



Faculty of Resource Science and Technology

Characterisation of *Ganoderma boninense* Isolates from Sarawak, the Causal Agent of Basal Stem Rot in *Elaeis guineensis*

Lo Mei Lieng

**Master of Science
2024**

Characterisation of *Ganoderma boninense* Isolates from Sarawak, the Causal Agent of Basal
Stem Rot in *Elaeis guineensis*

Lo Mei Lieng

A thesis submitted

In fulfilment of the requirements for the degree of Master of Science

(Plant Science)

Faculty of Resource Science and Technology
UNIVERSITI MALAYSIA SARAWAK

2024

DECLARATION

I declare that the work in this thesis was carried out in accordance with the regulations of Universiti Malaysia Sarawak. Except where due acknowledgements have been made, the work is that of the author alone. The thesis has not been accepted for any degree and is not concurrently submitted in candidature of any other degree.



.....
Signature

Name: Lo Mei Lieng

Matric No.: 20020035

Faculty of Resource Science and Technology

Universiti Malaysia Sarawak

Date : 22 September 2024

ACKNOWLEDGEMENT

First and foremost, I would like to express my sincere gratitude to my supervisors, Dr. Vu Thanh Tu Anh and Associate Professor Dr. Freddy Yeo Kuok San, for all of their assistance, guidance, and support. I appreciated the time and ideas that they spent on the completion of this study. As for providing me with an opportunity to pursue my master's degree, I am grateful to Datu Dr. Lulie Melling FASc, Director of the Sarawak Tropical Peat Research Institute (TROPI). I have been able to reach my potential thanks to her inspiration and support. I am also grateful to Sarawak Oil Palms Berhad (SOPB) for providing me with a scholarship. This scholarship brings me one step closer to achieving my academic goals. Also, I would like to express my sincere thanks to Dr. Sharon Lau, Head of the Molecular and Microbiology Research Division (M&M), for her faith in me and her words of advice and encouragement. I am really grateful to M&M team, especially Mr. Ewandy, Mr. Meldon, Ms. Laurina, Ms. Claudia, Ms. Mary, Mr. Rocky, Ms. Jacelyn, Mr. Simon Peter, Ms. Anathasia, Mr. Frazer, Ms. Jee Mui Sie, and Ms. Chin Mei Yee, for their assistance throughout my study. Thank you to Mr. Joseph and Dr. Ken Wong for their guidance in the measurement of the photosynthesis rate. I also like to thank the other TROPI members who have contributed to this study both directly and indirectly. This study would not have been possible without them. Thank you to Ms. Chanda Agom, who donated the rubber tree for this study, Mr. Belayong Sing, who did the tree-cutting, and Mr. Morgan Taylor Lai, Ms. Lo Mei Hua, Ms. Lo Mei Chieng, and Ms. Mona Anam, who prepared the rubber wood blocks. Last but not least, I would like to thank my parents for their unwavering love, support, and understanding, as well as for encouraging me to always do my best and be grateful in life. Thank you for your love and unending support, sibling.

ABSTRACT

Malaysia's oil palm industry has been threatened by basal stem rot (BSR), a difficult-to-cure disease caused by *Ganoderma boninense*. This disease causes yield and palm losses by shortening the economic life cycle of the oil palm. However, there is a critical knowledge gap on *G. boninense* aggressiveness in the Sarawak region, and their metabolic profile remain poorly explored. Therefore, this study employed various approaches to differentiate *G. boninense* isolates aggressiveness, including measurements of seedlings vegetative growth, chlorophyll content, photosynthetic rate, disease incidence (DI), disease severity index (DSI), and the *in vitro* growth rate of the isolates on different media. Subsequently, the metabolic profiles of the most and least aggressive *G. boninense* isolates in this study were characterised using BIOLOG Phenotype Microarray (PM). Six *G. boninense* isolates sampled from Balingian, Daro, and Kuala Igan, namely BLSM5B, DR51B, BLSM5A, BLSM4A, IGKI3, and DR56, were artificially inoculated onto two-month-old oil palm seedlings. Based on the aggressiveness parameters employed in this study, the isolates were categorised into three groups: highly aggressive (BLSM5B), moderately aggressive (DR51B, BLSM5A, BLSM4A, and IGKI3), and less aggressive (DR56). The measurements of chlorophyll content and photosynthetic rates proved to be highly sensitive to *G. boninense* infection. Notably, the bole size of the seedlings remained unaffected throughout the study. Spearman's rank correlation revealed that chlorophyll content and photosynthetic rate display a negative correlation with the DSI, whereas *in vitro* growth rate on malt extract agar (MEA) showed a positive correlation with DSI. Additionally, most *G. boninense* reisolated in this study exhibited faster growth than those from the original culture stock on MEA. Isolate BLSM5B stands out as a promising candidate for future studies related to BSR disease management and control strategies. In terms of substrate utilisation, isolate BLSM5B demonstrated the ability to

utilize a wide range of substrates (carbon (65.26%), nitrogen (72.63%), phosphorus (88.14%), and sulphur (74.29%) compared to the less aggressive isolate, DR56 (4.73%, 57.89%, 81.36%, 62.86%, and 64.89%, respectively). Additionally, isolate BLSM5B exhibited a robust biosynthetic pathway (93.62%) and growth on various pH conditions (81.91%) compared to isolate DR56 (21.28% and 64.89, respectively). However, isolate DR56B is more efficient in the utilisation of peptide nitrogen (72.34%) and the growth on various osmolytes condition (60%) in comparison to isolate BLSM5B (70.57% and 46.32%, respectively). Both isolates were unable to metabolize sodium benzoate at a pH of 5.2 (20–200 mM), preferred Ala-Asp (nitrogen source) and Met-His, Thr-Arg, Gly-Asn, and Thr-Gln (peptide nitrogen source), and a pH of 4.5 in the presence of 5-hydroxy tryptophan. In addition, the comparisons of substrate utilisation between isolates BLSM5B and DR56 showed a significant difference in their utilisation in certain substrates. These findings offering valuable insights for the development of new ways to manage BSR, highlighting the importance of identifying specific nutrients or conditions that support the growth of *G. boninense*, thereby enabling more precise and effective control measures. Among the disease confirmation techniques employed in this study, molecular detection of fungal DNA isolated from infected tissue demonstrated the highest recovery percentage. The amplification of fungal DNA extracted from the infected tissue using the ITS3/GanET primers without subsequent sequencing, proved to be reliable for disease detection. Incorporating molecular identification is essential to improve the precision and reliability of disease confirmation whenever a culture-based approach is required.

Keywords: Artificial inoculation, aggressiveness, phenotype microarray, disease confirmation, *Ganoderma boninense*

Pencirian isolat Ganoderma boninense dari Sarawak, Ejen Penyebab Reput Pangkal Batang Elaeis guineensis

ABSTRAK

Industri kelapa sawit Malaysia diancam oleh penyakit reput pangkal batang (BSR), penyakit yang sukar dikawal disebabkan oleh Ganoderma boninense. Penyakit ini menyebabkan kerugian hasil dengan memendekkan kitaran hayat ekonomi pokok kelapa sawit. Namun, terdapat kesenjangan pengetahuan mengenai keagresifan isolat G. boninense di wilayah Sarawak, dan profil metabolik isolat. Oleh itu, kajian ini menggunakan pelbagai pendekatan untuk membezakan keagresifan isolat G. boninense, termasuk pengukuran pertumbuhan vegetatif anak pokok, kandungan klorofil, kadar fotosintesis, kejadian penyakit (DI), indeks keparahan penyakit (DSI), dan kadar pertumbuhan in vitro isolate pada media yang berbeza. Seterusnya, profil metabolik isolat G. boninense yang paling agresif dan kurang agresif dikaji menggunakan BIOLOG Phenotype Microarray (PM). Enam isolat G. boninense yang disampel dari Balingian, Daro, dan Kuala Igan, iaitu BLSM5B, DR51B, BLSM5A, BLSM4A, IGKI3, dan DR56, digunakan untuk inokulasi buatan pada anak pokok kelapa sawit berusia dua bulan. Berdasarkan parameter keagresifan dalam kajian ini, isolat-isolat tersebut dikategorikan kepada tiga kumpulan: sangat agresif (BLSM5B), sederhana agresif (DR51B, BLSM5A, BLSM4A, dan IGKI3), dan kurang agresif (DR56). Pengukuran kandungan klorofil dan kadar fotosintesis terbukti sensitif terhadap jangkitan G. boninense. Saiz lilitan batang anak pokok adalah tidak terjejas sepanjang kajian. Korelasi "Spearman rank" menunjukkan bahawa kandungan klorofil dan kadar fotosintesis mempunyai korelasi negatif dengan DSI, manakala kadar pertumbuhan in vitro pada malt extract agar (MEA) menunjukkan korelasi positif dengan DSI. Selain itu, majoriti G. boninense yang dipencilkan semula menunjukkan pertumbuhan yang lebih cepat berbanding stok asal kultur pada MEA. Isolat

BLSM5B berpotensi sebagai calon untuk kajian masa depan berkaitan pengurusan penyakit BSR dan strategi kawalan. Dari segi penggunaan substrat, isolat *BLSM5B* menunjukkan kemampuan tinggi dalam penggunaan pelbagai substrat: karbon (65.26%), nitrogen (72.63%), fosforus (88.14%), dan sulfur (74.29%), berbanding isolat kurang agresif, *DR56* (masing-masing 4.73%, 57.89%, 81.36%, 62.86%, dan 64.89%). Isolat *BLSM5B* juga menunjukkan jalur biosintesis (93.62%) dan pertumbuhan pada pelbagai pH (81.91%) yang lebih tinggi berbanding isolat *DR56* (masing-masing 21.28% dan 64.89%). Walau bagaimanapun, isolat *DR56* lebih efisien dalam penggunaan nitrogen peptida (72.34%) dan pertumbuhan pada pelbagai osmolit (60%) berbanding isolat *BLSM5B* (masing-masing 70.57% dan 46.32%). Kedua-dua isolat tidak dapat menggunakan natrium benzoat pada pH 5.2 (20–200 mM), lebih menggemari Ala-Asp (sumber nitrogen) dan Met-His, Thr-Arg, Gly-Asn, dan Thr-Gln (sumber nitrogen peptida), dan pH 4.5 dalam kehadiran 5-hidroksi triptofan. Selain itu, perbandingan penggunaan substrat antara isolat *BLSM5B* dan *DR56* menunjukkan perbezaan yang signifikan dalam penggunaan substrat tertentu. Penemuan ini amat berharga dalam pengurusan penyakit BSR, menekankan kepentingan mengenal pasti nutrien atau keadaan yang menyokong pertumbuhan *G. boninense*, membolehkan langkah kawalan BSR yang lebih tepat dan berkesan. Antara teknik pengesanan penyakit yang digunakan, kejayaan pengesanan DNA kulat yang diektrak daripada tisu pokok yang dijangkiti melalui kaedah molekular menunjukkan kejayaan tertinggi. Amplifikasi DNA kulat yang diektrak daripada tisu pokok yang dijangkiti menggunakan primer ITS3/GanET tanpa penjujukan DNA, terbukti tepat untuk pengesanan penyakit. Penggunaan kaedah molekular meningkatkan kejituan dan ketepatan pengesanan penyakit dalam pendekatan konvensional.

Kata kunci: Inokulasi buatan, keagresifan, mikroarray fenotip, pengesanan penyakit, *Ganoderma boninense*

TABLE OF CONTENTS

	Page
DECLARATION	i
ACKNOWLEDGEMENT	ii
ABSTRACT	iii
<i>ABSTRAK</i>	v
TABLE OF CONTENTS	vii
LIST OF TABLES	xii
LIST OF FIGURES	xiv
LIST OF ABBREVIATIONS	xix
CHAPTER 1 INTRODUCTION	1
1.1 Study Background	1
1.2 Problem Statement	5
1.3 Objectives	7
CHAPTER 2 LITERATURE REVIEW	8
2.1 Oil Palm	8
2.2 Economic Importance	9
2.3 Basal Stem Rot	10
2.4 The Pathogen	14

2.4.1	<i>Ganoderma boninense</i>	14
2.4.2	Life Cycle	17
2.4.3	Mode of Infection	17
2.5	Pathogen Phenotype	19
2.6	Aggressiveness of the Pathogen	21
2.7	Factors for Development of Basal Stem Rot	22
2.7.1	Substrates, Inoculum Sizes and Inoculation Methods	22
2.7.2	Shade	24
2.7.3	Planting Material	25
2.8	Aggressiveness Assessment Parameters	25
2.8.1	Disease Incidence and Disease Severity Index	25
2.8.2	Physiological Aspects of an Infected Plant	26
2.8.3	<i>In Vitro</i> Growth Rate	28
2.9	Disease Confirmation Approach in <i>Ganoderma</i> Infected Oil Palm Seedlings	30
CHAPTER 3 MATERIALS AND METHODS		32
3.1	Source of Isolates and Culture Condition	32
3.2	<i>Ganoderma</i> Inoculum Preparation	33
3.3	Oil Palm Seedlings Artificial Inoculation	35
3.4	Characterisation of <i>Ganoderma boninense</i> Isolates	40

3.4.1	Aggressiveness Level	40
3.4.1.1	Vegetative Growth Measurement	40
3.4.1.2	Chlorophyll Content	42
3.4.1.3	Photosynthetic Rate	42
3.4.1.4	Disease Assessment	44
3.4.1.5	<i>In Vitro</i> Growth Rate	46
3.4.2	Statistical Analyses: Aggressiveness Assessment	47
3.4.3	Substrate Utilisation Profile	47
3.4.4	Statistical Analyses: Substrate Utilisation Profile	48
3.5	Disease Confirmation Methods	49
3.5.1	Re-isolation from Infected Tissue	49
3.5.2	Re-isolation from Fruiting Body	52
3.5.3	Molecular Identification	53
3.5.3.1	Fungal DNA Extracted from Fungi Isolated from the Bole and Root Tissue on <i>Ganoderma</i> Selective Medium	53
3.5.3.2	Fungal DNA Isolated from Fruiting Bodies on <i>Ganoderma</i> Selective Medium	59
3.5.3.3	Fungal DNA Isolated from Bole and Root Tissue	59
	CHAPTER 4 RESULTS	60
4.1	Characterisation of <i>Ganoderma boninense</i> Isolates	60
4.1.1	Aggressiveness Levels	60
4.1.1.1	Vegetative Growth Measurements of Oil Palm Seedlings	60
i.	Height	60
ii.	Bole Size	62
iii.	Number of Leaves	63

iv. Leaf Area	65
v. Fresh Root Mass	67
4.1.1.2 Chlorophyll Content	69
4.1.1.3 Photosynthesis Rate	71
4.1.1.4 Disease Progress	74
4.1.1.5 <i>In Vitro</i> Growth Rate	81
4.1.1.6 Aggressiveness Assessment	86
4.1.2 Spearman's Rank Correlation between Aggressiveness Parameters and Disease Severity Index	88
4.1.2.1 Vegetative Growth Parameters vs Disease Severity Index	88
4.1.2.2 Chlorophyll Content vs Disease Severity Index	89
4.1.2.3 Photosynthetic Rate vs Disease Severity Index	89
4.1.2.4 <i>In Vitro</i> Growth Rates and the Disease Severity Index	90
4.1.3 Substrate Utilisation Profile	91
4.1.3.1 Carbon Sources	91
4.1.3.2 Nitrogen Sources	94
4.1.3.3 Phosphorus and Sulphur Sources	94
4.1.3.4 Biosynthetic Pathways/Nutrient Supplements	97
4.1.3.5 Peptide Nitrogen Sources	100
4.1.3.6 Osmolytes	104
4.1.3.7 pH	106
4.1.3.8 Summary of Substrates Utilisation by Isolates BLSM5B and DR56	110
4.1.4 Substrate Utilisation Differences between Isolates BLSM5B and DR56	111
4.2 Disease Confirmation Methods	115
4.2.1 Re-isolation from Infected Tissue	115
4.2.2 Re-isolation from Fruiting Body	117
4.2.3 Molecular Identification	117

4.2.3.1	Identification of Fungi Isolated from Bole and Root Tissue on GSM	117
4.2.3.2	Identification of Fungi Isolated from Fruiting Body on GSM	118
4.2.3.3	Identification of Fungi Based on Genomic DNA of inoculated Bole and Root Tissues	118
4.2.3.4	Comparison of Disease Confirmation Methods	120
CHAPTER 5 DISCUSSION		121
5.1	<i>Ganoderma boninense</i> Isolates Aggressiveness	121
5.2	<i>Ganoderma boninense</i> Substrates Utilisation	126
5.3	<i>Ganoderma</i> Disease Confirmation Methods	131
CHAPTER 6 CONCLUSION AND RECOMMENDATIONS		134
6.1	Conclusions	134
6.2	Recommendations	135
REFERENCES		137
APPENDICES		166

LIST OF TABLES

	Page
Table 3.1: <i>Ganoderma boninense</i> isolates used in this study	32
Table 3.2: Fertilisation program used in this study (Heriansyah and Tan, 2005)	38
Table 3.3: Vegetative growth parameters measured in this study and the measuring procedure	41
Table 3.4: The leaf chamber setpoint	43
Table 3.5: Disease class value, signs and symptoms for disease severity index scoring (Lo et al., 2023)	45
Table 3.6: <i>Ganoderma boninense</i> aggressiveness level classification (Lo et al., 2023)	46
Table 3.7: Phenotype microarray plates	48
Table 3.8: Composition of <i>Ganoderma</i> selective medium	49
Table 3.9: Composition of CTAB buffer	54
Table 3.10: The components of PCR reaction mixture	58
Table 4.1: <i>In vitro</i> growth rate of <i>Ganoderma boninense</i> on malt extract agar (MEA), potato dextrose agar (PDA) and sabouraud dextrose agar (SDA)	84
Table 4.2: Summary of seedlings physiological parameters measured for <i>Ganoderma boninense</i> isolates aggressiveness assessment at six months after inoculation	87
Table 4.3: Substrates in PM1 and PM2 microplates that significantly supported the growth of isolate BLSM5B. There was no compound in PM1 and PM2 microplates that significantly supports the growth of isolate DR56	93
Table 4.4: Substrates in PM3 microplates that significantly supported the growth of isolate BLSM5B and DR56	96
Table 4.5: Substrates in PM4 microplates that significantly supported the growth of isolate BLSM5B and DR56	97
Table 4.6: Substrates in PM5 microplates that significantly supported the growth of isolate BLSM5B	99

Table 4.7:	Substrates in PM6 microplates that significantly supported the growth of isolate BLSM5B and DR56	102
Table 4.8:	Substrates in PM7 microplates that significantly supported the growth of isolate BLSM5B and DR56	103
Table 4.9:	Substrates in PM8 microplates that significantly supported the growth of isolate BLSM5B and DR56	104
Table 4.10:	Osmolytes conditions in PM9 microplates that significantly supported the growth of isolate BLSM5B. There were no osmolytes conditions that significantly support the growth of isolate DR56	108
Table 4.11:	pH conditions in PM10 microplates that significantly supported the growth of isolate BLSM5B and DR56	109
Table 4.12:	The substrates types and percentages utilized by isolates BLSM5B and DR56	110

LIST OF FIGURES

	Page
Figure 2.1: Basal stem rot sign and symptoms (Zakaria, 2023)	12
Figure 2.2: The basidiocarps of <i>Ganoderma boninense</i> on infected oil palm tree trunk (Flood et al., 2022)	15
Figure 2.3: Lignin degradation of oil palm infected by <i>Ganoderma boninense</i>	15
Figure 2.4: <i>Ganoderma boninense</i> grown on potato dextrose agar (Idris et al., 2000b)	16
Figure 2.5: Rubberwood block: 12 × 6 × 6 cm (Kok et al., 2013)	23
Figure 3.1: <i>Ganoderma boninense</i> isolates pure culture after nine day of incubation: (A) BLSM5A, (B) BLSM5B, (C) BLSM4A, (D) DR51B, (E) DR56, and (F) IGKI3	33
Figure 3.2: Well colonised rubberwood block after 60 days of incubation	34
Figure 3.3: Germinated oil palm seeds (Dura × PISOfera AA Hybrida IS)	36
Figure 3.4: Healthy two months old oil palm seedlings	36
Figure 3.5: (A) <i>Ganoderma</i> -colonised rubber wood block in a polybag half-filled with transplanting medium. (B) Artificial inoculation of oil palm seedlings	37
Figure 3.6: Vegetative growth measurements of oil palm seedlings	40
Figure 3.7: The root of the seedlings were cut at the base of the bole (blue line) for fresh root mass measurement	42
Figure 3.8: LI-6800F portable photosynthesis system (LI-COR Inc., USA).	43
Figure 3.9: Oil palm seedling bole cut into halves	51
Figure 3.10: The fruiting body grew around the artificially inoculated seedling	52
Figure 3.11: Fungal mycelia liquid culture in malt extract broth	53
Figure 3.12: Visible fungal DNA strands formed after being incubated overnight at 4°C in a cold room	57

- Figure 4.1: The height of the oil palm seedlings at 0, 3, 4, 5, and 6 months after inoculation. The means follow by the same letter per respective month, indicating no significant difference at 0.05 significance level. Error bars represent the standard error of the mean 62
- Figure 4.2: The bole size of the oil palm seedlings at 0, 3, 4, 5, and 6 months after inoculation. The means follow by the same letter per respective month, indicating no significant difference at 0.05 significance level. Error bars represent the standard error of the mean 63
- Figure 4.3: The number of leaves of the oil palm seedlings at 0, 3, 4, 5, and 6 months after inoculation. The means follow by the same letter per respective month, indicating no significant difference at 0.05 significance level. Error bars represent the standard error of the mean 65
- Figure 4.4: The leaf area of the oil palm seedlings was measured at 0, 3, 4, 5, and 6 months after inoculation. The means followed by the same letter for each respective month indicate that there is no significant difference at the 0.05 significance level. Error bars represent the standard error of the mean 67
- Figure 4.5: The fresh root mass of the oil palm seedlings was measured at 3, 4, 5, and 6 months after inoculation. The means followed by the same letter for each respective month indicate that there is no significant difference at the 0.05 significance level. Error bars represent the standard error of the mean 69
- Figure 4.6: The chlorophyll meter readings (in SPAD units) of the oil palm seedlings were taken at 3, 4, 5, and 6 months after inoculation. The means followed by the same letter for each respective month indicate no significant difference at the 0.05 significance level. Error bars represent the standard error of the mean. All seedlings selected for chlorophyll measurements in the treatment DR51B died six months after inoculation, whereas those in the treatment BLSM5B died five months after inoculation 71
- Figure 4.7: The photosynthesis rate of the oil palm seedlings was measured at 3, 4, 5, and 6 months after inoculation (MAI). The means followed by the same letter for each respective month indicate no significant difference at the 0.05 significance level. Error bars represent the standard error of the mean. All seedlings selected for chlorophyll measurements in the treatment DR51B died six months after inoculation, whereas those in the treatment BLSM5B died five months after inoculation 73
- Figure 4.8: The first fruiting body (indicated by the red arrow) was observed near the seedling inoculated with DR51B two months after inoculation. Additionally, necrotic leaves were noticed in seedlings that were inoculated with DR51B 74

Figure 4.9: Leaf necrosis (indicated by the red arrow) observed in seedlings inoculated with isolate BLSM5A (left) and BLSM5B (right)	75
Figure 4.10: Fruiting bodies grew on seedlings inoculated with the following isolates three months after inoculation: (A) BLSM5B, (B) DR56, (C) DR51B, (D) IGKI3, (E) BLSM4A, and (F) BLSM5A	76
Figure 4.11: Necrotic lesions and complete necrosis were observed on the boles of the seedlings inoculated with the following isolates four months after inoculation: (A) BLSM5B, (B) DR56, (C) DR51B, (D) IGKI3, (E) BLSM4A, and (F) BLSM5A	77
Figure 4.12: Necrotic lesion and necrotic roots of the seedlings inoculated with the following isolates four months after inoculation: (A) BLSM4A, (B) DR51B, and (C) BLSM5B	78
Figure 4.13: The disease incidence of the oil palm seedlings at 3, 4, 5, and 6 months after inoculation (MAI)	79
Figure 4.14: Disease severity index (DSI) of oil palm seedlings at 3, 4, 5, and 6 months after inoculation (MAI). The means followed by the same letter for each respective month indicate no significant difference at the 0.05 significance level. Error bars represent the standard error of the mean	81
Figure 4.15: The growth of <i>Ganoderma boninense</i> isolates on day eight after inoculation: (A) malt extract agar, (B) potato dextrose agar, and (C) sabouraud dextrose agar	83
Figure 4.16: <i>In vitro</i> growth rate of <i>Ganoderma boninense</i> isolates from original stock culture (OSC) and those reisolated from fruiting body (FB) in this study on malt extract agar. The same alphabet of each respective isolate indicate no significant different at the 0.05 significance level. Error bars represent standard error	85
Figure 4.17: Scatter plots showing the relationship between the vegetative growth parameters and disease severity index (DSI): (A) Number of leaves, (B) Bole size, (C) Height, (D) Leaf area, and (E) Fresh root mass. The Spearman's rank correlation coefficient (r_s) and corresponding P-values (p) for each relationship are shown	88
Figure 4.18: Scatter plot showing the relationship between chloropyll content (SPAD unit) and disease severity index (DSI). Spearman's rank correlation coefficient (r_s) and P-values (p) are presented	89
Figure 4.19: Scatter plot showing the relationship between leaf photosynthetic rate and disease severity index (DSI). Spearman's rank correlation coefficient (r_s) and P-values (p) are presented	90

- Figure 4.20: Scatter plots showing the relationship between *in vitro* growth rate (IVGR) of *Ganoderma boninense* isolates and disease severity index (DSI) on three different media: (A) Malt extract agar (MEA). (B) Potato dextrose agar (PDA). (C) Sabouraud dextrose agar (SDA). Spearman's rank correlation coefficient (r_s) and corresponding P-values (p) for each relationship are shown 91
- Figure 4.21: Data for biolog phenotype microarray PM1 and PM2. Utilisation of carbon sources by the isolates is indicated by red (BLSM5B) and green (DR56) areas in the growth curve for each substrate 92
- Figure 4.22: Data for biolog phenotype microarray PM3 and PM4. Utilisation of the nitrogen sources (PM3) and phosphorus (Well A2-E12) and sulfur source (PM4: Well F2-H12) by the isolates is indicated by red (BLSM5B) and green (DR56) areas in the growth curve for each substrate 95
- Figure 4.23: Data for biolog phenotype microarray PM5. Activity of biosynthetic pathways exhibited by the isolates was indicated by red (BLSM5B) and green (DR56) areas in the growth curve for each substrate 98
- Figure 4.24: Data for biolog phenotype microarray PM6, PM7, and PM8. Utilisation of the peptide nitrogen sources by the isolates was indicated by red (BLSM5B) and green (DR56) areas in the growth curve for each substrate 101
- Figure 4.25: Data for biolog phenotype microarray PM9 (Osmolytes) and PM10 (pH). The metabolic activity was indicated by red (BLSM5B) and green (DR56) areas in the growth curve for each tested condition 108
- Figure 4.26: Data for biolog phenotype microarray PM 1-10 plates comparing isolate BLSM5B (most aggressive) and isolate DR56 (least aggressive). Red presented the metabolic fingerprint of isolate BLSM5B; green presented the metabolic fingerprint of isolate DR56; and yellow presented the common fingerprints of both isolates. The boxed well indicates a significant difference in substrate utilisation 114
- Figure 4.27: Re-isolation on *Ganoderma* selective medium. (A) The bole and the roots of uninoculated seedlings. (B) The bole and the roots of inoculated seedlings. Brown pigmentation forms around the infected tissue (red arrow) 116
- Figure 4.28: Contaminated *Ganoderma* selective medium 116
- Figure 4.29: Fruiting body inoculated on *Ganoderma* selective medium exhibited brown pigmentation (red arrow) 117
- Figure 4.30: The amplification of fungal DNA recovered from the bole (top lane) and the root (bottom lane) tissue using the GanET/ITS3 primer pair after (A)

three, (B) four, (C) five, and (D) six months after inoculation. “L”, “P”, and “N” indicate 100bp DNA ladder, positive control, and negative control, respectively. Lane 1 and 2 (A to D) is the DNA recovered from uninoculated oil palm seedlings. The remainder is the DNA recovered from oil palm seedlings inoculated with isolate BLSM5B, DR56, DR51B, IGKI3, BLSM4A, and BLSM5A

119

Figure 4.31: Success rate of confirming the presence of *Ganoderma boninense* based on PCR amplification using genomic DNA of infected tissue and fungal culture established from re-isolation from infected tissue and fruiting body of *Ganoderma boninense*

120

LIST OF ABBREVIATIONS

%	Percent
<	Less than
>	More than
±	Plus or minus
×	Times
°C	Celsius
μM	Micromolar
μmol m ⁻² s ⁻¹	Micromoles per square meter per second
μmol mol ⁻¹	Micromoles per mole
A	Assimilation
ANOVA	Analysis of variance
ATP	Adenosine triphosphate
bp	Base pair
BS	Bole size
BSR	Basal stem rot
cm	Centimeter
cm.day ⁻¹	Centimeter per day
cm ³	Cubic Centimeter
CTAB	Cetyltrimethylammonium bromide
CWDEs	Cell wall degrading enzymes
DI	Disease incidence
DNA	Deoxyribonucleic acid

DSI	Disease severity index
DTT	Dithiothreitol
e.g.	Exempli gratia
et al.	Et alia
EtBr	Ethidium bromide
etc.	Et cetera
FFB	Fresh fruit bunches
FRM	Fresh root mass
g	Gram
g/L	Gram per liter
GPS	Global positioning system
GSM	<i>Ganoderma</i> selective medium
ha	Hectare
HPLC	High-performance liquid chromatography
ITS	Internal transcribed spacer
IVGR	<i>In vitro</i> growth rate
K	Potassium
kb	Kilobase pairs
L	Liter
LA	Leaf area
MAI	Month after inoculation
MEA	Malt extract agar
MEB	Malt extract broth
mg/mL	Milligrams per milliliter

mL	Milliliter
mM	Millimolar
NaCl	Sodium chloride
NADPH	Nicotinamide adenine dinucleotide phosphate
ng/ μ L	Nanograms per microliter
NOL	Number of leaves
OPEM	Oil palm extract medium
p	P-value
P	Phosphorus
PCR	Polymerase chain reaction
PDA	Potato dextrose agar
pH	Potential of hydrogen
PMs	Phenotype Microarrays
PP	Polypropylene
PVP	Polyvinylpyrrolidone
Rnase	Ribonucleases
rpm	Revolutions per minute
r_s	Spearman's rank correlation coefficient
RWBs	Rubberwood blocks
S	Sulfur
SDA	Sabouraud dextrose agar
SE	Standard error
SPAD	Soil plant analysis development
spp.	Species

TE	Tris-EDTA
™	Trademark
U	Unit
UPW	Ultra-pure water
USD	United States dollar
VGM	Vegetative growth measurement

CHAPTER 1

INTRODUCTION

1.1 Study Background

Since ancient times, phytopathogens have posed a threat to global food security, agricultural industries, and biodiversity (Thynne et al., 2015). Plant pathogens destroyed approximately 30% of world crop outputs, enough to feed 600 million people (Avery et al., 2019). According to Doehlemann et al. (2017), the majority of fungal plant pathogen species belong to the phyla Ascomycota and Basidiomycota, and they account for 70–80% of total plant diseases (Dayarathne et al., 2020), which greatly reduces crop yields and causes significant economic loss. Tackling plant pathogens is difficult because their populations are variable in time, space, and genotype (Strange and Scott, 2005). In addition, most developing countries have tropical climates that allow for continuous cropping, which results in the build-up of inoculum (Avery et al., 2019). As a result, one of the major issues that humanity is currently facing is how to maintain a sustainable, safe, and nutritious food supply for a growing human population.

In Malaysia, the primary cause of the basal stem rot (BSR) of oil palm (*Elaeis guineensis*) is *Ganoderma boninense*, a hemibiotroph basidiomycete from the Ganodermataceae family (Bharudin et al., 2022). Although Idris et al. (2000b) identified four species (*G. boninense*, *G. zonatum*, *G. tornatum*, and *G. miniatocinctum*) associated with BSR in Malaysia, *G. tornatum* was only found on dead palms, classified as non-pathogenic, and likely a saprophyte. Currently, *G. boninense* is recognised as the main species responsible for BSR in oil palms (Moncalvo, 2000). This pathogen poses a significant threat to Malaysia, the world's second-largest producer of palm oil, which accounts for almost one-third of global production (Hirschmann, 2022) and causes up

to USD 500 million of the annual yield loss (Zakaria, 2023). Consequently, Sarawak, the largest oil palm planting state in Malaysia, which accounts for 1.61 million hectares, or 28% of the country's total oil palm planted area (MPOB, 2021), has also been severely impacted by the BSR. Difficulties in detecting BSR at an early stage due to the late emergence of disease symptoms hinder disease management (Alexander et al., 2022). Besides, Paterson et al. (2015) projected that by 2050, the mean surface temperature in Malaysia would rise by 1.5 to 2 °C. Temperature increases of 1 to 4 °C may reduce oil palm productivity and increase the susceptibility to diseases and pests, which would exacerbate the BSR (Paterson et al., 2015; Paterson et al., 2017; Sarkar et al., 2020). As a consequence, the development of effective disease control measures is necessary for the sustainability of oil palm industry in the country.

Ganoderma boninense isolates from diverse locations have been shown to display a significant degree of genetic variation. Due to the high divergence of the genetic pool between distinct isolates, the aggressiveness (illustrated using the disease severity index) of different *G. boninense* strains varies (Kok et al., 2013; Midot et al., 2019; Wong et al., 2021; Bharudin et al., 2022). Additionally, the disease intensity and transmission rates of different *G. boninense* strains also differ. It has been identified that *G. boninense* is the main pathogen responsible for BSR-infected oil palm stands in Sarawak (Midot et al., 2019). Despite the fact that the pathogen has the potential to severely harm the oil palm industry, information on its aggressiveness is still scarce. Currently, only the aggressiveness of *Ganoderma* spp. isolated from Betong, Miri, and Balingian divisions has been determined in Sarawak (Rakib et al., 2015; Lo et al., 2023). Therefore, it is crucial to compare the aggressiveness of *G. boninense* isolates from various locations, as this information is essential for future studies such as the selection of a reference isolate for host

resistance screening and host-pathogen interaction gene expression studies. These findings will aid in the development of disease control strategies.

According to Alizadeh et al. (2013), the growth rate of *G. boninense* is influenced by both culture media and isolates. These factors can affect their growth rates and, therefore, their performance. In West Malaysia, Kok et al. (2013) reported differences in the *in vitro* growth rate among *G. boninense* isolates on two media: malt extract agar (MEA) and oil palm extract medium (OPEM). Even though the authors found weak linear relationships between the *in vitro* growth rate of *G. boninense* (on MEA and OPEM) and their aggressiveness, different *G. boninense* strains may exhibit different types of relationships or strengths. However, no study has been done on the *in vitro* growth rate of Sarawak *G. boninense* isolates. Besides, Zhan et al. (2016) suggest that the *in vitro* growth rate of a pathogen may play a significant contribution to pathogen aggressiveness. Therefore, it is essential to look into the *in vitro* growth rate of *G. boninense* isolates from different geographic regions in Sarawak, as well as their association with aggressiveness.

It is also known that the vegetative growth of seedlings infected with different *G. boninense* isolates varies greatly; for instance, seedlings challenged with the most aggressive isolate had significantly lower vegetative growth than seedlings challenged with the least aggressive isolates and controls (Goh et al., 2014). The authors also reported that the rate of infection and the emergence of symptoms occur at different rates depending on the isolates. The study also found that the two-month-old oil palm seedlings were more responsive in terms of DSI with vegetative growth measurements (VGM) parameters measured compared to older seedlings (five-month-old) (Goh et al., 2014). Furthermore, the stunted vegetative growth of *G. boninense* infected oil palm seedlings is due to extensive decay of the basal stem, which restricts water and nutrient uptake

(Sapak et al., 2008; Chong et al., 2017). Rakib et al. (2019) reported that the chlorophyll content decreased as the disease severity index (DSI) increased during the pathogenesis of *Ganoderma* in the oil palm seedlings. Water restrictions can limit photosynthesis efficiency due to thylakoid membrane damage and reduced chlorophyll content (Yang and Luo, 2021). Since plant leaf chlorophyll content is closely related to photosynthetic rate and nutritional status, physiological parameters such as vegetative growth, chlorophyll content, and photosynthetic rate could be used to differentiate the aggressiveness of *G. boninense* isolates.

During the last 10 years, the Biolog phenotypic microarray system (PMs) has been widely used to analyse the metabolic phenotypes of many microorganisms: *Bacillus subtilis* (Gusarov et al., 2009), *Escherichia coli* (Bochner et al., 2001), *Ralstonia solanacearum* (Chen et al., 2016), and *Alternaria alternata* (Wang et al., 2015). This system enables the simultaneous assay of nearly 1000 metabolic phenotypes, including the utilisation of carbon, nitrogen, sulphur, and phosphorus, as well as their biosynthetic pathways, osmotic pressure, ionic strength, and pH, which is rapid and easy to use (Singh, 2009) compared to the time-consuming traditional method (Wang et al., 2018). To date, no study has been conducted to investigate the substrate utilisation of the *G. boninense* isolates using the Biolog system. Moreover, other studies have found that manipulation of carbon and nitrogen supplies improves the fungus' ability to infect its host (Magan, 2001). The findings gained from this study will provide a comprehensive overview of the metabolic capability of *G. boninense*, which will be valuable for developing potential BSR control strategies in oil palms to decrease disease impacts as well as understanding the nutrient preferences for disease development. This information could also aid in the development of selective media for *G. boninense*.

Ganoderma selective medium (GSM) are widely employed to confirm disease in oil palm seedlings infected with *G. boninense*. This is accomplished by re-isolating *G. boninense* from diseased tissue and plating it on GSM (Goh et al., 2014; Rakib et al., 2015). However, this method is time-consuming and challenging at times, particularly if the Petri dish is overgrown by rapidly growing fungi, since *G. boninense* is a slow-growing fungus. Additionally, certain ingredients in the GSM, such as pentachloronitrobenzene (PCNB), are banned in countries like Indonesia due to their carcinogenic nature (Amanda and Prakoso, 2017). Moreover, ridomil is not available in some countries, complicating the future use of this medium (Amanda and Prakoso, 2017). As a result, there is an emerging need for alternatives, such as PCR-based molecular identification using DNA sample of infected seedling tissue, that serve the same purpose. Despite its drawbacks, GSM remains the superior medium for isolating *G. boninense* from field samples, particularly when a pure culture is required for research purposes.

1.2 Problem Statement

BSR, caused by *G. boninense*, is the most devastating oil palm disease in Malaysia. This disease has threatened the country's oil palm industry and resulted in economic losses by significantly reducing oil palm yields. Sarawak, as Malaysia's largest oil palm planting state, is also affected by this disease. Previous studies on *Ganoderma* spp. isolates' aggressiveness have shown substantial regional variations across Peninsular Malaysia, Sarawak, Indonesia, and Columbia (Kok et al., 2013; Goh et al., 2014; Rakib et al., 2015; Abdul Hamid, 2016; Castillo et al., 2022; Lo et al., 2023). These studies have underlined the fundamental relevance of understanding the aggressiveness of *Ganoderma* spp. isolates, as they pose a serious threat to the oil palm industry, which is a vital component of the agricultural economy in various regions. Despite the severe potential consequences of *Ganoderma* infection in the oil palm industry, there

is a lack of comprehensive data on the aggressiveness of *G. boninense* isolates found in Sarawak in a broader geographical context. Furthermore, by including various locales in the study, we may uncover commonalities and variations in the aggressiveness of *G. boninense* isolates, which can aid in the development of region-specific disease management strategies. Such strategies are crucial for the oil palm industry's long-term sustainability, not only in Sarawak but also in other oil palm-producing regions facing comparable issues.

While numerous studies have explored various aspects of *Ganoderma*'s biology, one critical area remains underexplored: the substrate utilisation patterns of *G. boninense* isolates. Substrate utilisation, which includes a wide range of organic compounds that this pathogen may degrade and use as a nutrition source, is a vital feature of its biology and pathogenicity. A few studies have been conducted to investigate nutritional conditions for *G. boninense* mycelial growth using high-performance liquid chromatography (HPLC) (Goh et al., 2013) and their growth on various sugar compounds under *in vitro* conditions (Peng et al., 2019). However, the metabolic diversity that can be studied using these approaches is limited. A comprehensive substrate utilisation pattern of *G. boninense* is critical in identifying potential nutrient sources in oil palm plantations that support growth as well as those that inhibit growth, which may then be used to design disease management strategies.

In addition, BSR-infected oil palms are asymptomatic in the early stages of the infection; the first symptoms typically appear on foliage when the infection has advanced by 60–70% (Chong et al., 2017). Current disease management efforts were hampered due to the late detection of *Ganoderma* infection in plantations, highlighting the urgent need for more targeted and effective disease management strategies to curb this disease. As a result, characterisation of *G. boninense*

isolates aggressiveness and substrate utilisation are critical for the development of preventive measures rather than reacting to outbreaks to reduce the risk of infection.

1.3 Objectives

The main objectives of this research were to characterise the aggressiveness levels and substrate utilisation of *G. boninense* isolates from Sarawak. This was achieved through the following set of objectives:

- i. To differentiate the aggressiveness levels of the *G. boninense* isolates based on physiological growth parameters of infected oil palm seedlings.
- ii. To investigate the substrate utilisation pattern of the most aggressive and least aggressive *G. boninense* isolates.

CHAPTER 2

LITERATURE REVIEW

2.1 Oil Palm

In 1917, Frenchman Henri Fauconnier pioneered the first commercial oil palm plantation in Tennamaram Estate, Selangor, Malaysia (Teoh, 2002). Oil palm, a woody monocotyledon of the Arecaceae family, is renowned as the “golden crop of Malaysia” due to its highly profitable export earnings (Dayou et al., 2014; Ferdous Alam et al., 2015). The two main species of oil palm are *Elaeis guineensis* (West Africa) and *E. oleifera* (South America) (Corley and Tinker, 2016). However, due to its superior yield, *E. guineensis* has been the species most commonly grown for commercial production and is recognised as the world’s leading source of vegetable oil and fat (Murphy, 2014; Jin et al., 2016). The term *Elaeis* derived from the Greek word *elaion*, which means “oil”, and *guineensis* comes from the name of the place where it was discovered, the Guinea coast of West Africa (Supramani et al., 2021). Dura, Pisifera, and Tenera are the three common varieties of the *E. guineensis* species, which have different shell thickness and mesocarp content (Teoh, 2002). In Malaysia, Tenera is the main variety cultivated due to its high yields (Basiron, 2007).

Oil palm agriculture has been linked to deforestation and the conversion of peat soils, which are directly connected to climate change and the production of severe haze and have a negative impact on biodiversity (Dislich et al., 2017). According to Supramani et al. (2021), soil moisture levels between 0.6% to 1.6% and temperatures between 24 °C to 28 °C are ideal for oil palm growth. Oil palms are at stressed when the temperature drops to 15 °C (cold stress) or rises to 36 °C (heat stress), or when soil moisture levels decrease to 0.4% (dry stress) or increase to 2%

(wet stress). Based on the climate projections presented by Paterson et al. (2017), growing oil palms in Malaysia will become more challenging at least until 2100 due to an unsuitable climate. This challenge is driven by rising temperatures, water stress, increased susceptibility to pests and diseases, yield reduction, and revenue losses (Sarkar et al., 2020). The productivity of oil palms may decline by 10 to 41% with temperature increases of 1 to 4 °C (Sarkar et al., 2020). The effects of water scarcity on oil palm are worsened by an increase in temperature since it speeds up the rate of soil water evaporation (Abubakar et al., 2021). Furthermore, rising temperatures alter the ecology of various pests and diseases, affecting factor such as their reproductive ability (Fleiss et al., 2017). Consequently, these pests and diseases gain greater resilience to environmental changes and experience population surges, raising the risk of an epidemic or even a pandemic outbreak within the plantations (Abubakar et al., 2021). Paterson (2020) also predicted that Malaysia's basal stem rot (BSR) incidence will go up significantly after 2050, along with an increase in oil palm mortality. The adaptation of more virulent *Ganoderma* strains to climate change could result in heightened disease risk for oil palm plantations (Zhou et al., 2015). Besides, the oil palm trees are expected to be less resistant to *Ganoderma* infections caused by both the changing climate and the increasingly aggressive fungal strains (Paterson, 2019).

2.2 Economic Importance

Oil palm is widely grown in Asia, Africa, and Latin America, with Malaysia and Indonesia among the top producers and exporters, followed by Thailand, Colombia, and Nigeria (Dayou et al., 2014; Jazuli et al., 2022). Over 72.27 million metric tonnes of palm oil were produced globally between 2020 and 2021, with Malaysia and Indonesia as the leading exporters of palm oil globally. Palm oil demand will continue to rise due to its availability and productivity advantage over other oil-producing crops such as soybean, sunflower, and rapeseed (Abdullah, 2011; Singh et al., 2013).

Malaysia, the second-largest palm oil producer in the world, contributed to 25.8 % of global palm oil output and 34.3% of global palm oil exports in 2020 (MPOC, 2020). The total oil palm planted areas in the country in 2021 was 5.74 million hectares. Sabah and Sarawak were the two states with the most oil palm planted areas in Malaysia in 2021, accounting for 26.6% and 28% of the total planted area (5.74 million hectares), respectively (MPOB, 2021). In terms of the country's agricultural gross domestic product oil palm accounted for 37.1% in 2021 (Mahidin, 2021). As a result, the sustainability of the oil palm industry is crucial for the country's future economic growth, social development, and environmental conservation.

2.3 Basal Stem Rot

Basal stem rot (BSR) has been devastating over the past 100 years, particularly in Malaysia and Indonesia, and projected to be increased when climate change favours infection by *Ganoderma boninense* (Paterson, 2019). BSR has also been recorded in Africa, Cameroon, Colombia, Ghana, Papua New Guinea, Southern Thailand, and Tanzania (Rebitanim et al., 2020). This disease poses a threat to Malaysia oil palm industry and results in economic losses by significantly reducing oil palm yields by up to 4.3 tonnes of fresh fruit bunches (FFB) per hectare, with more than 400,000 ha expected to be affected by 2020, amounting to 1.74 million tonnes of FFB yield decline (Chong et al., 2017). It was estimated that the annual yield loss caused by BSR was approximately USD 500 million (Kamu et al., 2021; Hilmi et al., 2022). Three states in Malaysia -Johor (1032.96 ha with 487 smallholders), Sabah (930.85 ha with 252 smallholders), and Perak (718.49 ha with 410 smallholders) - were discovered to have the highest number of oil palm trees infected with BSR (Jazuli et al., 2022).

The BSR infection is symptomless for a long period of time before the earliest signs and symptoms appeared. This will result in late detection of the disease and led to late response to

disease control. Once the infection has reached 60 to 70 %, the symptoms begin to emerge (Chong et al., 2017; Wong et al., 2021). Infection by *G. boninense* resembles those of drought and nutrient deficiency as the basal decay restricts water and nutrient uptake by the oil palm tree (Chong et al., 2017). Initially, BSR infection occurs through root contact with inoculum sources in the soil and spreads to the basal stem area (Rees et al., 2007; Rees et al., 2009). In the early infection stage, microhyphae, which resemble needle-like structures, are used by *G. boninense* to penetrate the oil palm root tissues (Govender and Wong, 2017). While the highly lignified endodermis of the root is still intact after colonization, the non-lignified cells disintegrate (Kamu, 2018). The pathogen can then penetrate the endodermis and invade the inner cortex. The infection causes ground parenchyma cells and sclerenchyma cells to disintegrate, resulting in cavities. Excessive hyphal growth of *G. boninense* could block xylem vessels, which compromises water and nutrient uptake and eventually results in yellowing and orange discoloration of the leaves and withering in infected palms. The crown flattening, thinning canopy, and multiple unopened spear leaves are among the symptoms of *Ganoderma* infected oil palm (Figure 2.1) (Turner, 1981; Hilmi et al., 2022). The most obvious feature of BSR is the emergence of basidiocarps and the deterioration of the basal stem (Figure 2.1). In severe cases, affected palm trees will die and topple.



Figure 2.1: Basal stem rot sign and symptoms (Zakaria, 2023)

BSR in Malaysia was first documented by Thompson (1931) in oil palm trees older than 25 years, due for replanting. Initially regarded as a disease of older palm trees, BSR began affecting younger trees (10 to 15 years old) from the late 1950s onward. In recent decades, infections have been detected in palm trees as young as 1 year old (Turner, 1981; Miller et al., 2000). This shift indicates an expanding susceptibility of oil palm to BSR across various oil palm age groups, driven by the extensive growth of the oil palm industry in recent decades. Normally, infected young palms die within 6–24 months after symptoms appeared, whereas mature palms take 2-3 years to die (Ariffin et al., 2000). Several factors contribute to *Ganoderma* infection in the field, including host susceptibility (oil palm variety), pathogen virulence (aggressiveness levels), environmental conditions (soil temperature, water content, fertility, etc.), and plantation management practices (e.g., no sanitation prior to replanting) (Jazuli et al., 2022). Additionally, the high starch content

in oil palm may be advantageous for *G. boninense*, as rapid depletion of starch was observed during early infection (Rees et al., 2009). This starch likely serves as a significant energy source, facilitating the host-pathogen interaction. Besides, oil palm planted in areas initially planted with coconut shows the highest BSR incidence compared to those in forest or former rubber planting areas (Gurmit, 1990). *Ganoderma boninense* was discovered as a symptomless endophyte in some live coconut palms (Idris et al., 2001), which could explain the high occurrence in plantings of succeeding coconuts. This suggests that the presence of *G. boninense* in live coconut palms does not initially cause harm to the host. However, it serves as a reservoir of inoculum, potentially explaining its high occurrence in subsequent plantings of oil palm. Furthermore, Turner (1981) discovered that oil palm planted in former coconut plantations had higher incidences of BSR than former rubber plantations and more prevalent in coastal areas with a history of previous coconut or oil palm planting than on inland soils.

Numerous interventions, including mechanical (cultural), chemical, and biological approaches, have been developed to combat this disease; nevertheless, these control measures have only served as temporary solutions to extend the lifespan of the infected oil palm stands, which makes the industries less sustainable. Additionally, the complex biology of *G. boninense*, the monoculture system of oil palm plantations, and the pathogen's wide range of hosts contribute to the challenge of effectively managing the disease (Rupaedah et al., 2024). Moreover, symptomless initial infections make it challenging to detect the disease at an early stage and hamper disease management attempts.

2.4 The Pathogen

2.4.1 *Ganoderma boninense*

Ganoderma boninense is a white-rot basidiomycete that belongs to the Ganodermataceae and is classed under Basidiomycetes (Bharudin et al., 2022). BSR, one of the most devastating oil palm diseases, is caused by *G. boninense* (Hilmi et al., 2022). *Ganoderma boninense* has a wide, fan-like structure with double-walled, truncate spores with inner layers ranging in colour from yellow to brown that grow on tree trunks (Figure 2.2). They also degrade lignin in wood (Figure 2.3), as well as cellulose and related polysaccharides (Bharudin et al., 2022). *Ganoderma boninense* pure cultures on potato dextrose agar are white on the surface, with a darkened (pigmented) undulating reverse surface that buckled the agar (Figure 2.4). This species is also known to have a wide range of hosts, including forest trees such as Acacia, Populus, and Macadamia, as well as plantations crops like coconut, Nipah, aren, areca nut, papyrus, grapevines, rubber, cocoa, tea, and guarana (As'wad et al., 2011; Purba et al., 2019).



Figure 2.2: The basidiocarps of *Ganoderma boninense* on infected oil palm tree trunk (Flood et al., 2022)



Figure 2.3: Lignin degradation of oil palm infected by *Ganoderma boninense*



Figure 2.4: *Ganoderma boninense* grown on potato dextrose agar (Idris et al., 2000b)

Early reports suggested that several *Ganoderma* species may be linked to the oil palm BSR, including *G. applanatum*, *G. boninense*, *G. chalceum*, *G. lucidum*, *G. miniatocinctum*, *G. pseudoferreum*, and *G. tornatum* (Turner, 1981). However, in later reports, Idris et al. (2000a) identified four *Ganoderma* species (*G. boninense*, *G. zonatum*, *G. tornatum*, and *G. miniatocinctum*) associated with oil palm BSR in Malaysia through an artificial infection study. *Ganoderma tornatum*, which was only found on dead palms, was identified as non-pathogenic and presumed to be a saprophyte, (Idris et al., 2000a). After the general consensus, it is generally agreed that the primary species responsible for BSR in oil palms is *G. boninense* (Moncalvo, 2000). Additionally, it was discovered that *G. boninense* was more prevalent and virulent than the other two species (*G. zonatum* and *G. miniatocinctum*) in a number of estates with a high incidence of BSR (Idris et al., 2001). In Peninsular Malaysia, *G. boninense* is the most common species associated with BSR (Ho and Nawawi, 1985). Similarly, *G. boninense* was also identified as the pathogen responsible for BSR-infected oil palm stands in Sabah and Sarawak, Malaysia (Chong et al., 2011; Midot et al., 2019), Southern Thailand, (Pornsuriya et al., 2013), Indonesia and Papua New Guinea (Pilotti et al., 2004; Purba et al., 2019). In Columbia and Cameroon, different species

of *Ganoderma* were associated with BSR: *G. zonatum* (Castillo et al., 2022) and *G. ryvardense* (Kinge and Mih, 2011), respectively.

2.4.2 Life Cycle

Ganoderma boninense, a basidiomycete, reproduces via two strategies: basidiospores and vegetative mycelia, where the primary mechanism of dispersal is believed to be through basidiospores (Chong et al., 2017). The discovery of highly diverse *G. boninense* isolates from oil palm-producing regions through molecular studies supports the theory that basidiospores play significant roles in BSR infection and spread (Pilotti et al., 2021; Wong et al., 2021). Basidiospores produced by mature basidiocarps are dispersed by winds or insects and germinate to develop a monokaryotic mycelium that feeds on dead plant material (Bharudin et al., 2022). At the germination stage, monokaryotic mycelia are not infectious. The nuclear exchange and migration occur, and dikaryotic mycelium forms, invades, and establishes itself within the plant host. When the climate is favourable, the dikaryotic mycelia later gives rise to the formation of the fruiting body. Karyogamy and the formation of meiotic spores occur in the multicellular reproductive structure (fruiting body), indicating that the *Ganoderma* sexual cycle is complete.

2.4.3 Mode of Infection

As a soil-borne fungus, it is widely accepted that the main mode of infection by *Ganoderma* is through root invasion, where infected debris comes into contact with healthy roots. This was evidence by numerous infection studies using oil palm seedlings and *Ganoderma*-colonised rubber wood blocks (RWB) (Sariah et al., 1994; Breton et al., 2006; Chan et al., 2011). *Ganoderma* required direct contact with the roots of the palm tree to develop infection (Cooper et al., 2011) and wounding is not required for infection (Flood et al., 2022). The needs of intimate contact

between inoculum and plant roots were probably due to the two main traits of *Ganoderma* that it is a rather weak pathogen that needs a substantial inoculum to attack and also a poor competitor against others saprotrophic microflora. Through microscopic observation, Alexander et al. (2017) and Rees et al. (2009) provided confirmation that root invasion as probably the main mode of infection by *G. boninense*.

Nevertheless, *Ganoderma* population in plantations has a high degree of heterogeneity based on the genetic studies conducted in the province of Sabah (Rakib et al., 2020), Papua New Guinea (Pilott et al., 2018), Sarawak (Rakib et al., 2014), Peninsular Malaysia, and Sumatra (Mercière et al., 2017), which suggests that basidiospores are responsible for the primary spread of the pathogen. Most studies to date have focussed on invasion through roots and little attention has been given to possible basidiospore infection through frond bases (Flood et al., 2022). Although Thompson (1931) suggested mode of infection via basidiospores, several attempts to initiate direct infection in oil palm seedlings by inoculation of basidiospores have failed in the past, which may suggest insufficient parasitic ability or that successful infection of aerial parts only occurs under certain circumstances (Flood et al., 2022). Therefore, the mode of spread is still highly debated.

Besides, production of a range of cell wall-degrading enzymes (CWDEs) (Cooper et al., 2011) are required to ensure a successful penetration and degradation of the host outermost tissues, which are made up of the resistant polymers cellulose, lignin, and suberin. Amylase, oxidase, invertase, coagulase, protease, rennetase, pectinase, and cellulose are CWDEs produced by *Ganoderma*. During *G. boninense* infection, the enzyme activity of *G. boninense* related to lignin and all other important structural cell wall polymers was discovered, as well as their effect on host wall composition (Rees et al., 2009).

Ganoderma infection appears to be associated with developmental shifts. *Ganoderma boninense* behaved as a hemibiotroph, where they switches from biotrophic to necrotrophic phase during infection (Bharudin et al., 2022). In the early infection, *G. boninense* behave as biotrophic where they absorb nutrient from the host by colonising the root cortex and stem base while keeping the host cells intact (Rees et al., 2009; Chong et al., 2017). This phase then followed by necrotrophic phase, where the *G. boninense* exudes CWDEs that eventually kill the host cells (Rees et al., 2009; Chong et al., 2017).

2.5 Pathogen Phenotype

The Biolog (Hayward, CA, United States) company has developed a semi-high throughput Phenotypic Microarray (PMs) system to assay nearly 1000 phenotypic traits simultaneously for characterisation and monitoring the cellular phenotypes of pure cultures or communities in an environmental sample (Borglin et al., 2012). This system has been widely utilized to assay microorganisms, including *Bacillus subtilis* (Gusarov et al., 2009), *Escherichia coli* (Bochner et al., 2001), *Ralstonia solanacearum* (Chen et al., 2016), *Alternaria alternata* (Wang et al., 2015), and *Botrytis cinerea* (Wang et al., 2018). This system is not only easy to operate but also allows for the rapid testing of microorganisms against various substrates including the utilisation of carbon, nitrogen, sulphur, phosphorus source, biosynthetic pathways and varying effects of osmotic, ionic, and pH environments (Wang et al., 2015; Pinzari et al., 2016).

Wang et al. (2015) used the PM system to analyse metabolic characteristics of an isolate of *Alternaria alternata*, the causal agent of tobacco brown spot. The authors found that *A. alternata* phenotypic traits related to the utilisation of diverse resources and their broad adaptability may offer substantial potential for study on pathogen-tobacco interactions and pathogen survival under varied environmental settings. Chen et al. (2016) also used the PM system to study phenotypic

fingerprints of *Ralstonia solanacearum* isolates under various osmolytes and pH environments and discovered that the information gained increased understanding of the bacterium's adaptability and provided valuable profiles for the development of effective disease control strategies. Similarly, the result of metabolic phenotype characterization of *Botrytis cinerea*, the causal agent of grey mold, also enriched knowledge of its ability to utilize nutritional substrates and its adaptability in different environments (Wang et al., 2018). This feature of the results has provided valuable clues to finding new methods of grey mold management. Full metabolic profiles of *Listeria monocytogenes* responsible for Listeriosis outbreak, also has provides data that useful for the future design of improved *Listeria* specific media to enhance routine detection and isolation of this pathogen as well as provide knowledge for developing novel methods for its control in food (Muchaamba et al., 2019).

During the emergence and manifestation of an infection, pathogenic microorganisms require nutritional support for development and replication by using the nutrients from hosts (Fleck et al., 2011). Variations in environmental factors including temperature, pH, osmolytes, and the availability of nutrients (carbon and nitrogen sources) may have an impact on the ability of pathogens to survive. For the formation of bioactive secondary metabolites, the ideal environmental conditions, including temperature, pH, and salinity, must be met; otherwise, production of bioactive secondary metabolites may fail or no growth may be seen (Akond et al., 2016). Under *in vitro* conditions, *G. boninense* grew better in growth media containing higher levels of sucrose (173 g/L), fructose (12.9 g/L), or both (Goh et al., 2013). In a different study, Peng et al. (2019) found that fructose and glucose were the best carbon sources for *G. boninense* mycelial growth, whereas ammonium citrate and ammonium nitrate were the best nitrogen sources. Furthermore, optimal conditions for *G. boninense* mycelial growth, as reported by Peng

et al. (2019), includes pH values between 4 and 5, humidity levels between 50% and 60%, and temperatures ranging from 25 to 32 °C . On the other hand, Nawawi and Ho (1990) reported that the ideal pH and temperature for *G. boninense* mycelial growth *in vitro* were 3.7–5.0 and 27–30 °C, respectively; however, their growth at 15 and 35 °C is critically hindered and impossible at 40 °C. All of the research described above were conducted using a conventional approach, which limits the metabolic diversity that can be studied within a specific microbe as opposed to the PMs system. Besides, little is known about the metabolic profile of the *G. boninense* isolate till now. As a result, metabolic profiling of *G. boninense* is required to provide a more comprehensive understanding of the pathogen's metabolic capabilities.

2.6 Aggressiveness of the Pathogen

The fitness of the individual pathogen genotypes in terms of transmission is primarily determined by two factors: virulence (pathogen's capacity to attack particular host genotypes) and aggressiveness (Burdon, 1987). Aggressiveness refers to a pathogen isolate's ability to infect a susceptible genotype to a greater extent than other isolates (Michalska et al., 2016). According to Wong et al. (2012), different species of *Ganoderma* display a range of traits and levels of aggression, owing to the high divergence of the genetic pool between distinct isolates (Kok et al., 2013; Midot et al., 2019; Wong et al., 2021; Bharudin et al., 2022). *Ganoderma boninense* genetic heterogeneity may result from the exchange of genetic material between isolates (outcrossing between isolates) over successive generations or between isolates from different geographic locations, with the pathogen potentially coming from the same species or closely related species (Miller et al., 1999; Pilotti, 2005; Zakaria et al., 2005). Pilotti (2005) revealed that *G. boninense* is heterothallic with a tetrapolar mating system that controls sexual reproduction, favouring outbreeding within a population and genetic variation in the same plantation region, resulting in

dynamic populations, which is the main cause of ineffective disease management. In Peninsular Malaysia, the aggressiveness of *G. boninense* isolates varied across the regions (Goh et al., 2014). Similarly, *Ganoderma* spp. in Betong, Balingian, and Miri, Sarawak also exhibits different levels of aggressiveness (Rakib et al., 2015; Lo et al., 2023). The variation in the aggressiveness of *Ganoderma* sp. isolates also reported in Indonesia (Breton et al., 2006) and Columbia (Castillo et al., 2022). For the development of efficient disease management strategies and the prediction of potential outbreaks for the sustainability of the oil palm industry in Sarawak, further research on the aggressiveness of *G. boninense* isolates from various divisions in Sarawak is required.

2.7 Factors for Development of Basal Stem Rot

2.7.1 Substrates, Inoculum Sizes and Inoculation Methods

In order to artificially establish basal stem rot (BSR) on oil palm seedlings, various substrates have been tested in the past to induce *Ganoderma* infection. For instance, wheat-oat medium (Lim et al., 1992), POPW medium (mixture of paddy and oil palm wood sawdust supplemented with sucrose, ammonium sulfate, calcium sulfate, and bacto peptone) (Idris et al., 2004), rubberwood blocks (Sariah et al., 1994; Breton et al., 2006; Rees et al., 2007; Kok et al., 2013), and *Ganoderma* mycelial suspension (Chong et al., 2012; Purnamasari et al., 2018). Among these substrates, *Ganoderma*-colonised rubberwood blocks (RWBs) (Figure 2.5) are still the most frequently used for infection study due to its effectiveness. Although mycelial suspension method for inducing *Ganoderma* infection shows promise; it still requires further optimisation and validation due to limited number of publications. Furthermore, this method might require the use of sterile soils to be effective.

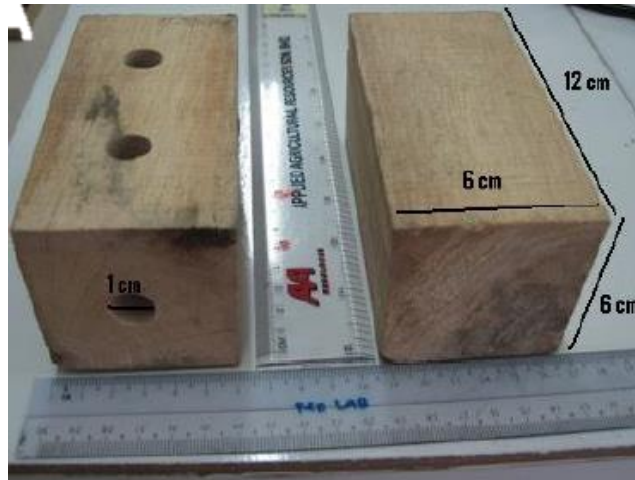


Figure 2.5: Rubberwood block: 12 × 6 × 6 cm (Kok et al., 2013)

Various sizes of RWB have been used for artificial inoculation: 3 × 3 × 3 cm³, 6 × 6 × 6 cm³, 6 × 3 × 3 cm³, 5 × 5 × 15 cm³, and 6 × 6 × 12 cm³ (Sariah et al., 1994; Breton et al., 2006; Rees et al., 2007). However, inoculation with *Ganoderma*-colonised RWBs of sizes 6 x 6 x 6, 6 x 3 x 3 and 6 x 6 x 12 cm³, has been reported as a successful substrate for supporting inoculum in the infection of oil palm seedlings (Rees et al., 2007). This approach has been adapted in the studies on aggressiveness of *Ganoderma* sp. (Kok et al., 2013; Goh et al., 2014; Rakib et al., 2015), transcriptome of oil palm roots infected with *G. boninense* (Tee et al., 2013), effects of incorporation of micronutrients into common compound fertiliser on BSR incidence and disease severity (Fabien et al., 2014) and the role of mineral nutrients against *Ganoderma* infections (Bivi et al., 2016).

Inoculation with *Ganoderma* mycelial suspension has recently gained popularity, and it is reported to be faster and more reliable than the rubberwood method in producing *Ganoderma* disease. Chong et al. (2012) conducted artificial inoculation by spraying *Ganoderma* suspension onto oil palm roots; however, it is unsure whether the oil palms infected using this technique will

develop common BSR symptoms when grown to maturity, as this was not determined in the study. Later, Purnamasari et al. (2018) were able to produce BSR symptoms such as necrotic leaves, severe wilting, and rotten stems, especially at the base, a week after inoculation by immersing oil palm roots in *Ganoderma* mycelial suspension for 30 minutes prior to replanting in sterile soil. Using sterile soil for infection studies, however, is impractical for large sample sizes. Furthermore, it did not reflect the field's environment, in which *Ganoderma* thrives. For this method to be effective and reliable, it certainly requires some improvements. As a result, rubberwood methods currently preferred for infection studies.

2.7.2 Shade

Shade had a substantial impact on BSR as evidenced by the fact that shaded seedlings manifested symptoms earlier and had higher levels of infection than exposed palms (Rees et al., 2007). Breton et al. (2006) found that disease kinetics were fastest under natural shade, while in the absence of shade, no symptoms emerged. Similarly, Rees et al. (2007) discovered that inoculated seedlings grown in the shade increase severity of the disease after eight months, but not seedlings exposed to the sun. This is in accordance with Nawawi and Ho (1990), who found that temperatures above 35 °C inhibited *Ganoderma* growth, whereas exposure to 45 °C for two days is lethal. This explains why *G. boninense* infections in plantations take a while to manifest because the temperature in exposed palms typically exceeds 40 °C. Initially, it was believed that BSR was a disease of senescent palms; however, fully grown canopies changed the environment (temperature, humidity, etc.) in a way that encouraged the accumulation of *Ganoderma* inoculum. Therefore, it is essential to incorporate artificial shade in the infection studies.

2.7.3 Planting Material

In the study of *Ganoderma* infection, several plant materials have been used, including germinated oil palm seeds and seedlings varying in age from two to twelve months, as well as one month old plantlets (Sariah et al., 1994; Idris et al., 2004; Breton et al., 2006; Rees et al., 2007; Kok et al., 2013; Goh et al., 2014; Goh et al., 2016). All were able to produce BSR symptoms, while younger seedlings will produce symptoms earlier; however, this depends on the size of the inoculum and the inoculation techniques used. Younger seedlings are desirable for faster disease induction because they are more susceptible to *G. boninense* infection in terms of disease incidence (DI), disease severity index (DSI), and vegetative growth measurement (VGM) (Goh et al., 2014).

2.8 Aggressiveness Assessment Parameters

2.8.1 Disease Incidence and Disease Severity Index

DI is the percentage of diseased plants in the samples regardless of their severity used for disease development assessment (Kranz, 1988), whereas DSI is the percentage of the host tissue or organ covered by symptoms that is quantified based on the external and internal disease symptoms scored according to a standardised disease scale (Breton et al., 2006). According to Kok et al. (2013), either one of the two parameters could be used to quantify *Ganoderma*'s level of aggressiveness due to the linear relationship between DI and DSI. For some diseases that are systemic, have low variation in severity levels within a sample unit, or have low severity levels, DI could be as informative as DSI (Seem, 1984; Kranz, 1988). Also, it might be possible to quantify DI and relate it to DSI if the correlation, linear regression, and nonlinear regression methods demonstrate that the association between DI and DSI is highly statistically significant (Seem, 1984). However, for some diseases, DI may be less informative and less precise than DSI

in terms of disease effects on plant growth and yield (Horsfall and Cowling, 1978; Seem, 1984). Furthermore, DI does not provide information about the severity caused by the disease. As a result, DSI is more suitable and reliable for assessing *Ganoderma* aggressiveness since it measures the severity of the disease to the host and takes into consideration aspects such as the intensity of the symptoms (e.g., lesion size). Nonetheless, the DI is essential for determining the rate of disease progression.

2.8.2 Physiological Aspects of an Infected Plant

Photosynthesis is the fundamental function of green plants: it allows them to convert light energy into chemical energy, which they can use in all cell functions. This process occurs in the chloroplast that contain a green substance called chlorophyll. During photosynthesis, plants use solar energy to generate ATP, NADPH, and carbohydrates (Lu and Yao, 2018). Many important compounds, such as primary metabolites, defence-related hormones, and antimicrobial compounds, are synthesised using these resources. When a pathogen infects a plant, it alters its nutrient availability, metabolism, and physiology. This frequently results in a reduction in a plant's growth (size or yield), fitness, and susceptibility to infection, and, in some cases, death (Burdon, 1987; Khankahdan et al., 2021; van Dijk et al., 2021).

Reduced growth and yields are common symptoms in plant that have been attacked by pathogen that degrade part of a plant's photosynthetic area, resulting in significantly reduced photosynthetic production (Agrios, 2005). *Ganoderma*-infected oil palm seedlings often exhibit stunted growth in relation to non-infected seedlings due to the extensive decay of the basal stem of the infected seedlings that restricts the water and nutrient uptake (Sapak et al., 2008; Chong et al., 2017). Water restrictions can limit photosynthesis efficiency due to thylakoid membrane damage and reduced chlorophyll content (Yang and Luo, 2021). Consequently, this will affect the

plant's ability to perform normal photosynthesis, disrupting plant growth and degenerating the oil palm tree's physical condition. All these effects lead to a decline in vegetative growth, photosynthesis rate, and chlorophyll content (Husin et al., 2020; van Dijk et al., 2021; Yang and Luo, 2021).

Parkash et al. (2021) studied the effect of cotton leafroll dwarf virus on physiological processes in cotton plants and found that the net photosynthesis and photochemical efficiency of the thylakoid reactions of symptomatic plants declined with stunted growth at advanced disease stages. Similarly, Rebitanim et al. (2020) discovered that *G. boninense*-infected oil palm seedlings without GanoCare® treatment also have a lower photosynthesis rate, including reduction in vegetative growth, and chlorophyll content. According to Rakib et al. (2019), chlorophyll content in *G. boninense*-infected oil palm seedlings declines at early phases of pathogenesis. A reduction in leaf chlorophyll content in inoculated oil palm plantlets also reported by Goh et al. (2016).

The growth of oil palm seedlings infected with different *G. boninense* isolates varies significantly. For example, seedlings infected with the most aggressive isolate showed much lower vegetative growth compared to those infected with the least aggressive isolates and the control group (Goh et al., 2014). The authors also observed varying rates of infection and symptom emergence depending on the isolates. Additionally, the study found that two-month-old oil palm seedlings were more responsive in terms of DSI with measured vegetative growth measurements (VGM) compared to older seedlings (five-month-old) (Goh et al., 2014). Furthermore, stunted growth in *G. boninense* infected oil palm seedlings result from extensive decay of the basal stem, limiting water and nutrient uptake (Sapak et al., 2008; Chong et al., 2017). A linear correlation between vegetative growth and the DSI of infected seedlings reported by Goh et al. (2014) also

indicates that vegetative growth could be used to differentiate the aggressiveness of *Ganoderma* isolates. As a result, the vegetative growth, photosynthesis rate, and chlorophyll content of infected plants may be used as an additional criterion for a more precise and reliable assessment of *Ganoderma* aggressiveness. Moreover, it is also essential to determine the relationship of seedling vegetative growth, photosynthesis rate, and chlorophyll content with the disease severity to improve understanding of plant-pathogen interaction and management approach.

2.8.3 *In Vitro* Growth Rate

In natural environments, the growth and dispersal of fungi vary among fungal genera, species, and strains (Knudsen and Stack, 1991). There are numerous approaches to measuring the *in vitro* growth rate in filamentous fungi; however, measurement of the radial expansion of the fungal colony on nutritional agar in a Petri dish is a frequently used direct method to quantify growth (Slowik et al., 2023). Typically, measurements are taken perpendicularly and can be an average of multiple pairs of measurements by either measuring using lines already drawn before adding the fungus plug or drawing them during assessing (Hendricks et al., 2017). The linear growth rate has been widely utilized in the study of *in vitro* growth of *G. boninense* on novel palm extract medium (Kok et al., 2013), media incorporated with various sugar compounds (Goh et al., 2013), and medium incorporated with industrial wood waste supplements (Alizadeh et al., 2013).

In plant pathology, the use of *in vitro* growth rate as a quantitative host-pathogen interaction indicator of aggression has been highly debated until recently (Zhan et al., 2016). Faster-growing pathogen strains are expected to cause more disease in the host. This was observed for pathogens such as *Ophiostoma ulmi* (Brasier and Webber, 1987), *Gnomonia leptosyla* (Belisario et al., 2008), *Alternaria brassicicola* (Thrall et al., 2005), and *Ceratocystis albifundus*

(Lee et al., 2015). However, no such correlation was found for *Gaeumannomyces graminis* (Irzykowska and Bocianowski, 2008) and *Microdochium nivale* (Brennan et al., 2003). This indicated that differences in the correlation between aggressiveness and *in vitro* growth could exist within the same host-pathogen system. For instance, *Plasmodium falciparum* isolates from Asia have been reported to have a positive correlation between virulence and multiplication rate in the human malaria system (Chotivanich et al., 2000), but the same isolates from Africa exhibit a negative correlation (Deans et al., 2006). This outcome can be attributed to variations in hosts immunity, in density and nutritive status of hosts and pathogens, regulatory mechanisms for pathogen invasiveness in particular host-pathogen interactions, or the quality and amount of phytotoxins that pathogens produce. Kok et al. (2013) found low linear correlation relationships between the mycelia growth rate of *G. boninense* on malt extract agar (MEA) and oil palm extract medium (OPEM) and degree of virulence (DI and DSI) among the *G. boninense* isolates; however, different *Ganoderma* isolates may exhibit different relationships of varying strength.

According to Alizadeh et al. (2013), the growth rate of *G. boninense* is influenced by both culture media and isolates. In Peninsular Malaysia, *G. boninense* grows better on medium incorporated with substances such as oil palm trunk sawdust (Kok et al., 2013), coconut trunk sawdust (Goh et al., 2013), and wood powder obtained from rubber or oil palm wood (Alizadeh et al., 2013), as compared to conventional media such as MEA and potato dextrose agar (PDA) under *in vitro* conditions. However, custom agar media preparation is more complex and prone to inconsistency in quality, which could affect the media's performance and introduce variation into experimental results. Furthermore, the substances used are also not readily available. Apart from culture media, environmental parameters, and pathogen species, the region from which the pathogen was isolated could also affect fungus growth rate. There is currently no data available on

the *in vitro* growth rate of Sarawak *G. boninense* isolates. Consequently, evaluating the *in vitro* growth rate of *G. boninense* from Sarawak is crucial to better predicting and designing responses to disease outbreaks interventions.

2.9 Disease Confirmation Approach in *Ganoderma* Infected Oil Palm Seedlings

In the past, reisolation on *Ganoderma* selective medium (GSM) was the commonly used approach to confirm disease in *Ganoderma*-infected oil palm seedlings. This method involves plating the diseased plant parts, such as the bole and roots, on the GSM (Idris et al., 2000a; Breton et al., 2006; Chan et al., 2011; Kok et al., 2013; Goh et al., 2014; Rakib et al., 2015). However, due to its semi-selective nature, other fungi could grow on it and outcompete the *G. boninense* growth, indicating that an alternative is needed. Lo et al. (2023) performed disease confirmation through reisolation on GSM, sequencing of internal transcribed spacer (ITS) region of DNA isolated from fungus isolated on GSM, and fungal DNA extracted from infected plant tissue and discovered that molecular identification of fungal DNA extracted from infected seedling tissues is the fastest and precise method. However, the comparison process for the disease confirmation approach was not described in detail by the author. Furthermore, disease confirmation via identification of fruiting bodies formed around the seedlings was not conducted.

The following primer sets have been developed for PCR-based confirmatory diagnostics for the detection of *Ganoderma* in infected tissues: Gan1 (5' TTG ACT GGG TTG TAG CTG 3') and Gan2 (5' GCG TTA CAT CGC AAT ACA 3') (Utomo and Niepold, 2000); GanET (5'GAGTTGTCCCAATAAC 3') and ITS3 (5' GCATCGATGAAGAACGCAGC 3') (Bridge et al., 2000); and PER44-123 and LR1 (Idris et al., 2003). Gan1/Gan2 primer pair were generated from the ITS region 1 of the rDNA of *G. boninense* and produced a PCR product of 167 bp in size

(Utomo and Niepold, 2000). The GanET/ITS3 primer pair was derived from the ITS region of *Ganoderma*, with an expected PCR product of 320 bp, where the ITS3 primer was designed to be universal for fungi, reducing the possibility of amplifying DNA from other organisms or the palm itself, and the specificity of the GanET primer ensuring that only oil-palm associated *Ganoderma* DNA was amplified (Bridge et al., 2000). Mandal et al. (2014) found that 320 bp fragment produced by the GanET/ITS3 primer pairs was more prominent than the 167 bp fragment produced by the Gan1/Gan2 primer pair. As for primer PER44-123, it was constructed from ITS region rDNA and used with LR1 primer to yield an approximately 580 bp product specific to *G. boninense* (Idris et al., 2003); however, the sequence was not publicly available.

CHAPTER 3

MATERIALS AND METHODS

3.1 Source of Isolates and Culture Condition

Six *G. boninense* isolates from this study were obtained from the Sarawak Tropical Peat Research Institute (STROPI) (Figure 3.1). The selection was based on the haplotype described by Midot et al. (2019) (Table 3.1). All the pure cultures were kept as stock cultures on malt extract agar (MEA) (Difco™, MD, USA) at 16 °C and in sterile tap water at room temperature (27 ± 1 °C) in the dark. The sterile tap water stock cultures of the *G. boninense* isolates were revived on MEA and incubated for nine days at 27 ± 1 °C in the dark. The revived *G. boninense* isolates were subsequently subcultured onto MEA plates and incubated under the same conditions. The second transfer of culture was used to prepare the *Ganoderma* inoculum.

Table 3.1: *Ganoderma boninense* isolates used in this study

No.	Isolate	Location	Haplotype	GPS Coordinates
1	BLSM5B	Sg. Meris, Balingian	GbHap1	N 02° 57' 51.7", E 112° 30' 28.8"
2	DR56	Daro	GbHap2	N 02° 29' 30.9", E 111° 32' 21.3"
3	BLSM5A	Sg. Meris, Balingian	GbHap3	N 02° 57' 51.7", E 112° 30' 28.8"
4	IGKI3	Igan, Kuala Igan	GbHap4	N 02° 46' 17.4", E 111° 43' 26.8"
5	BLSM4A	Sg. Meris, Balingian	GbHap6	N 02° 57' 53.1", E 112° 30' 30.0"
6	DR51B	Daro	GbHap7	N 02° 29' 02.6", E 111° 32' 53.3"

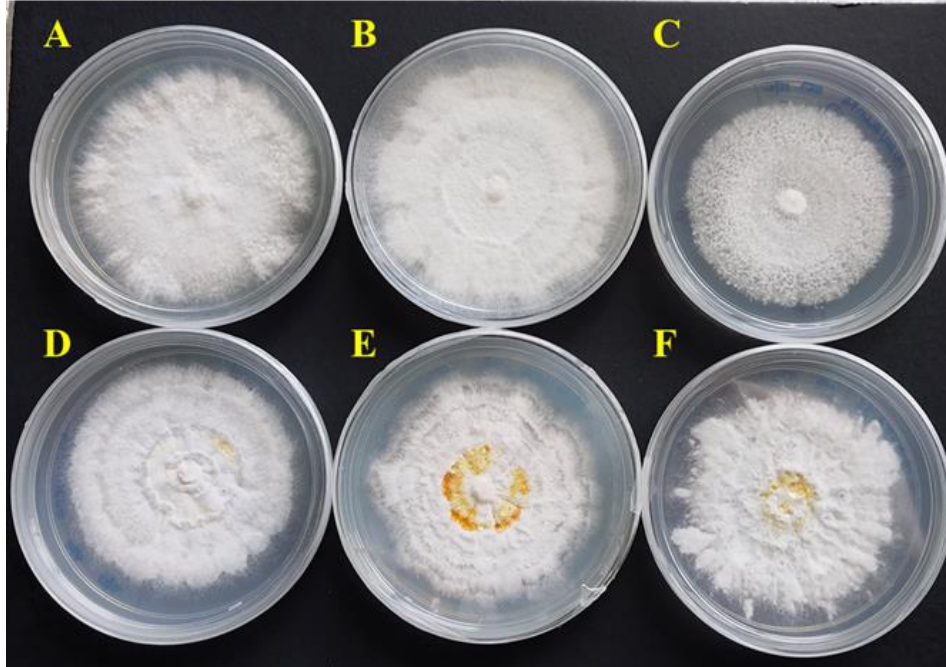


Figure 3.1: *Ganoderma boninense* isolates pure culture after nine day of incubation: (A) BLSM5A, (B) BLSM5B, (C) BLSM4A, (D) DR51B, (E) DR56, and (F) IGKI3

3.2 *Ganoderma* Inoculum Preparation

RWBs, with a dimension of 6 x 6 x 6 cm (Rebitanim et al., 2020) were cleaned and soaked overnight (Naher et al., 2012) in a plastic storage box containing ultra-pure water (UPW) before being autoclaved at 121°C for 45 minutes (15 psi). The sterilisation step was repeated three times. The extended duration of the temperature and repeated autoclaving process was to enhance the sterilisation process because it increases the total exposure time of the microorganisms to the lethal conditions of heat and pressure. Subsequently, each RWB was packed in a double-layered polypropylene (PP) plastic bag (18 x 25 cm) before adding 50 mL of malt extract broth (MEB). The PP plastic bag containing RWB and MEB were autoclaved at 121 °C for 20 minutes and allowed to cool to ambient temperature before being inverted to ensure that the MEB came into contact with all the RWB surfaces.

The entire full plate of a nine-day-old *G. boninense* pure culture grown on MEA was cut into small pieces of mycelial plugs using a scalpel. These mycelial plugs were then placed into a PP plastic bag containing autoclaved RWB and MEB. Then the PP plastic bag was inverted to ensure full contact between the mycelial plugs and all RWB surfaces. Subsequently, the inoculated RWB was incubated for 60 days at room temperature (ca. 27 ± 1 °C) in the dark to allow *G. boninense* mycelium to colonise the RWB (Rebitanim et al., 2020). Before incubation, the weight of each RWB was recorded. Throughout the 60-day incubation period, regular inspections were conducted twice a week to monitor both the growth of *G. boninense* and any potential contamination. After 60 days of incubation, the weight of each RWB was recorded once again. RWB with uniformly colonised mycelia (Figure 3.2) were selected as a source of inoculum (Turner, 1981).



Figure 3.2: Well colonised rubberwood block after 60 days of incubation

3.3 Oil Palm Seedlings Artificial Inoculation

The germinated oil palm seeds used in this study were Dura x Pisifera AA Hybrida IS (Figure 3.3), purchased from Applied Agricultural Resources Sdn. Bhd., Malaysia. Before sowing, the germinated seeds were evaluated for plumule and radicle damage, as well as fungal infection. All healthy germinated seeds were sown individually in polybags (5" × 8") filled with sieved topsoil. They were maintained in a net house under 70% shade and watered twice daily (early morning and late evening) with an equal amount of water (150 mL per seedling). Before artificial inoculation, the transplanting medium was prepared by sieving the topsoil, peat, and sand separately before being mixed in a 3:2:1 ratio, respectively (Sapak et al., 2008). For each polybag, the soil mixture was then pre-mixed with 10 grams of rock phosphate.

Prior to artificial inoculation, the vegetative growth measurement of two-month-old oil palm seedlings were also recorded to select seedlings with uniform growth. Only a healthy two-month-old seedlings with uniform growth were uprooted for artificial inoculation (Figure 3.4). One *Ganoderma*-colonised RWB was placed in each polybag (12" × 14") half-filled with the soil mixture of equal amount (Figure 3.5A). Subsequently, a two-month-old oil palm seedling was placed on top of the *Ganoderma*-colonised RWB as shown in Figure 3.5B (Kok et al., 2013; Goh et al., 2014; Rebitanim et al., 2020). The seedlings roots were then covered with the soil mixture and arranged in a randomised complete block design under 70% shade. Each isolate of *G. boninense* was inoculated to the oil palm seedlings with 10 replications of oil palm seedlings for each destructive sampling month (3-, 4-, 5-, and 6-months post inoculation). Seedlings without the RWB served as a control. A total of 280 seedlings were used in this study. The fertilisation program was conducted as per Table 3.2.



Figure 3.3: Germinated oil palm seeds (Dura × PISOfera AA Hybrida IS)



Figure 3.4: Healthy two months old oil palm seedlings

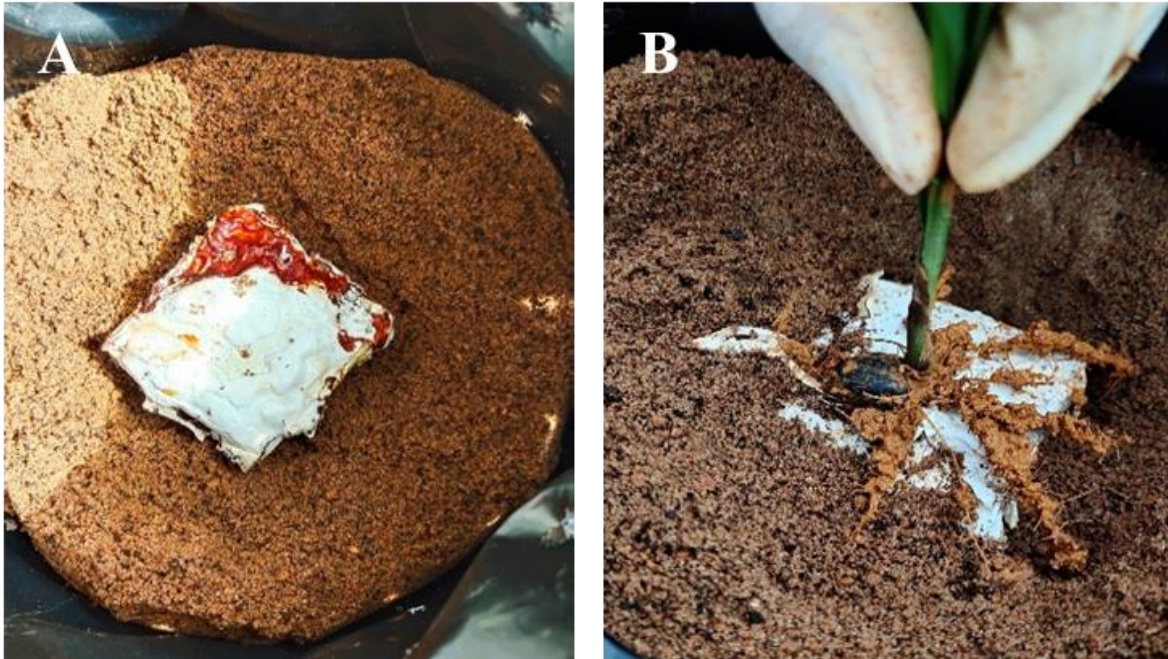


Figure 3.5: (A) *Ganoderma*-colonised rubber wood block in a polybag half-filled with transplanting medium. (B) Artificial inoculation of oil palm seedlings

Table 3.2: Fertilisation program used in this study (Heriansyah and Tan, 2005)

Seedling Age		Fertilisation Schedule		
Week	Month	Duration	Fertiliser	Rate
1 – 4	1		No fertiliser until one complete new leaf appears	
5 – 8	2	Weekly (drench)	Grofas kuning soluble foliar fertiliser (22:22:10:1 formulation)	15 g in 4 L water per 100 seedlings at 40 mL per seedling
9 – 12	3	Transplanting		
		Weekly (drench)	Grofas kuning soluble foliar fertiliser (22:22:10:1 formulation)	15 g in 4 L water per 25 seedlings at 160 mL per seedling
13 – 16	4	Weekly (drench)	Grofas kuning soluble foliar fertiliser (22:22:10:1 formulation)	15 g in 4 L water per 25 seedlings at 160 mL per seedling

Table 3.2 continued

20	5	Weekly (drench)	Grofas kuning soluble foliar fertiliser (22:22:10:1 formulation) *For chlorotic seedling only	15 g in 4 L water per 25 seedlings at 160 mL per seedling
		Once (solid)	Compound CCM 45 (12:12:17:2+B+TE)	5 g per seedling
		Once (drench)	High Grade Fine Borate (HGBF 48)	1 g per 10 L for <7 months old seedling at 500 mL per seedling
24	6	Once	Compound CCM 45 (12:12:17:2+B+TE)	10 g per seedling
		Once	Kieserite	10 g per seedling

3.4 Characterisation of *Ganoderma boninense* Isolates

3.4.1 Aggressiveness Level

3.4.1.1 Vegetative Growth Measurement

After transplanting, the seedlings' stems were marked at 1 cm above the soil level as a reference point throughout the study (Figure 3.6). The vegetative growth parameters measured include seedling height (H, cm), bole size (BS, cm), number of leaves (NOL), leaf area (LA, cm²), and fresh root mass (FRM, g) (Table 3.3). Monthly recordings of these parameters were carried out before each destructive sampling.

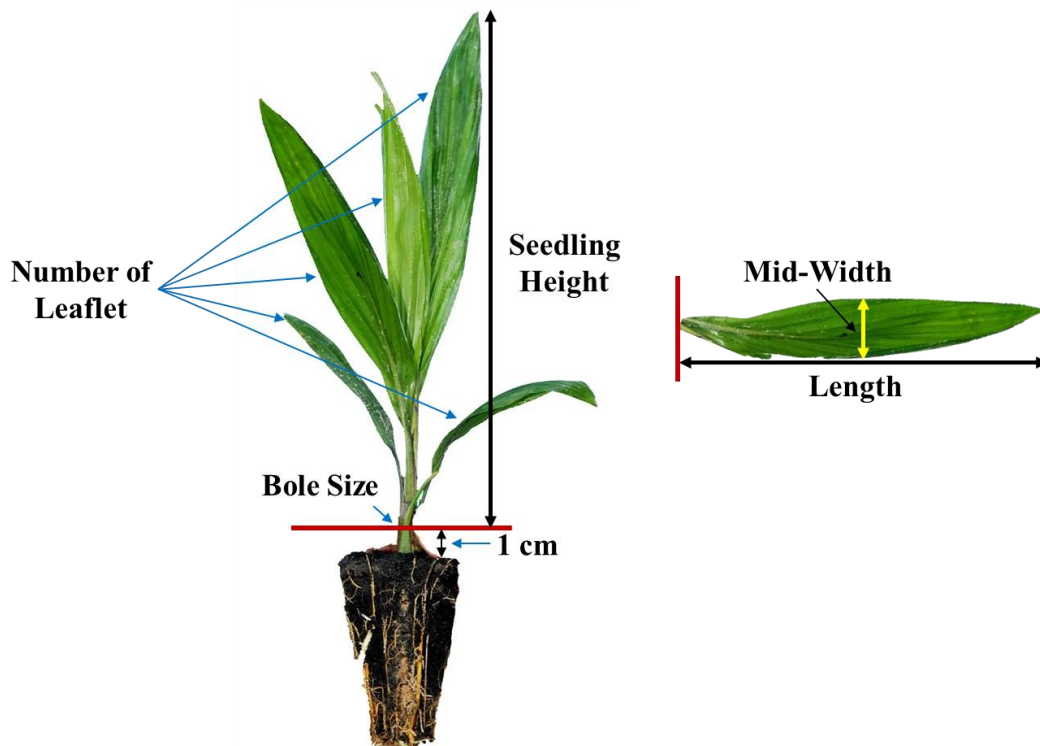


Figure 3.6: Vegetative growth measurements of oil palm seedlings

Table 3.3: Vegetative growth parameters measured in this study and the measuring procedure

No.	Parameter	Procedure
1.	Heigh, H	Measured from the base of the stem (marked) to the longest leaf tip, as illustrated in Figure 3.6.
2.	Bole size, BS	Measured at 1 cm above the soil level (marked) using a digital calliper.
3.	Number of leaves, NOL	Count all the healthy leaflet except for necrotic leaflet.
4.	Leaf area, LA	<p>Estimate using formula by (Corley et al., 1971):</p> $LA = b \times (nlw) \quad \text{Equation 3.1}$ <p>b = correction factor (0.57)</p> <p>n = number of leaflets</p> <p>lw = mean of length \times mid-width (cm) of the largest leaflet</p>
5.	Fresh root mass, FRM	Separated at the base of the bole (Figure 3.7), cleaned, and patted dry with tissue paper before weighing.



Figure 3.7: The root of the seedlings were cut at the base of the bole (blue line) for fresh root mass measurement

3.4.1.2 Chlorophyll Content

The chlorophyll content of the oil palm seedlings was measured with a SPAD chlorophyll meter (SPAD-502Plus, Konica Minolta, Japan) (Rakib et al., 2019; Rebitanim et al., 2020; Aziz et al., 2021). Five seedlings representative of each treatment were chosen randomly for chlorophyll content measurement at three, four, five, and six months after artificial inoculation. All measurements were consistently taken at the centre of the third lanceolate or bifurcate leaf of the same set of seedlings.

3.4.1.3 Photosynthetic Rate

The photosynthetic rate (A) of oil palm seedlings was measured using a portable photosynthesis system (LI-6800F, LI-COR Inc., USA), as in the Figure 3.8 (Rebitanim et al., 2020). The measurement of net A of the oil palm seedlings was taken at the same set of seedlings and same leaf as those that were used to determine the chlorophyll content at three, four, five-, and

six-months post-inoculation. Prior to the measurement, the third lanceolate or bifurcate leaf of the seedling was wiped with a clean cloth to remove dirt on the leaf surface. The leaf chamber environment tab was configured according to the user manual, as outlined in Table 3.4. The time of measurement taken was consistently between 14.30 and 16.45.



Figure 3.8: LI-6800F portable photosynthesis system (LI-COR Inc., USA).

Table 3.4: The leaf chamber setpoint

Environment Tab	Setpoint
Relative Humidity	65%
Fan Speed	10,000 rpm
CO ₂	400 $\mu\text{mol mol}^{-1}$
Flow Control	700 $\mu\text{mol s}^{-1}$
Txchg	33 °C
Fluorometer	600 $\mu\text{mol m}^{-2} \text{s}^{-1}$

3.4.1.4 Disease Assessment

All the signs (e.g., white mycelium and basidiocarp) and symptoms (necrotic and chlorotic leaves) observed throughout the study were recorded for aggressiveness assessment. During destructive sampling, internal symptoms such as the number of necrotic primary roots and a visual estimation of the proportion of necrotic bole tissue were recorded (Breton et al., 2006). The percentage of necrotic primary roots, leaves, and bole were calculated using Equation 3.2 and Equation 3.3, respectively.

$$\begin{aligned} & \text{\% Necrotic primary root} && \text{Equation 3.2} \\ & = \left(\frac{\text{Number of necrotic primary root or leave}}{\text{Total number of primary root}} \right) \times 100 \end{aligned}$$

$$\text{\% Necrotic bole} = \left(\frac{\text{Necrotic bole tissue area}}{\text{Total bole tissue area}} \right) \times 100 \quad \text{Equation 3.3}$$

The disease severity index (DSI, %) was scored based on disease class adapted from Lo et al. (2023) (Table 3.5). The DSI was measured by the proportion of host tissue or organ covered by symptoms and calculated using Equation 3.4 (Liu et al., 1995). Whereas disease incidence (DI, %) was determined by the proportion of infected plants in the sample, regardless of their severity (Kranz, 1988), and calculated using Equation 3.5 (Campbell and Madden, 1990). The aggressiveness of *G. boninense* isolates was grouped based on the classification by Lo et al. (2023) (Table 3.6).

$$\text{DSI} = \left(\frac{\text{Number of plants in the rating} \times \text{rating number}}{\text{Total number of plants} \times \text{highest rating}} \right) \times 100 \quad \text{Equation 3.4}$$

$$DI = \left(\frac{\text{Number of seedlings identified as diseased}}{\text{Number of seedlings per treatment set}} \right) \times 100 \quad \text{Equation 3.5}$$

Table 3.5: Disease class value, signs and symptoms for disease severity index scoring (Lo et al., 2023)

Disease Class Value	Signs and Symptoms on Oil Palm Seedling
0	Healthy seedlings with green leaves/healthy bole tissue/root tissue without appearance of fungal mycelium on any part of plants
1	Presence of fungal mycelium or basidiocarp on any parts of plants without necrosis or chlorosis leaves/rotting of bole/root tissue
2	Presence of fungal mycelium or basidiocarp on any parts of plants with rotting of necrosis or chlorosis leaves/rotting of bole/root tissue (>1%<10%)
3	Presence of fungal mycelium or basidiocarp on any parts of plants with necrosis or chlorosis leaves/rotting of bole/root tissue (>10%<25%)
4	Presence of fungal mycelium or basidiocarp on any parts of plants with necrosis or chlorosis leaves/rotting of bole/root tissue (>25%<75%)
5	Presence of fungal mycelium or basidiocarp on any parts of plants with necrosis or chlorosis leaves/rotting of bole/root tissue (>75%) or seedling dead

Table 3.6: *Ganoderma boninense* aggressiveness level classification (Lo et al., 2023)

Aggressiveness Level	Disease Severity Index (%)
Highly Aggressive	>81
Moderately Aggressive	40 to 80
Less Aggressive	21 to 40
Least Aggressive	0 to 20

3.4.1.5 *In Vitro* Growth Rate

Three different microbiological media were used to determine the *in vitro* growth rates (IVGR) of the *G. boninense* isolates: potato dextrose agar (PDA, HiMedia, Mumbai, India), malt extract agar (MEA, Difco™, MD, USA), and sabouraud dextrose agar (SDA) [peptone 10 g/L (Oxoid, Hampshire, England), D-Glucose 40 g/L (Merck, Darmstadt, Germany), and microbiology agar 15 g/L (Merck, Darmstadt, Germany)]. These media are widely used in fungal cultivation due to their ability to support the growth and development of a broad range of fungal species. Each isolate was subcultured in five replicates on each medium (PDA, MEA, and SDA) in 90 mm Petri dishes. Eight millimetres of mycelial plug were then cut from actively growing mycelia (the margin of nine-day-old cultures) and subcultured in the centre of the Petri dishes. The Petri dishes were double-sealed with Parafilm and incubated at 27 ± 1 °C in the dark for eight days. Radial increments of the fungal mycelium were measured daily at four different points along two perpendicular lines until all five replicate cultures within one treatment had reached the edge of the Petri dishes. The IVGR of the *G. boninense* isolates was calculated using Equation 3.6. Subsequently, the IVGR of the original culture stock of *G. boninense* isolates (BLSM5B, DR56,

DR51B, IGKI3, BLSM4A, and BLSM5A) revived from culture stocks was also compared to the IVGR of the same confirmed *G. boninense* isolates reisolated from the fruiting body (representative of each isolate) in this study. Similarly, each isolate was subcultured in five replicates on MEA, , the most common medium used for growing *G. boninense*.

$$\text{IVGR} = \frac{\text{Maximum radial length (cm)}}{\text{Number of days of incubation}} \quad \text{Equation 3.6}$$

3.4.2 Statistical Analyses: Aggressiveness Assessment

The Shapiro-Wilk test was used to assess data normality. Analysis of variance (ANOVA) was used to determine significant differences in normally distributed data, followed by Tukey's test at the 0.05 significance level. For non-normally distributed data, the Kruskal-Wallis test was utilized, followed by multiple comparisons at the 0.05 significance level with the function Kruskal in the package agricolae (Mendiburu and Yaseen, 2020). Spearman's rank correlation coefficient (r_s) was employed for correlation between the disease severity index and eight parameters, namely NOL, H, LA, BS, FRM, leaf photosynthetic rate, chlorophyll content, and IVGR. All tests and analyses were performed using the RStudio (Version 1.4.1106) software (R Core Team, 2021).

3.4.3 Substrate Utilisation Profile

After assessing the aggressiveness of the *G. boninense* isolates, the most and least aggressive isolates were selected for substrate utilisation characterisation using a biolog phenotypic microarray system. Ten microplates were used to characterise the substrate utilisation of the isolates: PM1 to PM10 (Table 3.7). The differences in metabolic properties between the most and least aggressive *G. boninense* isolates were also investigated. Pure cultures of the isolates

were sent to Focus Biotech Sdn. Bhd. for phenotypic microarray analysis. The experiment was conducted three times.

Table 3.7: Phenotype microarray plates

No.	Plate	Substrate
1	PM1 & 2	Carbon Sources
3	PM3	Nitrogen Sources
4	PM4	Phosphorus and Sulfur Sources
5	PM5	Nutrient Supplements
6	PM6, 7, & 8	Peptide Nitrogen Sources
9	PM9	Osmolytes
10	PM10	pH

3.4.4 Statistical Analyses: Substrate Utilisation Profile

The metabolic performance of the most and least aggressive *G. boninense* isolates was determined based on the area under the kinetic curve of dye formation. To score growth in the various PM conditions, the product of the average area and the average slope of the time course data of each well was calculated, followed by Z normalization. Multiplication by the average slope ensured that only wells displaying an increasing signal and a sufficient total area represent a “metabolically active” growth condition (Biondi et al., 2009). For PM 9-10 and PM 1-8, distinct threshold values were established, specifically 6,000 and 1,000, respectively. The well was scored as “metabolized by the isolate” if the product exceeded the threshold value. Z-scores greater than

1 were weighted as “effectively metabolized by the isolate”. However, any well that surpassed these threshold value but exhibiting a negative slope or a flat slope with minimal change in the signal over time and those less than threshold value was scored as “could not be metabolized by the isolate”. For the comparative phenotypic microarray profiles of the most and least aggressive *G. boninense* isolates, the analyses were performed by Focus Biotech Sdn. Bhd. using Biolog Phenotypic Microarray Data Analysis software v1.7.

3.5 Disease Confirmation Methods

3.5.1 Re-isolation from Infected Tissue

Ganoderma selective medium (GSM) was prepared earlier before re-isolation, as described in Table 3.8 (Ariffin and Idris, 1992). During the destructive sampling, ten oil palm seedlings from each treatment were uprooted. The soil around the roots was carefully removed and then cleaned under running tap water to remove excess soil particles. The uprooted seedlings were then separated into roots and bole. The bole was cut into approximately 5-6 cm in length from the bole base and then cut again into two parts, as shown in Figure 3.9.

Table 3.8: Composition of *Ganoderma* selective medium

PART A (900 mL) ^[1]	
Composition	Amount
Bacto™ Peptone (Difco™, MD, USA)	5.00 g
Bacto™ Agar (Difco™, MD, USA)	20.00 g

Table 3.8 continued

Magnesium Sulfate Heptahydrate, $\text{MgSO}_4 \cdot 7\text{H}_2\text{O}$	0.25 g
(Amresco, Solon, Ohio)	
Dipotassium Hydrogen Orthophosphate, K_2HPO_4	0.50 g
(Univar, NSW, Australia)	
Ultra-Pure Water	Top up to 900.00 mL
PART B (100 mL)^[2]	
Streptomycin Sulfate (Duchefa, Haarlem, The Netherlands)	0.30 g
Chloramphenicol (Duchefa, Haarlem, The Netherlands)	0.10 g
Pentachloronitrobenzene, PCNB (Merck, Darmstadt, Germany)	0.29 g
Sensor™ 25 WP	0.13 g
Ethanol 70% (HmbG® Chemicals, Germany)	20.00 mL
Lactic Acid 85% (Sigma-Aldrich, MO, USA)	1.25 mL
Benlate T-20	0.15 g
Tannic Acid (Sigma-Aldrich, MO, USA)	1.25 g
Ultra-Pure Water	Top up to 100.00 mL

^[1] Firstly, the mixture for part A was stirred on a hot plate before being autoclaved at 121 °C for 15 minutes and allowed to cool to approximately 50 °C before mixing with mixture of part B.

^[2] The mixture of part B, on the other hand, was stirred constantly at room temperature (2–3 hours) until completely dissolved and then filtered-sterilised with a 0.2 µM syringe filter (Pall, Portsmouth, UK) before being added to part A. Lastly, combine part A and B, swirled to ensure thorough mixing, and then pour into petri dishes.



Figure 3.9: Oil palm seedling bole cut into halves

Prior to surface sterilisation, two to three drops of wetting agent TWEEN® 80 (Merck, Darmstadt, Germany), were added to two sterilants: 10% commercial bleach (Clorox®, Malaysia) containing 5% sodium hypochlorite and 70% ethanol (HmbG® Chemicals, Hamburg, Germany) to allow better surface contact. Two-step surface sterilisation was carried out by immersing the roots and bole (before being cut into halves) in a 500 mL beaker containing 10% commercial bleach for 10 minutes, followed by 5 minutes in 70% ethanol. The beaker containing the roots, bole, and sterilant was swirled during the surface sterilisation. Three consecutive changes of ultra-pure water (UPW) were used to rinse the bole and roots. The bole and roots were then placed in a beaker containing UPW. Blotted dry bole and roots were immersed in absolute ethanol (HmbG® Chemicals, Hamburg, Germany) and then quickly flamed before being sliced into medium-sized pieces (approximately 1–2 cm) and subcultured on a GSM plate (embedded in the agar). The GSM plates were incubated in an incubator at 27 ± 1 °C until white mycelium grew from the bole or root tissue. The white mycelium that grew around the infected tissue that produce brown pigmentation

on GSM was subcultured onto MEA, and its colony morphology was compared to that of the *G. boninense* pure culture for pathogen confirmation.

3.5.2 Re-isolation from Fruiting Body

The fruiting body that formed around the oil palm seedlings was harvested during destructive samplings (Figure 3.10). A clean tissue was used to wipe dirt from the outer surface of the fruiting body. Surface sterilisation of the outer surface of the fruiting body was carried out using tissue paper that had been sprayed with 70% ethanol. Using a sterilised scalpel, the fruiting body was dissected and cut into medium-sized pieces (approximately 1–2 cm) and subcultured on a GSM plate with the soft internal tissue embedded in the agar. The incubation conditions were similar to those for the bole and roots (27 ± 1 °C). The white mycelium that grew around the fruiting body on GSM was then subcultured onto MEA, and its colony morphology was compared to that of the *G. boninense* pure culture for pathogen confirmation.



Figure 3.10: The fruiting body grew around the artificially inoculated seedling

3.5.3 Molecular Identification

3.5.3.1 Fungal DNA Extracted from Fungi Isolated from the Bole and Root Tissue on *Ganoderma* Selective Medium

Fungal mycelia liquid cultures were prepared by scraping the active growing fungal mycelia grown on MEA with a sterile scalpel. Subsequently, these mycelia were inoculated into a 200 mL conical flask containing autoclaved malt extract broth (MEB). Conical flask containing MEB and fungal mycelia was then incubated for 6–7 days at 27 ± 1 °C in an incubated shaker (SI-600R, Jeio Tech, Korea) at 180 rpm. The resulting cultured fungal mycelia formed in the conical flask were harvested by filtration through a sterilised strainer (Figure 3.11). Following that, the fungal mycelia were rinsed with 2× phosphate buffered saline (PBS) by diluting 10× PBS (prepared as described in Appendix 1) with sterile UPW and kept in a 50 mL Falcon tube before being stored at -80 °C in an ultra-low temperature freezer (MDF-DU900V, Panasonic, Japan) prior to DNA extraction.



Figure 3.11: Fungal mycelia liquid culture in malt extract broth

A CTAB method modified by Voigt et al. (1999) was employed for DNA extraction of fungi isolated from bole and root tissue on GSM. Prior to the lysis step, the fungal mycelia were placed in a mortar containing liquid nitrogen and ground to a fine powder with a pestle. The ground samples were then transferred into a 50 mL Falcon tube containing 15 mL of CTAB buffer, mixed thoroughly, and incubated in a shaking water bath (BS-31, Jeio Tech, Korea) for 30 minutes at 65 °C. The composition of the CTAB buffer is presented in Table 3.9.

Table 3.9: Composition of CTAB buffer

Composition	Working Concentration	Amount
1 M Tris(hydroxymethyl) aminomethane hydrochloride, Tris-HCl, pH 8 (Vivantis, Selangor, Malaysia) ^[1]	100 mM	10.00 mL
0.5 M Diaminoethanetetra Acetic Acid Disodium Salt, EDTA, pH 8 (Acros Organics, Geel, Belgium) ^[2]	20 mM	4.00 mL
5 M Sodium Chloride, NaCl (Fisher, Leicestershire, UK) ^[3]	1.4 M	28.00 mL
Cetyltrimethylammonium Bromide, CTAB (Acros Organics, Geel, Belgium)	2% w/v	2.00 g
Polyvinylpyrrolidone, PVP (Bio Basic Canada Inc., Ontario, Canada)		0.08 g

Table 3.9 continued

Dithiothreitol, DTT	0.10 g
(Thermo Scientific, Vilnius, Lithuania)	
Sterilised Ultra-Pure Water, UPW	Top up to 100 mL

^[1] 80 mL of UPW was added to 12.11 g of Tris base and stirred until fully dissolved. The pH was then adjusted with 37% hydrochloric acid (Fisher, Leicestershire, UK) and topped-up with UPW to 100 mL when the pH reached 8.

^[2] 18.61 g of EDTA salt was added to 80 mL of UPW and stirred vigorously. Subsequently, adjust the pH with sodium hydroxide, NaOH (Merk, Darmstadt, Germany) pellets until the solution pH reached 7, then slowly add 5 M NaOH solution until the pH rose to 8. The EDTA salt will not dissolve until the pH is near 8. Lastly, top up the solution to 100 mL with UPW, followed by filter-sterilised and autoclaving at 121 °C for 15 minutes.

^[3] 29.2 g of NaCl was added to 80 mL of UPW and stirred until fully dissolved. Then, top up the solution to 100 mL with UPW, followed by autoclaving at 121 °C for 15 minutes. Finally, combine all the composition of CTAB buffer in a sterilised 100 mL Schott bottle according to the amount specified in Table 3.9, stir with sterilised stirrer until dissolves and top up with sterile UPW.

Note: CTAB buffer must be freshly prepared before used.

After incubation, a three-quarter volume of chloroform (Avantor, Gliwice, Poland) was added to the lysis buffer containing grounded materials and inverted for 15 minutes (20 rpm) using an overhead shaker (IKA® Trayster basic, IKA-Werke GmbH & Co. KG, Germany). Then, the mixture was centrifuged at $7000 \times g$ for 10 minutes in a refrigerated centrifuge (5430R, Eppendorf, Germany). The supernatant was carefully transferred (10–15 mL, approximately) to a new 50 mL Falcon tube. Then, two volumes of ice-cold absolute ethanol (HmbG® Chemicals, Hamburg, Germany) were added to the aqueous solution, which was then inverted gently for three times. Subsequently, the mixture was incubated overnight at 4 °C in a cold room. The following day, the visible DNA strands (Figure 3.12) were harvested and transferred into a 2 mL microcentrifuge

tube. To separate the excess liquid from the DNA strands, centrifugation on a refrigerated microcentrifuge (Mikro 200R, Hettich, Germany) at $14,000 \times g$ for 1 minute was performed. The excess liquid was then aspirated using a pipette and discarded. This step was repeated until there was no excess liquid left.

After removal of excess liquid, Tris-EDTA (TE) buffer (500 μL) was then added to the DNA pellet, followed by the addition of 2 μL of 10 mg/mL RNase A. On a thermomixer (Thermomixer comfort, Eppendorf, Germany), the suspension was incubated at 65 °C for 1 hour. The suspension was kept at 4 °C until the DNA completely dissolved and later stored at -20 °C for long term storage. The quality, yield, and integrity of the DNA were assessed using a NanoPhotometer® (P360, Implen GmbH, Germany) and by electrophoresis on a 1% agarose gel at 90 V for 35 minutes together with 1 kb DNA ladder (Vivantis, Selangor, Malaysia). The agarose gel was then stained with ethidium bromide (EtBr) (Merck, Darmstadt, Germany). Following that, the agarose gel was viewed on a molecular imager (Universal Hood II, Bio-Rad, USA) for quality, yield, and integrity assessment.

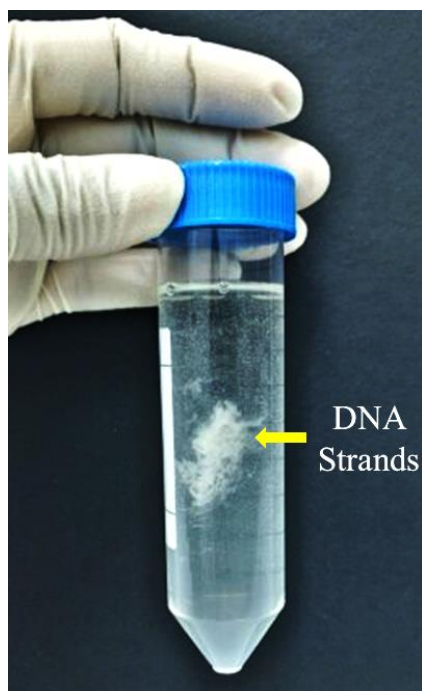


Figure 3.12: Visible fungal DNA strands formed after being incubated overnight at 4°C in a cold room

The primer sets (ITS1, 5' -TCCGTAGGTGAACCTGCGG-3') and (ITS4, 5' -TCCTCCGCTTATTGATATGC-3') were used to amplify an approximately 650 bp DNA fragment of the ITS region (White et al., 1990). The components of the PCR reaction mixture used are shown in Table 3.10. PCR was performed on a thermal cycler (Mastercycler Nexus GX2, Eppendorf, Germany) using the following protocol: initial denaturation at 95 °C for 2 minutes; 35 cycles of denaturation at 95 °C for 1 minute; annealing at 51 °C for 30 seconds; extension at 72 °C for 30 seconds; and a final extension at 72 °C for 5 minutes.

Table 3.10: The components of PCR reaction mixture

Reagent	Final Concentration
Colourless Buffer (GoTaq® Flexi, Promega, USA)	1×
Magnesium Chloride, MgCl ₂ (GoTaq® Flexi, Promega, USA)	2 mM
dNTP Mix (Vivantis, Selangor Malaysia)	0.2 mM
Bovin Serum Albumin (Acros Organics, Geel, Belgium)	0.16 mg/mL
Forward Primer	0.5 μM
Reverse Primer	0.5 μM
DNA Polymerase (GoTaq® Flexi, Promega, USA)	0.025 U
DNA Template	1 ng/μL

The quality, yield, and integrity of the PCR product were assessed using a NanoPhotometer® (P360, Implen GmbH, Germany) and by electrophoresis on a 2% agarose gel at 90 V for 35 minutes together with 100 bp DNA ladder (Thermo Scientific, MA, USA). The agarose gel was then stained with ethidium bromide (EtBr) (Merck, Darmstadt, Germany). Following that, the agarose gel was viewed on a molecular imager (Universal Hood II, Bio-Rad, USA) for quality, yield, and integrity assessment. The amplified products were sent to a commercial sequencing service (Next Gene Scientific Sdn. Bhd., Malaysia). Identification of the fungi was based on Basic Local Alignment Search Tool (BLAST) searches of ITS sequences against those of deposited ITS sequences in GenBank (National Centre for Biotechnology Information, NCBI).

3.5.3.2 Fungal DNA Isolated from Fruiting Bodies on *Ganoderma* Selective Medium

The fungal DNA isolation, PCR, and sequencing was performed using the method described in section 3.5.3.1.

3.5.3.3 Fungal DNA Isolated from Bole and Root Tissue

For sample preparation, the bole and root tissue oil palm seedling were sliced into small pieces (0.5–1 cm) and placed in a separate mortar containing liquid nitrogen and ground to a fine powder with a pestle. Then, the DNA isolation was performed using the method described in section 3.5.3.1. Screening of the fungal DNA recovered from inoculated and uninoculated (control) oil palm seedling tissue (bole and root) was carried out with *Ganoderma*-specific primers GanET (5'-GAGTTGTCCCAATAAC-3') and ITS3 (5'-GCATCGATGAAGAACGCAGC-3') (Bridge et al., 2000). The PCR protocol for this primer set was the same as described in section 3.5.3.1. The expected PCR product was 320 bp. Subsequently, the fungal DNA that produced a PCR product of 320 bp was amplified with the ITS1/ITS4 primer pair for identification using the methods described in section 3.5.3.1.

CHAPTER 4

RESULTS

4.1 Characterisation of *Ganoderma boninense* Isolates

4.1.1 Aggressiveness Levels

4.1.1.1 Vegetative Growth Measurements of Oil Palm Seedlings

i. Height

There was an increase in the height (H) of both *G. boninense*-inoculated and uninoculated (control) oil palm seedlings during the study period (Figure 4.1). Three months after inoculation, the seedlings inoculated with isolates BLSM4A, BLSM5A, DR51B, and BLSM5B (39.47 cm, 39.55 cm, 40.22 cm, and 40.15 cm, respectively) were significantly shorter than that of the control seedlings (45.94 cm; $p < 0.05$). However, there was no significant difference in H of seedlings inoculated with isolates DR56 and IGKI3 (42.98 cm and 40.71 cm, respectively) compared to the control (45.94 cm; $p > 0.05$). Overall, there was no significant difference in H among all the inoculated seedlings three months after inoculation: DR56, IGKI3, BLSM4A, BLSM5A, DR51B, and BLSM5B (42.98 cm, 40.71 cm, 39.47 cm, 39.55 cm, 40.22 cm, and 40.15 cm, respectively; $p > 0.05$). After four months post-inoculation, the H of oil palm seedlings inoculated with IGKI3, BLSM4A, BLSM5A, DR51B, and BLSM5B was significantly shorter (46.45 cm, 44.79 cm, 42.67 cm, 45.18 cm, and 45.21 cm, respectively) compared to the control (57.38 cm; $p < 0.05$). However, there was no significant difference between the H of seedlings inoculated with isolate DR56 (56.26 cm) and the control (57.38 cm; $p > 0.05$).

Five months after inoculation, the seedlings inoculated with isolates IGKI3, BLSM4A, BLSM5A, DR51B, and BLSM5B were significantly shorter (53.99 cm, 53.40 cm, 50.04 cm,

49.05cm, and 48.09 cm, respectively) than those in the control (65.32 cm; $p < 0.05$). However, there was no significant difference between the H of seedlings inoculated with isolate DR56 (64 cm) and the control (65.32 cm; $p > 0.05$). There was also no significant difference in H between seedlings inoculated with isolate DR56 (64 cm) and IGKI3 (53.99 cm; $p > 0.05$). Similarly, there was no significant difference in H among seedlings inoculated with isolate IGKI3, BLSM4A, BLSM5A, DR51B, and BLSM5B (53.99 cm, 53.40 cm, 50.04 cm, 49.05 cm, and 48.09 cm, respectively; $p > 0.05$).

After six months post-inoculation, the H of seedlings inoculated with isolates IGKI3, BLSM4A, BLSM5A, DR51B and BLSM5B was significantly shorter (61.05 cm, 61.85 cm, 61.93, 59.63 cm and 50.95 cm, respectively) compared to the control (78.45 cm; $p < 0.05$). However, there was no significant difference in H between seedlings inoculated with isolate DR56 (73.45 cm) and the control (78.45 cm; $p > 0.05$). Additionally, there was no significant difference among the seedlings inoculated with isolates DR56, IGKI3, BLSM4A, and BLSM5A (73.45 cm, 61.05 cm, 61.85 cm, and 61.93 cm, respectively; $p > 0.05$). Similarly, there was no significant difference in H among seedlings inoculated with isolate IGKI3, BLSM4A, BLSM5A, DR51B, and BLSM5B (53.99 cm, 53.40 cm, 50.04 cm, 49.05 cm, and 48.09 cm, respectively; $p > 0.05$).

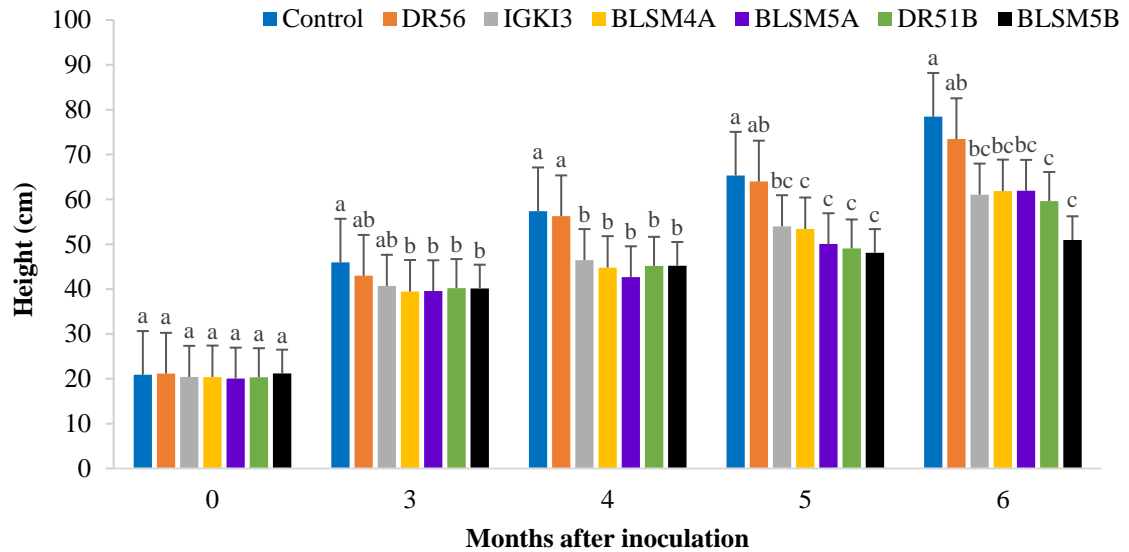


Figure 4.1: The height of the oil palm seedlings at 0, 3, 4, 5, and 6 months after inoculation. The means follow by the same letter per respective month, indicating no significant difference at 0.05 significance level. Error bars represent the standard error of the mean

ii. Bole Size

Overall, the bole size (BS) of the inoculated and control oil palm seedlings increased over time. There was no significant difference in the BS between seedlings treated with different isolates of *G. boninense* when compared to those of the control group throughout the study ($p > 0.05$) (Figure 4.2).

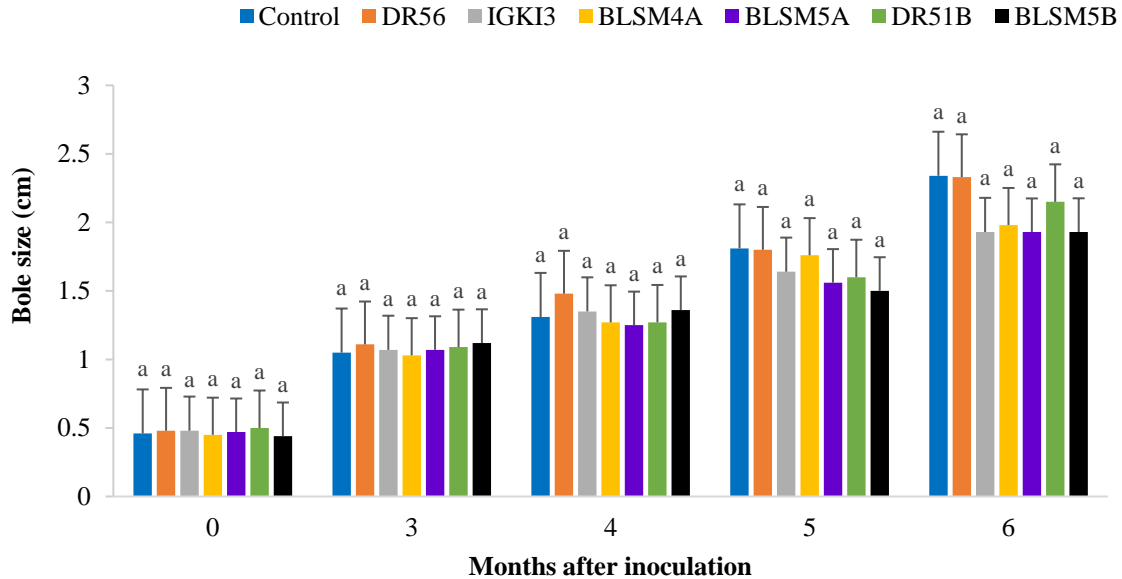


Figure 4.2: The bole size of the oil palm seedlings at 0, 3, 4, 5, and 6 months after inoculation. The means follow by the same letter per respective month, indicating no significant difference at 0.05 significance level. Error bars represent the standard error of the mean

iii. Number of Leaves

Generally, the number of leaves (NOL) of inoculated and the control oil palm seedlings increased throughout the study, except for seedlings inoculated with isolate BLSM5B (Figure 4.3). There was no significant difference in the NOL between oil palm seedlings inoculated with different *G. boninense* isolates three months after inoculation. Four months after inoculation, the NOL of the oil palm seedlings inoculated with isolates IGKI3, BLSM4A, BLSM5A, DR51B, and BLSM5B was significantly lower (6.53, 6.67, 6.45, 6.36, and 6.32, respectively) when compared to that of the control seedlings (7.42; $p < 0.05$). However, there was no significant difference in the NOL between seedlings inoculated with isolate DR56 (7.53) and the control (7.42; $p > 0.05$). Five months after inoculation, the NOL of the oil palm seedlings inoculated with isolate IGKI3, BLSM4A, BLSM5A, DR51B, and BLSM5B was significantly lower (6.86, 6.77, 6.58, 6.60, and

4.69, respectively) than those in the control (7.95; $p < 0.05$). However, there was no significant difference in the NOL between seedlings inoculated with isolate DR56 (8.00) and the control (7.95; $p > 0.05$). In addition, the NOL of seedlings inoculated with isolate BLSM5B was significantly lower (4.69) than those inoculated with isolates DR56, IGKI3, BLSM4A, BLSM5A, and DR51B (8.00, 6.86, 6.77, 6.58, and 6.60, respectively; $p < 0.05$). Six months after inoculation, the NOL of seedlings inoculated with isolate IGKI3, BLSM4A, BLSM5A, DR51B, and BLSM5B was significantly lower (7.00, 7.50, 8.25, 7.67, and 4.50, respectively) than those in the control (9.30; $p < 0.05$). Again, there was no significant difference in NOL between seedlings inoculated with isolate DR56 (9.27) and the control (9.30; $p > 0.05$). Additionally, the NOL of seedlings inoculated with isolate BLSM5B was significantly lower (4.50) compared to those inoculated with isolates IGKI3 and BLSM5A (8.00 and 8.00, respectively; $p < 0.05$), but not significantly different from the seedlings inoculated with isolates BLSM4A and DR51B (7.50 and 7.67, respectively; $p > 0.05$).

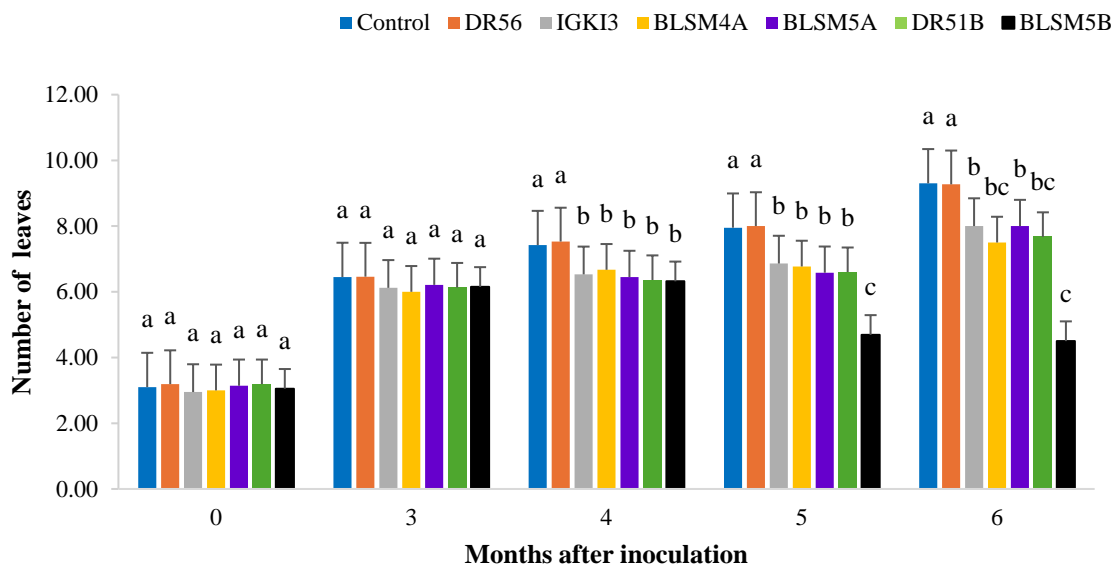


Figure 4.3: The number of leaves of the oil palm seedlings at 0, 3, 4, 5, and 6 months after inoculation. The means follow by the same letter per respective month, indicating no significant difference at 0.05 significance level. Error bars represent the standard error of the mean

iv. Leaf Area

All the leaf area (LA) of inoculated and the control seedlings increased throughout the study (Figure 4.4). There was no significant difference in the LA between treatments three months after inoculation. However, after four months post-inoculation, the LA of the oil palm seedlings inoculated with BLSM5B was significantly smaller (800.06 cm²) than that of the seedlings in the control (1093.02 cm²; $p < 0.05$). In addition, there was no significant difference in the LA between the seedlings inoculated with isolates DR56, IGKI3, BLSM4A, BLSM5A, and DR51B (1083.59 cm², 876.90 cm², 818.89 cm², 865.15 cm², and 830.65 cm², respectively) and the control seedlings (1093.02 cm²; $p > 0.05$). There was also no significant difference in LA among seedlings inoculated with isolates DR56, IGKI3, BLSM4A, BLSM5A, DR51B, and BLSM5B (1083.59 cm², 876.90 cm², 818.89 cm², 865.15 cm², 830.65 cm², and 800.06 cm², respectively; $p > 0.05$).

Five months after inoculation, the seedlings inoculated with isolates IGKI3, BLSM4A, BLSM5A, DR51B, and BLSM5B had significantly smaller LA (922.09 cm², 937.67 cm², 882.55 cm², 872.52 cm², and 844.15 cm², respectively) compared to those in the control (1374.80 cm²; $p < 0.05$). However, there was no significant difference in the LA between seedlings inoculated with DR56 (1381.66 cm²) and the control (1374.80 cm²; $p > 0.05$). After six months post-inoculation, the LA of the oil palm seedlings inoculated with isolates BLSM4A and BLSM5B were significantly smaller (903.23 cm² and 973.84 cm², respectively) compared to those in the control (1894.98 cm²; $p < 0.05$). However, there was no significant difference in LA between seedlings inoculated with isolates DR56, IGKI3, BLSM5A, and DR51B (1500.22 cm²; 1032.62 cm², 941.83 cm², and 990.48 cm², respectively) compared to the control (1894.98 cm²; $p > 0.05$). Additionally, there was no significant difference in LA among seedlings inoculated with isolates DR56, IGKI3, BLSM4A, BLSM5A, DR51B, and BLSM5B (1500.22 cm², 1032.62.67 cm², 903.23 cm², 941.83 cm², 990.48 cm², and 973.84 cm², respectively; $p > 0.05$).

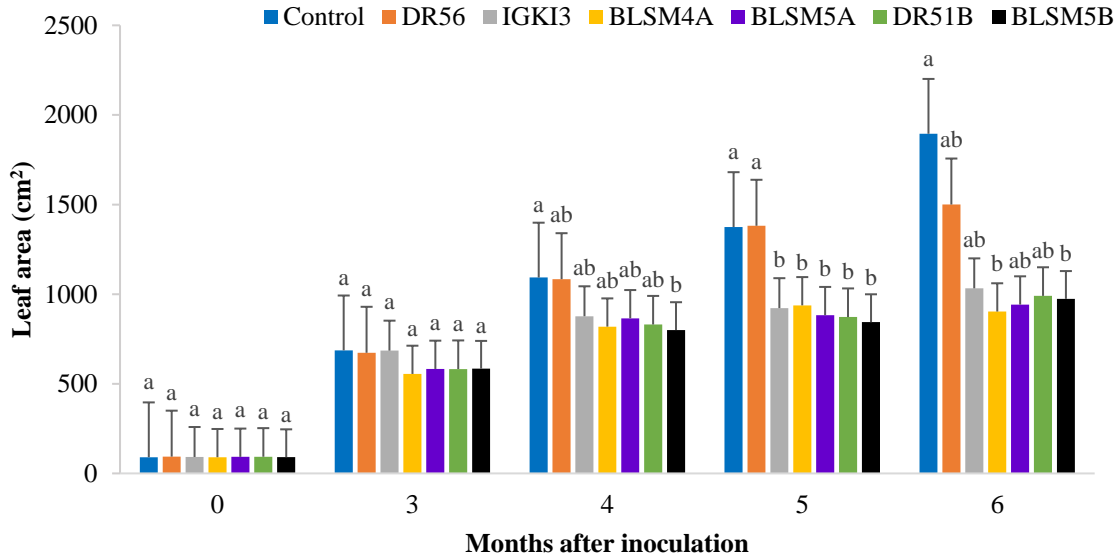


Figure 4.4: The leaf area of the oil palm seedlings was measured at 0, 3, 4, 5, and 6 months after inoculation. The means followed by the same letter for each respective month indicate that there is no significant difference at the 0.05 significance level. Error bars represent the standard error of the mean

v. Fresh Root Mass

All the fresh root mass (FRM) of inoculated and the control seedlings increased throughout the study (Figure 4.5). There was no significant difference in FRM between treatments three months after inoculation. Four months after inoculation, the seedlings inoculated with isolates IGKI3, BLSM4A, BLSM5A, DR51B, and BLSM5B had significantly lower (3.81 g, 3.39 g, 3.74 g, 3.52 g, and 2.22 g, respectively) FRM than those in the control (6.61 g; $p < 0.05$). However, there was no significant difference in FRM between seedlings inoculated with isolate DR56 (6.01 g) and the control (6.61 g; $p > 0.05$). Also, there was no significant difference between FRM of seedlings inoculated with isolates DR56, IGKI3, BLSM4A, BLSM5A, and DR51B (6.01 g, 3.81 g, 3.39 g, 3.74 g, and 3.52 g, respectively; $p > 0.05$) four months after inoculation. However, the FRM of seedlings inoculated with isolate BLSM5B was significantly lower (2.22 g) than those

inoculated with isolate DR56 (6.01 g; $p < 0.05$), but not significantly different with those inoculated with isolates IGKI3, BLSM4A, BLSM5A, and DR51B (3.81 g, 3.39 g, 3.74 g, and 3.52 g, respectively; $p > 0.05$). Five months after inoculation, the FRM of the seedlings inoculated with isolates IGKI3, BLSM4A, BLSM5A, DR51B, and BLSM5B were significantly lower (6.12 g, 3.60 g, 4.69 g, 4.30 g, and 2.71 g) than those in the control (13.73 g; $p < 0.05$). However, there was no significant difference in FRM between seedlings inoculated with isolate DR56 (11.93 g) and the control (13.73 g; $p > 0.05$). After six months post-inoculation, the FRM of the seedlings inoculated with isolates IGKI3, BLSM4A, BLSM5A, DR51B, and BLSM5B was significantly lower (6.77 g, 4.40 g, 5.98 g, 5.04 g, and 3.34 g, respectively) compared to those in the control (20.70 g; $p < 0.05$). However, there was no significant difference in FRM between seedlings inoculated with isolate DR56 (19.83 g) and the control (20.70 g; $p > 0.05$). Additionally, the FRM of the seedlings inoculated with isolate BLSM5B was significantly lower (3.34 g) than those inoculated with isolate IGKI3 (6.77 g; $p < 0.05$), but not significantly different with those inoculated with isolates BLSM4A, BLSM5A, and DR51B (4.40 g, 5.98 g, and 5.04 g, respectively; $p > 0.05$).

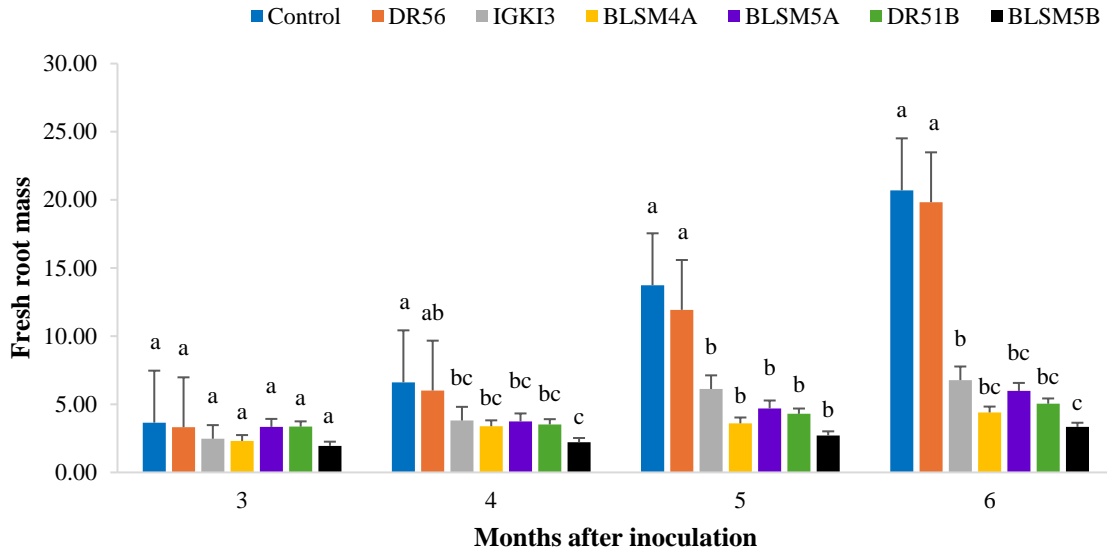


Figure 4.5: The fresh root mass of the oil palm seedlings was measured at 3, 4, 5, and 6 months after inoculation. The means followed by the same letter for each respective month indicate that there is no significant difference at the 0.05 significance level. Error bars represent the standard error of the mean

4.1.1.2 Chlorophyll Content

Three months after inoculation, only chlorophyll content of the seedlings inoculated with isolate BLSM5B was significantly lower (53.33) than that of the control (61.72; $p < 0.05$) (Figure 4.6). In addition, there was no significant difference in the chlorophyll content between seedlings inoculated with isolates DR56, IGKI3, BLSM4A, BLSM5A, and DR51B (62.81, 61.28, 59.89, 59.60, and 62.91, respectively) and the control (61.72; $p > 0.05$). Four months after inoculation, the chlorophyll content of the seedlings inoculated with isolate BLSM5B was significantly lower (46.02) than those in the control (61.91; $p < 0.05$). However, the chlorophyll content of the seedlings inoculated with isolates DR56, IGKI3, BLSM4A, BLSM5A, and DR51B (59.80, 59.62, 56.03, 55.05, and 56.85, respectively) were not significantly different than those in the control (61.91; $p > 0.05$). Besides, there was no significant difference in the chlorophyll content between

isolates IGKI3, BLSM4A, BLSM5A, DR51B, and BLSM5B (59.80, 59.62, 56.03, 55.05, 56.85, and 46.02, respectively; $p > 0.05$) four months after inoculation.

Five months after inoculation, the chlorophyll content of the seedlings inoculated with isolates IGKI3, BLSM4A, BLSM5A and DR51B was significantly lower (56.22, 54.82, 52.58, and 51.03, respectively) than those in the control (61.75; $p < 0.05$). However, there was no significant difference in the chlorophyll content between seedlings inoculated with isolate DR56 (58.21) and the control (61.75; $p > 0.05$). Also, there was no significant difference in the chlorophyll content between seedlings inoculated with isolates DR56, IGKI3, and BLSM4A (58.21, 56.22, and 54.82, respectively; $p > 0.05$) five months after inoculation. Additionally, the chlorophyll content of seedlings inoculated with BLSM5A and DR51B was significantly lower (52.58 and 51.03, respectively) than those inoculated with isolate DR56 (58.21; $p < 0.05$), but not significantly different compared to those inoculated with isolates IGKI3 and BLSM4A (56.22 and 54.82, respectively; $p > 0.05$). In addition, all seedlings selected for chlorophyll measurements in the treatment BLSM5B died five months after inoculation. Six months post-inoculation, the chlorophyll content of the seedlings inoculated with isolates BLSM4A and BLSM5A was significantly lower (53.77 and 51.20, respectively) than those in the control (59.77; $p < 0.05$). However, there was no significant difference in the chlorophyll content between seedlings inoculated with isolates DR56 and IGKI3 (57.79 and 57.68, respectively) and the control (59.77, $p > 0.05$). Additionally, there was no significant difference between seedlings inoculated with isolates DR56, IGKI3, BLSM4A, and BLSM5A (57.79, 57.68, 53.77, and 51.20, respectively; $p > 0.05$). All seedlings selected for chlorophyll measurements in the treatment DR51B died six months after inoculation.

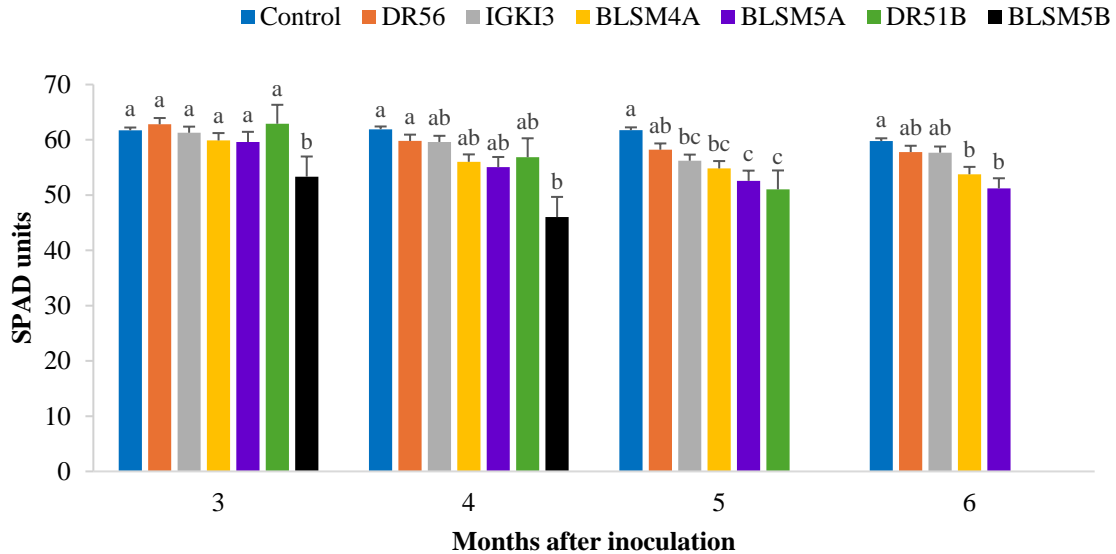


Figure 4.6: The chlorophyll meter readings (in SPAD units) of the oil palm seedlings were taken at 3, 4, 5, and 6 months after inoculation. The means followed by the same letter for each respective month indicate no significant difference at the 0.05 significance level. Error bars represent the standard error of the mean. All seedlings selected for chlorophyll measurements in the treatment DR51B died six months after inoculation, whereas those in the treatment BLSM5B died five months after inoculation

4.1.1.3 Photosynthesis Rate

Three months after inoculation, the photosynthesis rate of the seedlings inoculated with isolate BLSM5B was significantly lower ($2.20 \mu\text{mol m}^{-2} \text{s}^{-1}$) than that of control seedlings ($6.44 \mu\text{mol m}^{-2} \text{s}^{-1}$; $p < 0.05$). However, there was no significant difference in the photosynthesis rates of the seedlings inoculated with isolates DR56, IGKI3, BLSM4A, BLSM5A and DR51B ($5.59 \mu\text{mol m}^{-2} \text{s}^{-1}$, $4.28 \mu\text{mol m}^{-2} \text{s}^{-1}$, $3.99 \mu\text{mol m}^{-2} \text{s}^{-1}$, $3.30 \mu\text{mol m}^{-2} \text{s}^{-1}$, and $2.31 \mu\text{mol m}^{-2} \text{s}^{-1}$, respectively) compared to the control seedlings ($6.44 \mu\text{mol m}^{-2} \text{s}^{-1}$; $p > 0.05$) (Figure 4.7). Additionally, there was no significant difference between seedlings inoculated with isolates DR56, IGKI3, BLSM4A, BLSM5A, DR51B, and BLSM5B ($5.59 \mu\text{mol m}^{-2} \text{s}^{-1}$, $4.28 \mu\text{mol m}^{-2} \text{s}^{-1}$, $3.99 \mu\text{mol m}^{-2} \text{s}^{-1}$, $3.30 \mu\text{mol m}^{-2} \text{s}^{-1}$, $2.31 \mu\text{mol m}^{-2} \text{s}^{-1}$, and $2.20 \mu\text{mol m}^{-2} \text{s}^{-1}$, respectively; $p > 0.05$).

Four months after inoculation, the photosynthesis rate of the seedlings inoculated with isolate BLSM5B was significantly lower ($0.42 \mu\text{mol m}^{-2} \text{s}^{-1}$) than those in the control ($5.75 \mu\text{mol m}^{-2} \text{s}^{-1}$; $p < 0.05$). However, there was no significant difference in the photosynthesis rates of the seedlings inoculated with isolates DR56, IGKI3, BLSM4A, BLSM5A and DR51B ($4.49 \mu\text{mol m}^{-2} \text{s}^{-1}$, $3.83 \mu\text{mol m}^{-2} \text{s}^{-1}$, $2.47 \mu\text{mol m}^{-2} \text{s}^{-1}$, $2.86 \mu\text{mol m}^{-2} \text{s}^{-1}$, and $1.53 \mu\text{mol m}^{-2} \text{s}^{-1}$, respectively) compared to the control seedlings ($5.75 \mu\text{mol m}^{-2} \text{s}^{-1}$; $p > 0.05$). Additionally, there was no significant difference between seedlings inoculated with isolates DR56, IGKI3, BLSM4A, BLSM5A, DR51B, and BLSM5B ($4.49 \mu\text{mol m}^{-2} \text{s}^{-1}$, $4.49 \mu\text{mol m}^{-2} \text{s}^{-1}$, $3.83 \mu\text{mol m}^{-2} \text{s}^{-1}$, $2.47 \mu\text{mol m}^{-2} \text{s}^{-1}$, $2.86 \mu\text{mol m}^{-2} \text{s}^{-1}$, and $1.53 \mu\text{mol m}^{-2} \text{s}^{-1}$, respectively; $p > 0.05$).

Five months after inoculation, the seedlings inoculated with isolate IGKI3, BLSM4A, BLSM5A, and DR51B ($2.57 \mu\text{mol m}^{-2} \text{s}^{-1}$, $2.08 \mu\text{mol m}^{-2} \text{s}^{-1}$, $1.95 \mu\text{mol m}^{-2} \text{s}^{-1}$, and $0.77 \mu\text{mol m}^{-2} \text{s}^{-1}$, respectively) had a significantly lower photosynthesis rate compared to those in the control ($4.95 \mu\text{mol m}^{-2} \text{s}^{-1}$; $p < 0.05$). Additionally, there was no significant difference between the photosynthesis rates of the seedlings inoculated with isolate DR56 ($4.08 \mu\text{mol m}^{-2} \text{s}^{-1}$) and those of the control group ($4.95 \mu\text{mol m}^{-2} \text{s}^{-1}$; $p > 0.05$). In addition, the photosynthesis rates of the seedlings inoculated with isolate DR51B ($0.77 \mu\text{mol m}^{-2} \text{s}^{-1}$) was significantly lower than those inoculated with isolates IGKI3 and BLSM4A ($2.57 \mu\text{mol m}^{-2} \text{s}^{-1}$ and $2.08 \mu\text{mol m}^{-2} \text{s}^{-1}$, respectively; $p < 0.05$), but not significantly different with seedlings inoculated with isolate BLSM5A ($1.95 \mu\text{mol m}^{-2} \text{s}^{-1}$; $p > 0.05$).

Six months post-inoculation, the photosynthesis rate of the seedlings inoculated with isolates IGKI3, BLSM4A, and BLSM5A ($2.24 \mu\text{mol m}^{-2} \text{s}^{-1}$, $1.77 \mu\text{mol m}^{-2} \text{s}^{-1}$, and $1.45 \mu\text{mol m}^{-2} \text{s}^{-1}$, respectively) was significantly lower than those of the control ($4.61 \mu\text{mol m}^{-2} \text{s}^{-1}$; $p <$

0.05). There was no significant difference between the photosynthesis rates of the seedlings inoculated with isolate DR56 ($3.27 \mu\text{mol m}^{-2} \text{s}^{-1}$) and those of the control group ($4.61 \mu\text{mol m}^{-2} \text{s}^{-1}$; $p > 0.05$). Similarly, there was no significant difference between the photosynthesis rates of the seedlings inoculated with isolate DR56 ($3.27 \mu\text{mol m}^{-2} \text{s}^{-1}$) and those inoculated with isolate IGKI3 ($2.24 \mu\text{mol m}^{-2} \text{s}^{-1}$; $p > 0.05$). However, the photosynthesis rate of the seedlings inoculated with isolates BLSM4A and BLSM5A ($1.77 \mu\text{mol m}^{-2} \text{s}^{-1}$ and $1.45 \mu\text{mol m}^{-2} \text{s}^{-1}$, respectively) was significantly lower than those inoculated with isolate DR56 ($3.27 \mu\text{mol m}^{-2} \text{s}^{-1}$; $p < 0.05$), but not significantly different with those inoculated with isolate IGKI3 ($2.24 \mu\text{mol m}^{-2} \text{s}^{-1}$; $p > 0.05$).

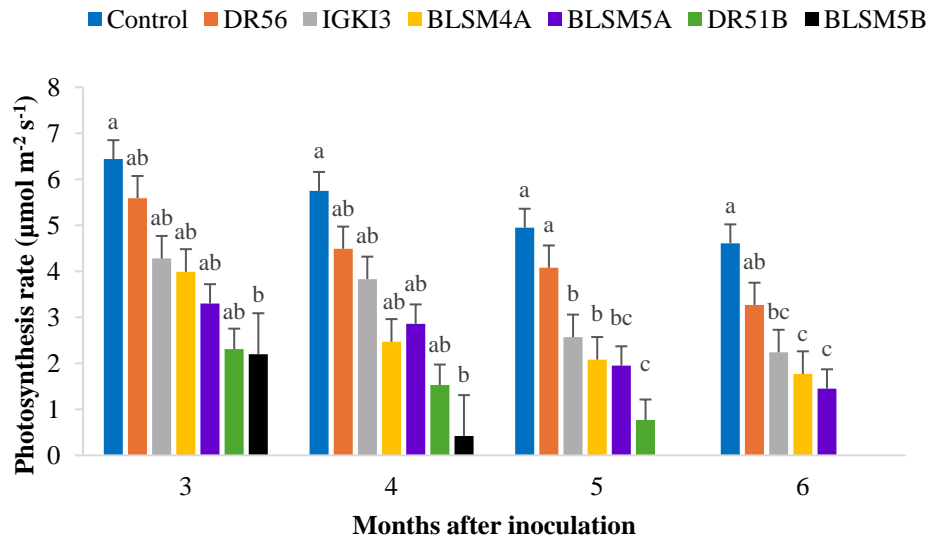


Figure 4.7: The photosynthesis rate of the oil palm seedlings was measured at 3, 4, 5, and 6 months after inoculation (MAI). The means followed by the same letter for each respective month indicate no significant difference at the 0.05 significance level. Error bars represent the standard error of the mean. All seedlings selected for chlorophyll measurements in the treatment DR51B died six months after inoculation, whereas those in the treatment BLSM5B died five months after inoculation

4.1.1.4 Disease Progress

The fruiting bodies of *G. boninense* began forming as early as two months after inoculation, with the first fruiting bodies was observed near the seedlings inoculated with isolate DR51B (Figure 4.8). Within the same two-month period, seedlings infected with isolates BLSM5B and BLSM5A also displayed leaf necrosis, though later than those inoculated with DR51B (Figure 4.9). Interestingly, despite the presence of necrotic leaves, seedlings infected with isolates BLSM5B and BLSM5A did not produce any fruiting bodies (Figure 4.9). By the end of three months post-inoculation, most inoculated seedlings had developed fruiting bodies (Figure 4.10), lesions, and rotten in the bole and root (Figure 4.11 and Figure 4.12).

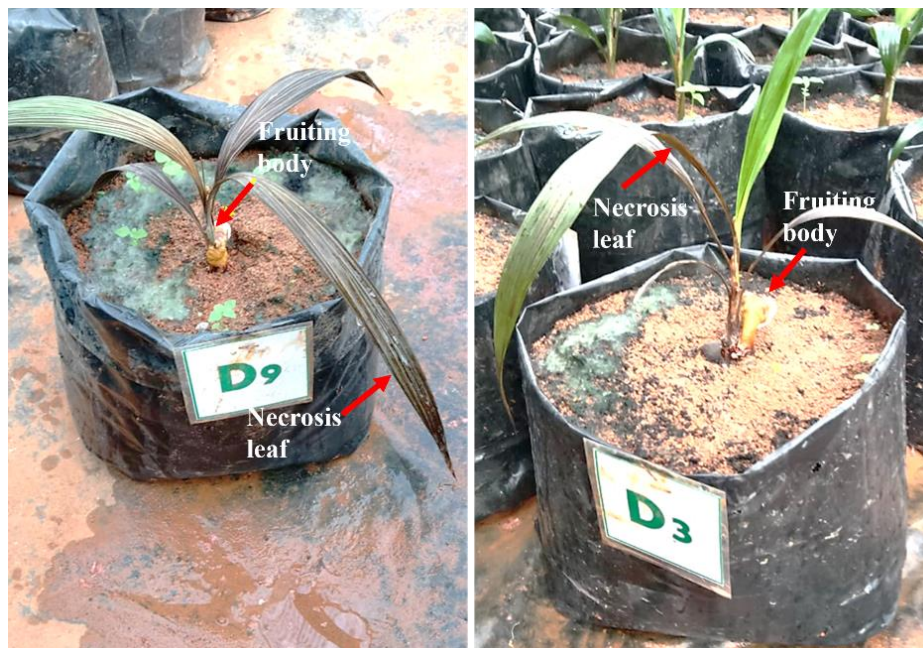


Figure 4.8: The first fruiting body (indicated by the red arrow) was observed near the seedling inoculated with DR51B two months after inoculation. Additionally, necrotic leaves were noticed in seedlings that were inoculated with DR51B

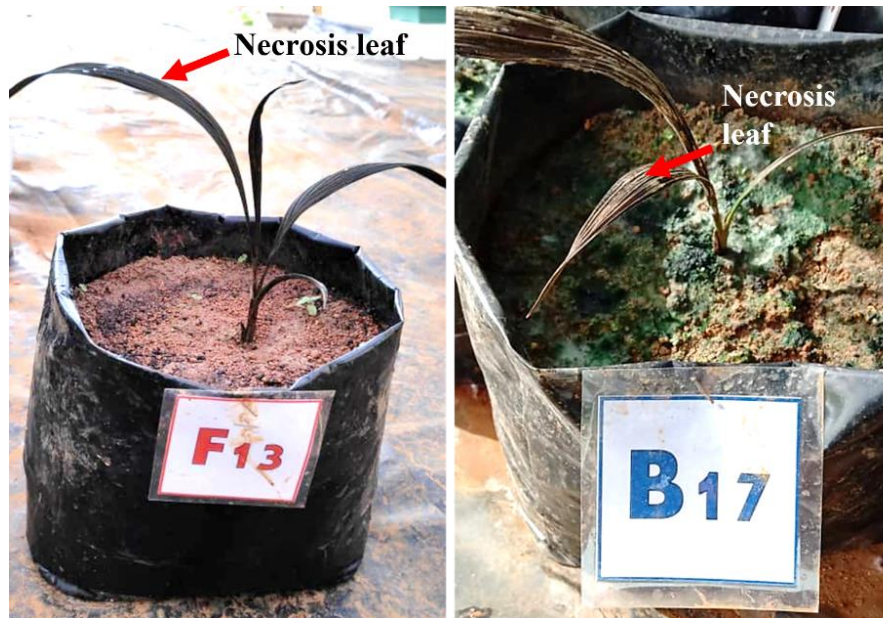


Figure 4.9: Leaf necrosis (indicated by the red arrow) observed in seedlings inoculated with isolate BLSM5A (left) and BLSM5B (right)



Figure 4.10: Fruiting bodies grew on seedlings inoculated with the following isolates three months after inoculation: (A) BLSM5B, (B) DR56, (C) DR51B, (D) IGKI3, (E) BLSM4A, and (F) BLSM5A

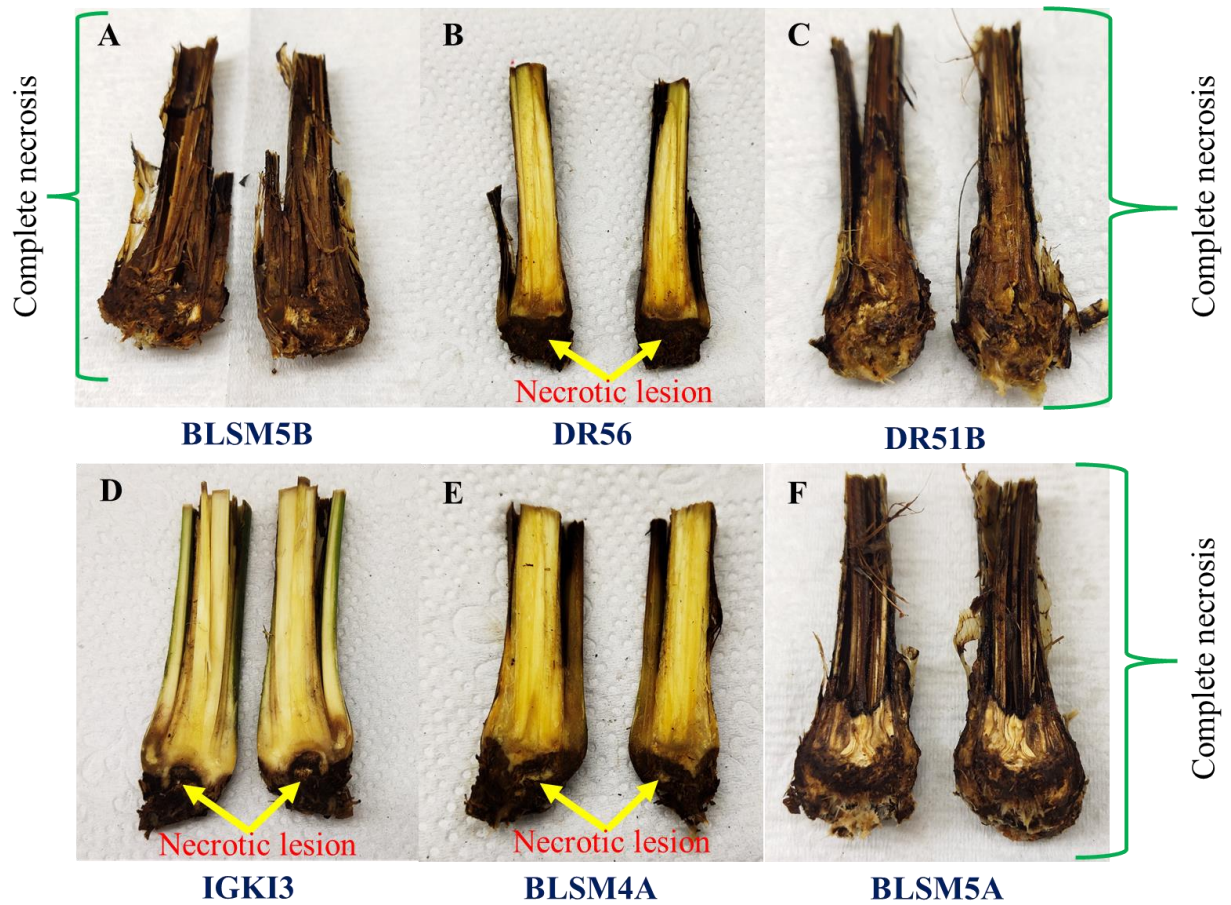


Figure 4.11: Necrotic lesions and complete necrosis were observed on the boles of the seedlings inoculated with the following isolates four months after inoculation: (A) BLSM5B, (B) DR56, (C) DR51B, (D) IGKI3, (E) BLSM4A, and (F) BLSM5A

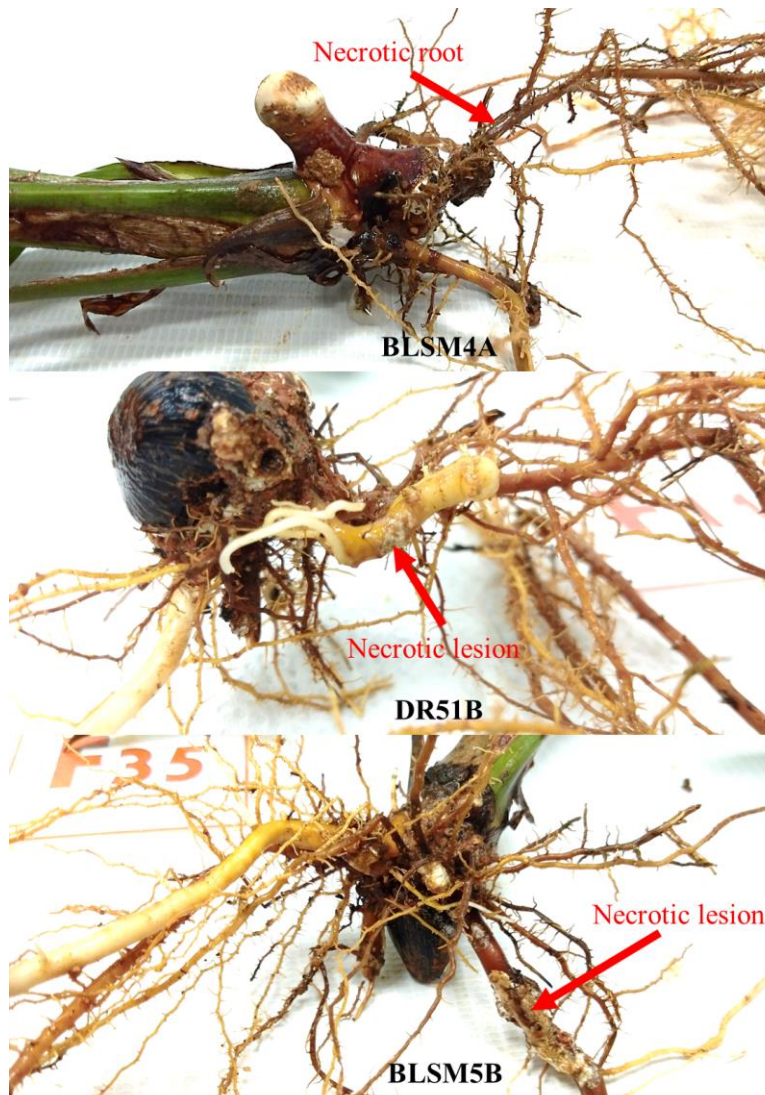


Figure 4.12: Necrotic lesion and necrotic roots of the seedlings inoculated with the following isolates four months after inoculation: (A) BLSM4A, (B) DR51B, and (C) BLSM5B

In this study, disease incidence (DI) was monitored in oil palm seedlings at different time points (3, 4, 5, and 6 months after inoculation) following the inoculation with isolates BLSM5B, DR51B, BLSM5A, BLSM4A, IGKI3, and DR56 (Figure 4.13). Three months after inoculation, seedlings inoculated with isolates DR51B and BLSM5A both caused 70% DI, while seedlings inoculated with isolates BLSM5B (50%), BLSM4A (20%), IGKI3 (30%), and DR56 (10%),

caused 50%, 20%, 30%, and 10% DI, respectively. Four months after inoculation, seedlings inoculated with isolate DR51B produce 80% DI, while seedlings inoculated with isolates BLSM5A, BLSM5B, BLSM4A, IGKI3, and DR56 were only causing 10-70% DI. Five months after inoculation, seedlings inoculated with isolates BLSM5B, DR51B, and BLSM5A was the first to achieve 100% DI, except for seedlings inoculated with isolates BLSM4A (60%), IGKI3 (80%), and DR56 (40%). Seedlings inoculated with isolates BLSM4A achieve 100% DI six months after inoculation, except for seedlings inoculated with isolates IGKI3 and DR56 (90% and 80%, respectively). Throughout the study period, the treatment with isolate DR56 consistently produced low DI. There was no disease incidence observed in the control seedlings throughout the study.

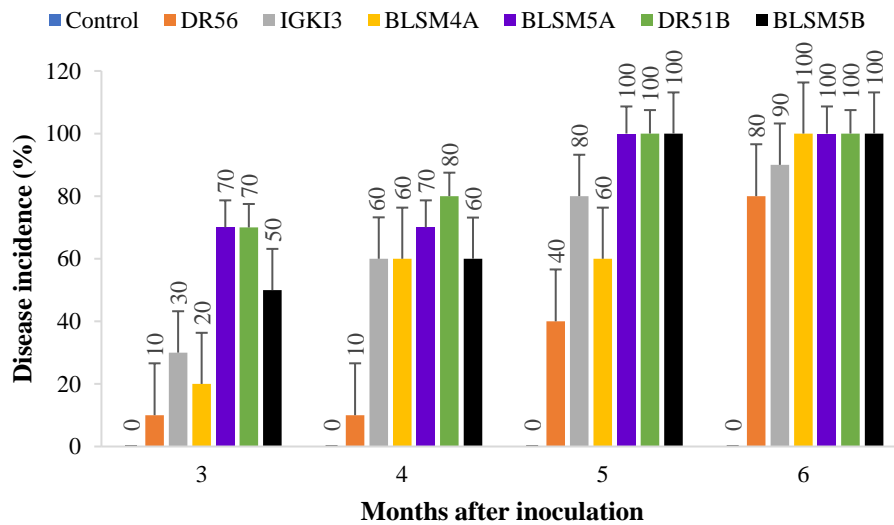


Figure 4.13: The disease incidence of the oil palm seedlings at 3, 4, 5, and 6 months after inoculation (MAI)

For disease severity index (DSI), after three months post-inoculation, the seedlings inoculated with isolate DR56, IGKI3, BLSM4A, BLSM5A, DR51B, and BLSM5B had significantly higher DSI values (25.31%, 50.67%, 44.66%, 53.99%, 55.99%, and 53.99%,

respectively; $p < 0.05$) than the control (0%, $p < 0.05$) (Figure 4.14). The DSI values of the seedlings inoculated with isolate IGKI3, BLSM4A, BLSM5A, DR51B, and BLSM5B were significantly higher (50.67%, 44.66%, 53.99%, 55.99%, and 53.99%, respectively; $p < 0.05$) than those inoculated with isolate DR56 (25.31%; $p < 0.05$). Similarly, four months after inoculation, the DSI values of the seedlings inoculated with isolates DR56, IGKI3, BLSM4A, BLSM5A, DR51B, and BLSM5B remained significantly higher (28.67%, 66.00%, 66.68%, 71.34%, 61.33%, and 62.66%, respectively; $p < 0.05$) compared to the control (0%, $p < 0.05$). Again, seedlings inoculated with isolate IGKI3, BLSM4A, BLSM5A, DR51B, and BLSM5B had significantly higher DSI values (66.00%, 66.68%, 71.34%, 61.33%, and 62.66%, respectively; $p < 0.05$) than those inoculated with isolate DR56 (28.67%; $p < 0.05$). Five months after inoculation, the DSI values of the seedlings inoculated with isolates DR56, IGKI3, BLSM4A, BLSM5A, DR51B, and BLSM5B remained significantly higher (42.00%, 70.66%, 74.00%, 79.33%, 79.99%, and 87.33%, respectively; $p < 0.05$) than that of the control (0%, $p < 0.05$). The DSI of the seedlings inoculated with isolate IGKI3, BLSM4A, BLSM5A, DR51B, and BLSM5B were significantly higher (70.66%, 74.00%, 79.33%, 79.99%, and 87.33%, respectively; $p < 0.05$) than those inoculated with isolate DR56 (42.00%; $p < 0.05$). By six months post-inoculation, seedlings inoculated with isolates DR56, IGKI3, BLSM4A, BLSM5A, DR51B, and BLSM5B continued to display significantly higher DSI values (43.99%, 76.66%, 82.00%, 83.33%, 88.00%, and 98.67%, respectively; $p < 0.05$) compared to control (0%; $p < 0.05$). Additionally, the DSI values of the seedlings inoculated with isolates IGKI3, BLSM4A, BLSM5A, DR51B, and BLSM5B were significantly higher (76.66%, 82.00%, 83.33%, 88.00%, and 98.67%, respectively; $p < 0.05$) than those of DR56 (43.99%, , $p < 0.05$).

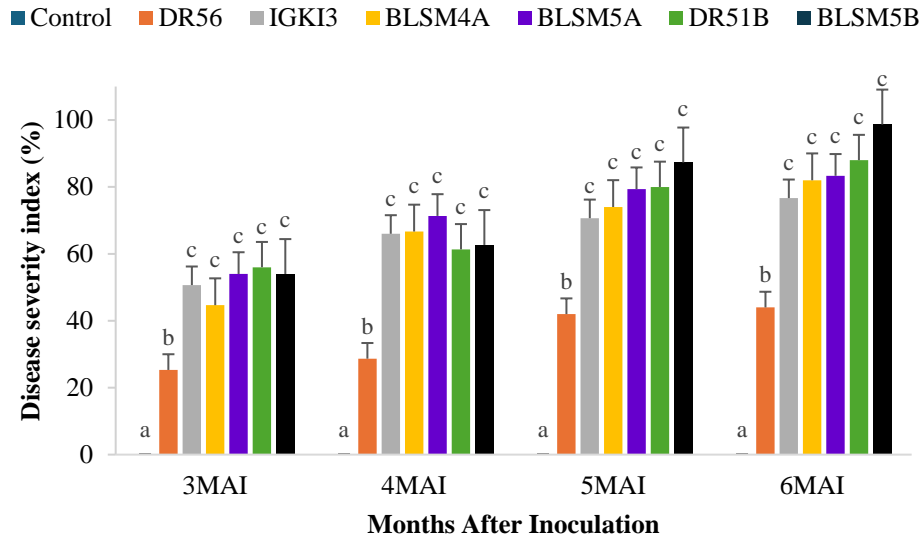


Figure 4.14: Disease severity index (DSI) of oil palm seedlings at 3, 4, 5, and 6 months after inoculation (MAI). The means followed by the same letter for each respective month indicate no significant difference at the 0.05 significance level. Error bars represent the standard error of the mean

4.1.1.5 *In Vitro* Growth Rate

Overall, all the three-culture media, viz., malt extract agar (MEA), potato dextrose agar (PDA), and sabouraud dextrose agar (SDA), supported the growth of *G. boninense* isolates tested in this study (Figure 4.15). All six isolates (BLSM5B, DR51B, BLSM5A, BLSM4A, IGKI3, and DR56) exhibit their maximum mycelial growth on MEA after eight days of inoculation (Figure 4.15A). On PDA, all isolates (except BLSM4A) achieved their maximum mycelial growth after eight days of inoculation (Figure 4.15B). In contrast, slow growth of the isolates was observed on SDA (Figure 4.15C). After eight days of inoculation, isolates BLSM5B (on MEA) and BLSM5A (on PDA) were the first to reach the edge of the 90 mm Petri dish wall (Figure 4.15A & B). However, none of the isolates on SDA reached full plate on day eight (Figure 4.15C).

In addition, the pigmentation produced by the *G. boninense* isolates varied depending on the culture medium and the isolates. On MEA, isolates DR51B and IGKI3 exhibited distinct yellow-to-brown ring at the centre, while isolate DR56 produced a light-yellow pigmentation at the centre (Figure 4.15A). When cultured on PDA, isolates BLSM5A, BLSM4A, and DR56 displayed centralised pigmentation (Figure 4.15B). Notably, isolates BLSM4A and DR56 displayed the most intense yellow-to-brown colour pigmentation, while isolate BLSM5A exhibited a lighter yellow pigmentation (Figure 4.15B). Conversely, none of the isolates produced pigmentation at the centre of the cultures on SDA (Figure 4.15C).

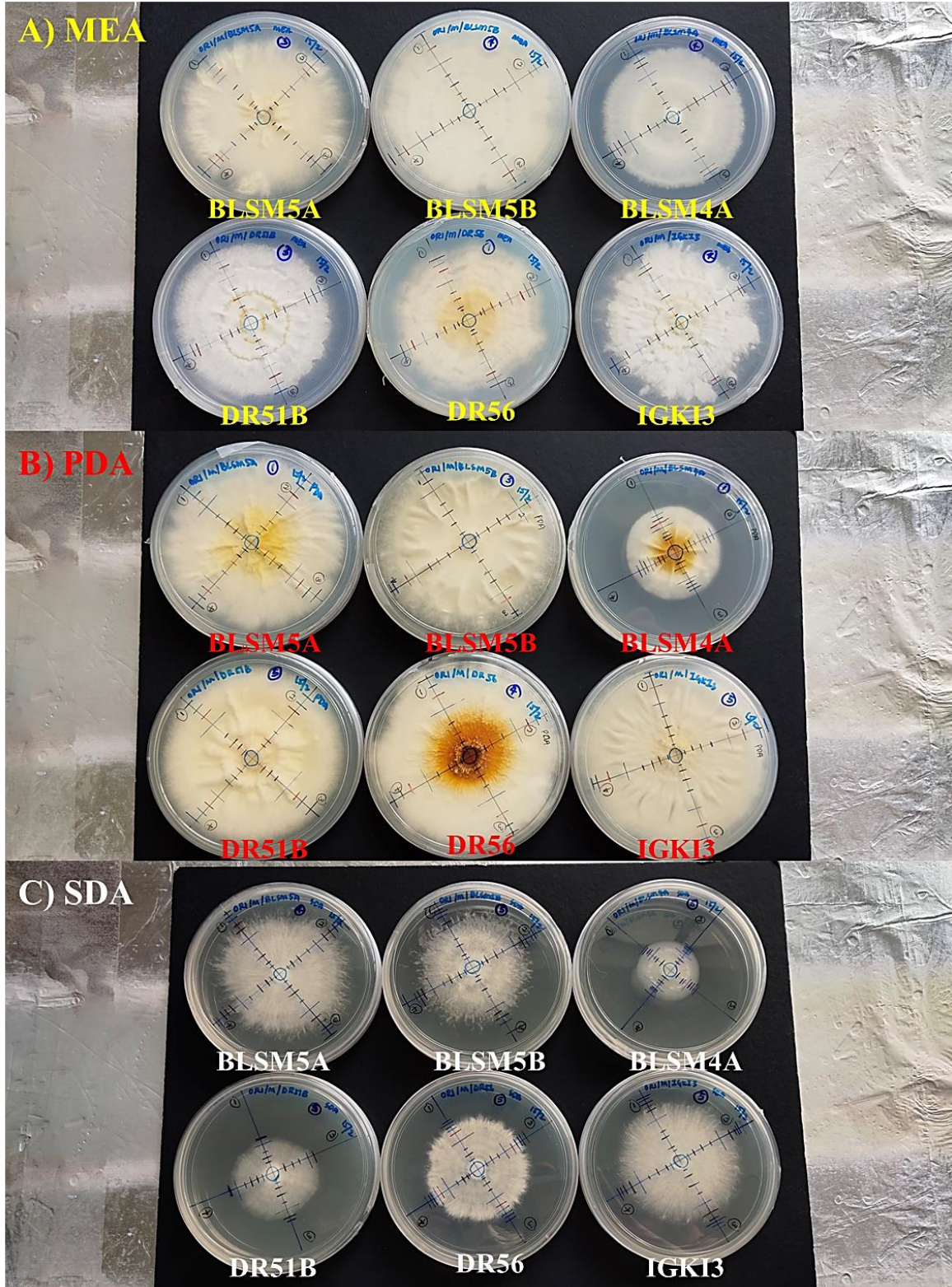


Figure 4.15: The growth of *Ganoderma boninense* isolates on day eight after inoculation: (A) malt extract agar, (B) potato dextrose agar, and (C) sabouraud dextrose agar

The *in vitro* growth rates of the six *G. boninense* isolates ranged from 0.47 to 0.32 cm.day⁻¹ on MEA, 0.45 to 0.20 cm.day⁻¹ on PDA, and 0.38 to 0.11 cm.day⁻¹ on SDA (Table 4.1). Isolate BLSM5B exhibited significantly faster growth on MEA compared to all other isolates. On the other hand, isolates BLSM5B, BLSM5A and IGKI3 grew the fastest on PDA. On SDA, isolate BLSM5A grew significantly faster compared to all other isolates. Isolate BLSM4A exhibited the slowest growth on both PDA and SDA, whereas isolate BLSM4A and DR56 grew the slowest on MEA. Overall, majority of the isolates grew uniformly on MEA compared to PDA and SDA.

Table 4.1: *In vitro* growth rate of *Ganoderma boninense* on malt extract agar (MEA), potato dextrose agar (PDA) and sabouraud dextrose agar (SDA)

Isolate	<i>In Vitro</i> Growth Rate (cm.day ⁻¹)		
	MEA *	PDA *	SDA *
BLSM5B	0.47 ± 0.01 ^a	0.42 ± 0.01 ^{ab}	0.33 ± 0.01 ^b
DR51B	0.38 ± 0.02 ^b	0.38 ± 0.03 ^{bc}	0.24 ± 0.01 ^c
BLSM5A	0.39 ± 0.01 ^b	0.45 ± 0.02 ^a	0.38 ± 0.01 ^a
BLSM4A	0.36 ± 0.01 ^{bc}	0.20 ± 0.01 ^d	0.11 ± 0.00 ^d
IGKI3	0.40 ± 0.01 ^b	0.44 ± 0.01 ^a	0.34 ± 0.01 ^b
DR56	0.32 ± 0.02 ^c	0.37 ± 0.01 ^c	0.23 ± 0.00 ^c

*Data are presented as mean ± SE. Means of five replications with the same letters within each column of culture medium were not significantly different at 0.05 significance level

Both *G. boninense* pure culture revived from the original stock culture and those reisolated from the fruiting body in this study reached the edge of 90 mm Petri dishes eight days after inoculated on MEA. Four out of six *G. boninense* isolates (IGKI3, BLSM4A, BLSM5A, and DR51B) reisolated from the fruiting body in this study grew significantly faster (0.45 cm.day⁻¹, 0.42 cm.day⁻¹, 0.46 cm.day⁻¹, and 0.49 cm.day⁻¹, respectively; $p < 0.05$) than their original stock culture (0.40 cm.day⁻¹, 0.36 cm.day⁻¹, 0.39 cm.day⁻¹, and 0.38 cm.day⁻¹, respectively; $p < 0.05$) (Figure 4.16). Isolate BLSM5B reisolated from fruiting body grew significantly slower (0.36 cm.day⁻¹; $p < 0.05$) than their original stock culture (0.47 cm.day⁻¹; $p < 0.05$). There was no significant difference between the *in vitro* growth rates of isolate DR56 revived from the original stock culture and those reisolated from the fruiting body (0.32 cm.day⁻¹ and 0.36 cm.day⁻¹, respectively; $p < 0.05$).

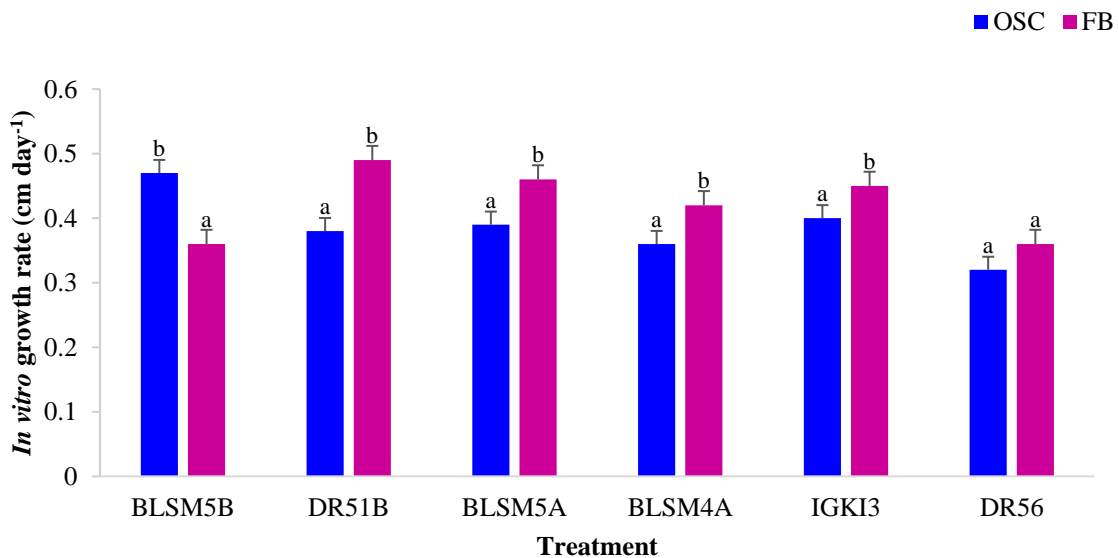


Figure 4.16: *In vitro* growth rate of *Ganoderma boninense* isolates from original stock culture (OSC) and those reisolated from fruiting body (FB) in this study on malt extract agar. The same alphabet of each respective isolate indicate no significant different at the 0.05 significance level. Error bars represent standard error

4.1.1.6 Aggressiveness Assessment

According to the classification by Lo et al. (2023) (Table 3.6), isolates BLSM4A, BLSM5A, DR51B, and BLSM5B (82%, 83.33%, 88%, and 98.67%, respectively) were grouped as highly aggressive (>81%). Among these, isolate BLSM5B showed the highest DSI value of 98.67%, which suggests it may be the most aggressive isolate in this study, although these differences were not statistically significant (Table 4.2). Whereas isolates DR56 and IGKI3 (43.99% and 76.66%, respectively) were categorised as moderately aggressive (40 to 80%). Therefore, DR56 was identified as the least aggressive isolate in this study, with the lowest DSI values of 43.99% and also caused the least effect on the physiological parameters of the infected seedlings among the isolates.

Table 4.2: Summary of seedlings physiological parameters measured for *Ganoderma boninense* isolates aggressiveness assessment at six months after inoculation

Isolate	Vegetative Growth Measurement					Chlorophyll Content, SPAD Units	Photosynthetic Rate, $\mu\text{mol m}^{-2} \text{s}^{-1}$	Sign and Symptom, Yes/No	DI ^f , %	DSI ^g , %	IVGR ^h on MEA, cm.day^{-1}
	NOL ^a	BS ^b	H ^c	LA ^d	FRM ^e						
	cm	cm	cm	g							
BLSM5B	4.50 ^c	1.93 ^a	50.95 ^c	973.84 ^b	3.34 ^c	Dead	Dead	Yes	100	98.67 ^b	0.47 ^a
DR51B	7.67 ^{bc}	2.15 ^a	59.63 ^c	990.48 ^{ab}	5.04 ^{bc}	Dead	Dead	Yes	100	88.00 ^b	0.38 ^b
BLSM5A	8.00 ^b	1.93 ^a	61.93 ^{bc}	941.83 ^{ab}	5.98 ^{bc}	51.20 ^b	1.45 ^c	Yes	100	83.33 ^b	0.39 ^b
BLSM4A	7.50 ^{bc}	1.98 ^a	61.85 ^{bc}	903.23 ^b	4.40 ^{bc}	53.77 ^b	1.77 ^c	Yes	100	82.00 ^b	0.36 ^{bc}
IGKI3	8.00 ^b	1.93 ^a	61.05 ^{bc}	1032.62 ^{ab}	6.77 ^b	57.68 ^{ab}	2.24 ^{bc}	Yes	90	76.66 ^b	0.40 ^b
DR56	9.27 ^a	2.33 ^a	73.45 ^{ab}	1500.22 ^{ab}	19.83 ^a	57.79 ^{ab}	3.27 ^{ab}	Yes	80	43.99 ^a	0.32 ^c
Control	9.30 ^a	2.34 ^a	78.45 ^a	1894.98 ^a	20.70 ^a	59.77 ^a	4.61 ^a	No	0	0 ^a	-

^a Number of leaves

^e Fresh root mass

^b Bole size

^f Disease incidence

^c Height

^g Disease severity index

^d Leaf area

^h *In vitro* growth rate

4.1.2 Spearman's Rank Correlation between Aggressiveness Parameters and Disease Severity Index

4.1.2.1 Vegetative Growth Parameters vs Disease Severity Index

The relationship between all the vegetative growth parameters [number of leaves ($r_s = -0.1600$; $p = 0.4159$), bole size ($r_s = 0.3430$; $p = 0.07393$), height ($r_s = 0.010$; $p = 0.9603$), leaf area ($r_s = 0.0276$; $p = 0.8888$), and fresh root mass ($r_s = -0.1689$; $p = 0.39$)] and the disease severity index was not significant (Figure 4.17A-E).

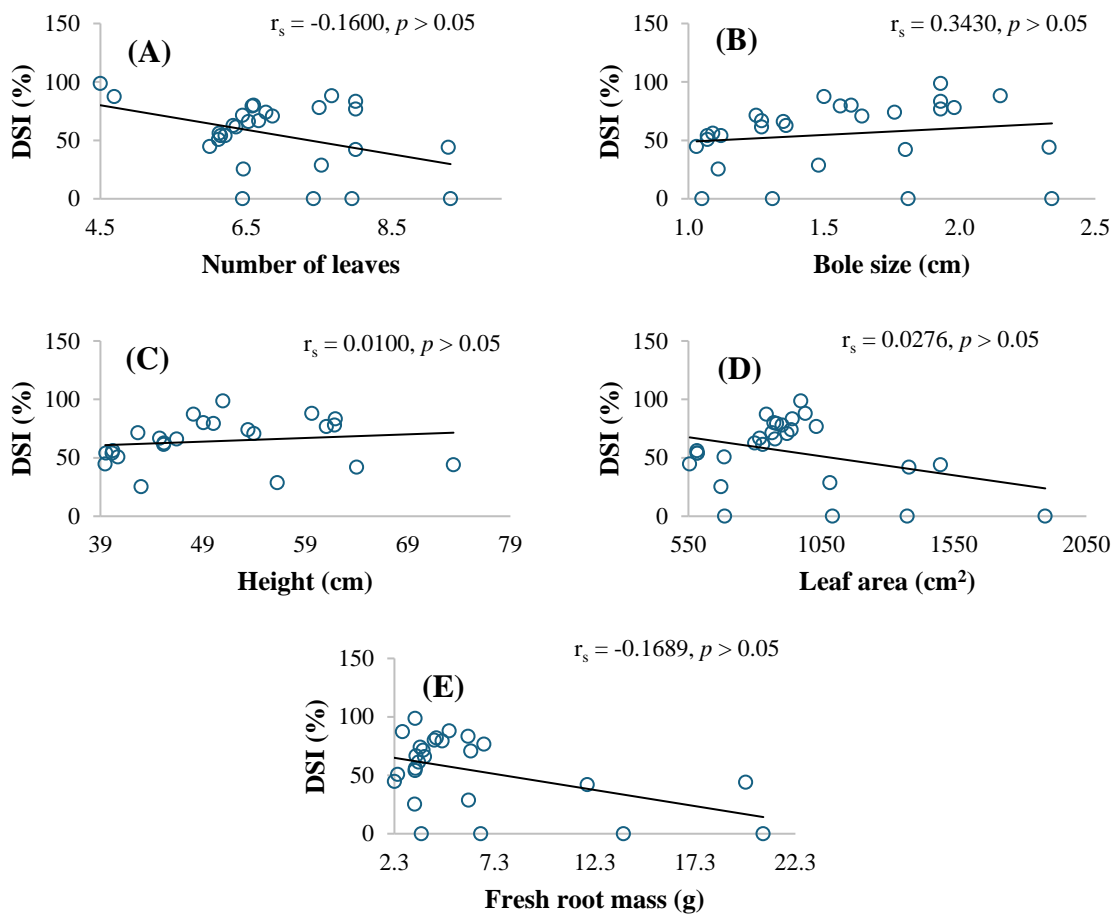


Figure 4.17: Scatter plots showing the relationship between the vegetative growth parameters and disease severity index (DSI): (A) Number of leaves, (B) Bole size, (C) Height, (D) Leaf area, and (E) Fresh root mass. The Spearman's rank correlation coefficient (r_s) and corresponding P-values (p) for each relationship are shown

4.1.2.2 Chlorophyll Content vs Disease Severity Index

The spearman's rank correlation coefficient indicates a moderately strong negative correlation between chlorophyll content ($r_s = -0.7759$, $p = 5.183e-06$) and the disease severity index (DSI) (Figure 4.18) (Chan, 2003; Akoglu, 2018). There is an inverse relationship between chlorophyll content and DSI in this study, which indicates that as the DSI increases, the chlorophyll content tends to decrease.

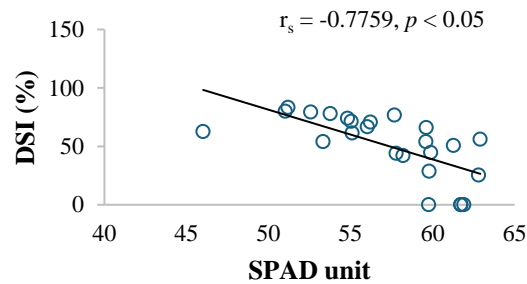


Figure 4.18: Scatter plot showing the relationship between chlorophyll content (SPAD unit) and disease severity index (DSI). Spearman's rank correlation coefficient (r_s) and P-values (p) are presented

4.1.2.3 Photosynthetic Rate vs Disease Severity Index

The spearman's rank correlation coefficient also indicates a very strong negative correlation between leaf photosynthetic rate ($r_s = -0.8521$, $p = 6.449e-08$) and the disease severity index (DSI) (Figure 4.19) (Chan, 2003; Akoglu, 2018). This implies an inverse relationship between photosynthesis rate and DSI in this study, indicating that as the DSI increases, the photosynthesis rate tends to decrease.

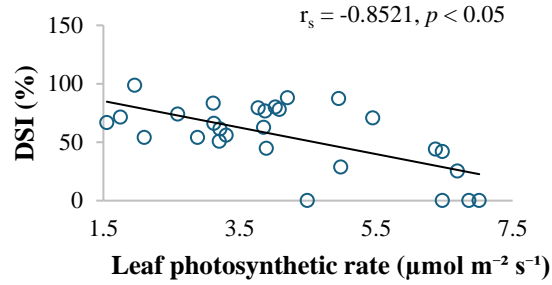


Figure 4.19: Scatter plot showing the relationship between leaf photosynthetic rate and disease severity index (DSI). Spearman's rank correlation coefficient (r_s) and P-values (p) are presented

4.1.2.4 *In Vitro* Growth Rates and the Disease Severity Index

The spearman's rank correlation coefficient indicates a fair positive correlation between the IVGR of the *G. boninense* isolates on MEA ($r_s = 0.4378, p = 0.03239$) and the DSI (Figure 4.20A) (Chan, 2003; Akoglu, 2018). A positive correlation coefficient implies that as the IVGR of *G. boninense* isolates on MEA increases, the DSI tends to increase as well. However, the relationship of IVGR of the *G. boninense* isolates on PDA ($r_s = 0.3652, p = 0.07926$) and SDA ($r_s = 0.2166, p = 0.3093$) with the disease severity index (DSI) was not significant (Figure 4.20B & C).

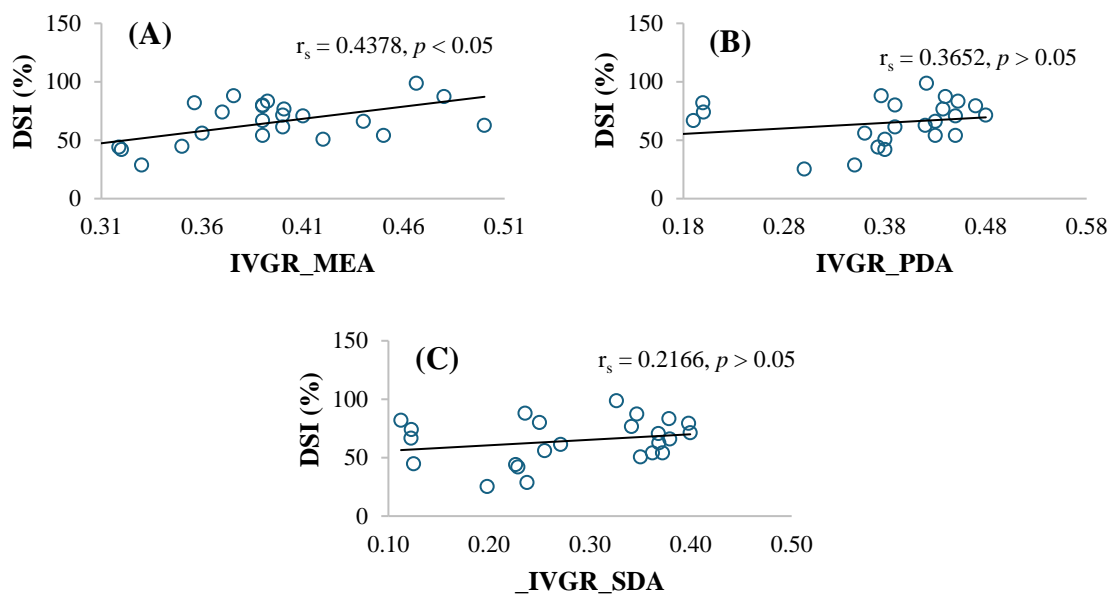


Figure 4.20: Scatter plots showing the relationship between *in vitro* growth rate (IVGR) of *Ganoderma boninense* isolates and disease severity index (DSI) on three different media: (A) Malt extract agar (MEA). (B) Potato dextrose agar (PDA). (C) Sabouraud dextrose agar (SDA). Spearman's rank correlation coefficient (r_s) and corresponding P-values (p) for each relationship are shown

4.1.3 Substrate Utilisation Profile

4.1.3.1 Carbon Sources

In this study, the most aggressive isolate, BLSM5B, could metabolize 65.26% (80/95 in plate PM1 and 44/95 in plate PM2) of tested carbon sources. In contrast, the least aggressive isolate, DR56, could only metabolize 4.73% (5/95 in plate PM1 and 4/95 in plate PM2) (Figure 4.21). About 23 compounds significantly support the growth of isolate BLSM5B (Table 4.3), while no compound significantly supports the growth of isolate DR56. In comparison, around 66 compounds inhibited the growth of the isolate BLSM5B (Appendix 2). In the case of isolate DR56, there were 181 different compounds that inhibited the growth (Appendix 2). Overall, isolate BLSM5B was more efficient at using carbon sources than isolate DR56.

PM1

PM2

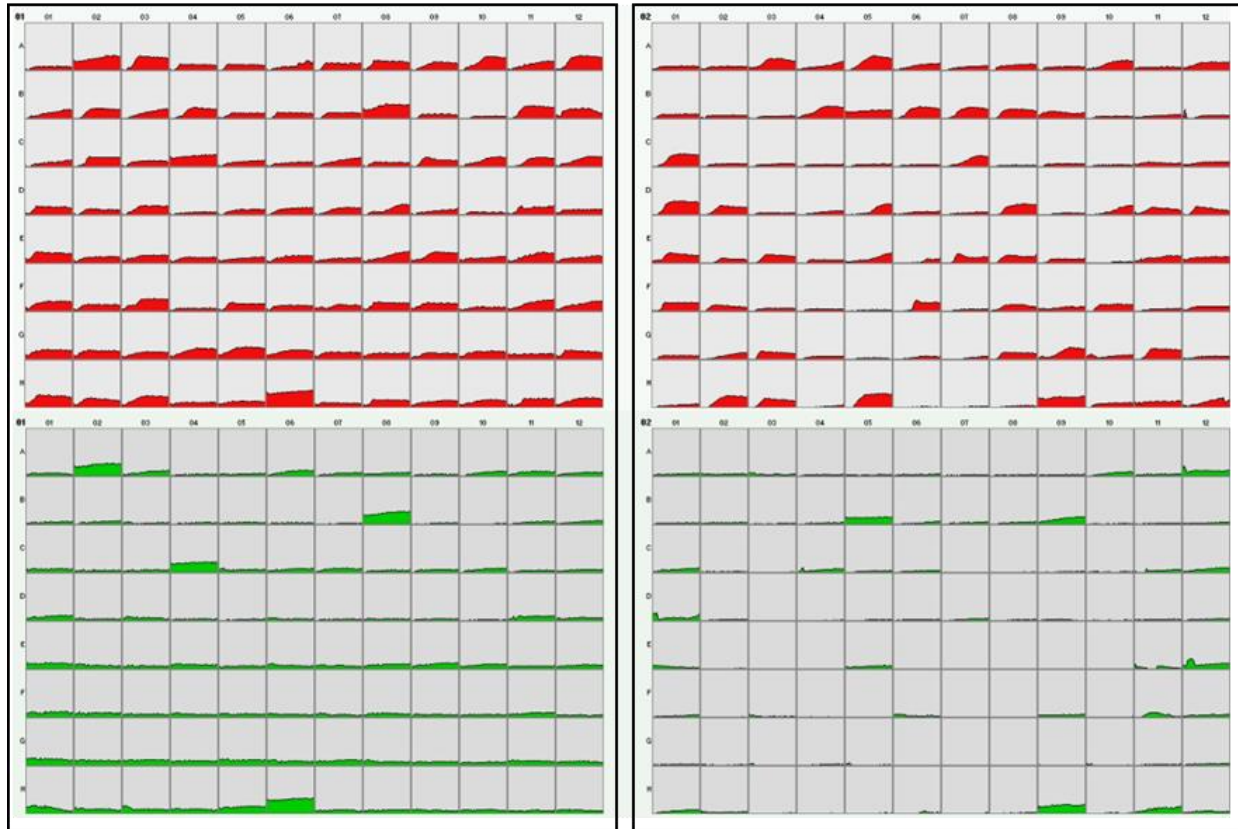


Figure 4.21: Data for biolog phenotype microarray PM1 and PM2. Utilisation of carbon sources by the isolates is indicated by red (BLSM5B) and green (DR56) areas in the growth curve for each substrate

Table 4.3: Substrates in PM1 and PM2 microplates that significantly supported the growth of isolate BLSM5B. There was no compound in PM1 and PM2 microplates that significantly supports the growth of isolate DR56

PM1		PM2	
Well	Substrate	Well	Substrate
A3	N-Acetyl-D-Glucosamine	A3	α -Cyclodextrin
A10	D-Trehalose	A5	γ -Cyclodextrin
A12	Dulcitol	B4	Amygdalin
B4	L-Fucose	B6	D-Arabitol
B11	D-Mannitol	B7	L-Arabitol
E8	β -Methyl-D-Glucoside	C1	Gentiobiose
E9	Adonitol	C7	β -Methyl-D-Galactoside
F3	Myo-Inositol	D1	D-Raffinose
F11	D-Cellobiose	D8	Xylitol
H3	m-Hydroxy Phenyl Acetic Acid	G9	L-Isoleucine
		H11	2,3-Butanone
		H2	L-Phenylalanine
		H5	D,L-Carnitine

4.1.3.2 Nitrogen Sources

As for the nitrogen sources utilisation (PM3), the isolate BLSM5B was able to use around 72.63% (69/95 in plate PM3), while isolate DR56 was only able to use 57.89% (55/95 in plate PM3) (Figure 4.22). There were nine compounds that significantly supported the growth of isolate BLSM5B (Table 4.4). However, only one compound significantly supported the growth of isolate DR56 (Table 4.4). Notably, both isolates displayed a shared preference for Ala-Asp, which significantly supported their growth (Table 4.4). The growth of isolates BLSM5B and DR56 was inhibited by 26 and 40 different compounds, respectively (Appendix 2). There was an apparent growth in the negative control without any nitrogen substrate (PM3, Well A1) inoculated with DR56 (Figure 4.22). Overall, the most aggressive isolate, BLSM5B, was more efficient using nitrogen sources than the least aggressive isolate, DR56.

4.1.3.3 Phosphorus and Sulphur Sources

Isolate BLSM5B was able to use 88.14% phosphorus sources (52/59 in plate PM4; Well A2-E12) and 74.29% sulphur sources (26/35 in plate PM4; Well F2-H12), whereas isolate DR56 was able to metabolize 81.36% phosphorus sources (48/59 in plate PM4) and 62.86% sulphur sources (22/35 in plate PM4) (Figure 4.22). There were eight phosphorus compounds that significantly supported the growth of the isolate BLSM5B, while three compounds significantly supported the growth of isolate DR56 (Table 4.5). As for sulphur compounds, two compounds significantly supported the growth of the isolate BLSM5B, while no sulphur compound tested significantly supported the growth of the isolate DR56 (Table 4.5). In contrast, the growth of isolates BLSM5B and DR56 was inhibited by seven and 11 different phosphorus compounds, respectively (Appendix 2). Besides that, the number of sulphur compounds that inhibited the growth of the isolates BLSM5B and DR56 was eight and 13, respectively (Appendix 2). Both

isolates showed apparent growth in the negative control without any phosphorus source (PM4, Well 1), but only the growth of isolate DR56 was significant (Figure 4.22 and Table 4.5).

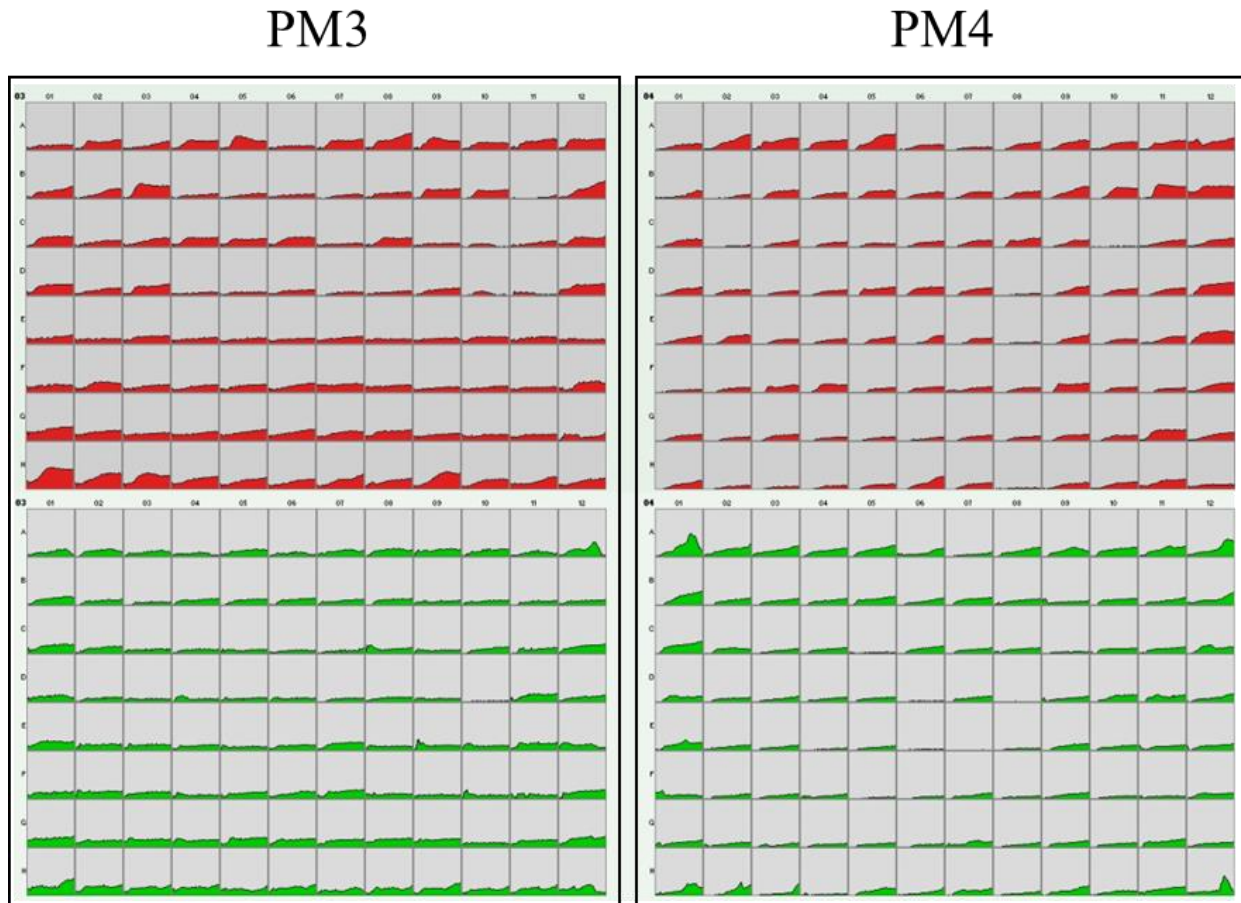


Figure 4.22: Data for biolog phenotype microarray PM3 and PM4. Utilisation of the nitrogen sources (PM3) and phosphorus (Well A2-E12) and sulfur source (PM4: Well F2-H12) by the isolates is indicated by red (BLSM5B) and green (DR56) areas in the growth curve for each substrate

Table 4.4: Substrates in PM3 microplates that significantly supported the growth of isolate BLSM5B and DR56

BLSM5B		DR56	
Well	Substrate	Well	Substrate
A8	L-Arginine	H1	Ala-Asp
B3	L-Histidine		
B12	L-Tryptophan		
H1	Ala-Asp		
H2	Ala-Gln		
H3	Ala-Glu		
H4	Ala-Gly		
H7	Ala-Thr		
H9	Gly-Gln		

Note: The substrates that supported the growth of both isolates DR56 and BLSM5B are indicated in bold text

Table 4.5: Substrates in PM4 microplates that significantly supported the growth of isolate BLSM5B and DR56

BLSM5B		DR56	
Well	Substrate	Well	Substrate
A2	Phosphate	A1	Negative Control
A3	Pyrophosphate	A12	Adenosine-3',5'-Cyclic Monophosphate
A5	Tripoly-Phosphate	B1	Thiophosphate
B9	Guanosine-3'-Monophosphate	C1	Phosphoenol Pyruvate
B10	Guanosine-5'-Monophosphate		
B11	Guanosine-2',3'-Cyclic Monophosphate		
D12	Uridine-3',5'-Cyclic Monophosphate		
E12	Thymidine 3',5'-Cyclic Monophosphate		
G11	L-Methionine Sulfoxide		
H6	Taurine		

4.1.3.4 Biosynthetic Pathways/Nutrient Supplements

Isolate BLSM5B demonstrated 88/94 (93.62%) different biosynthetic pathways, while isolate DR56 presented only 20/94 (21.28%) biosynthetic pathways (Figure 4.23). There were 30

substrates in PM5 microplate that significantly supported the growth of isolate BLSM5B (Table 4.6). However, none of the substrates in PM5 microplate that significantly supported the growth of isolate DR56. Isolate BLSM5B could not metabolized only six substrates in PM5 microplate, while DR56 could not metabolized more than 70 substrates (Appendix 2). Both isolates showed apparent growth in the negative control (PM5, Well A1) without any nutrient supplements (Figure 4.23). However, only the growth of isolate BLSM5B was significant (Table 4.6).

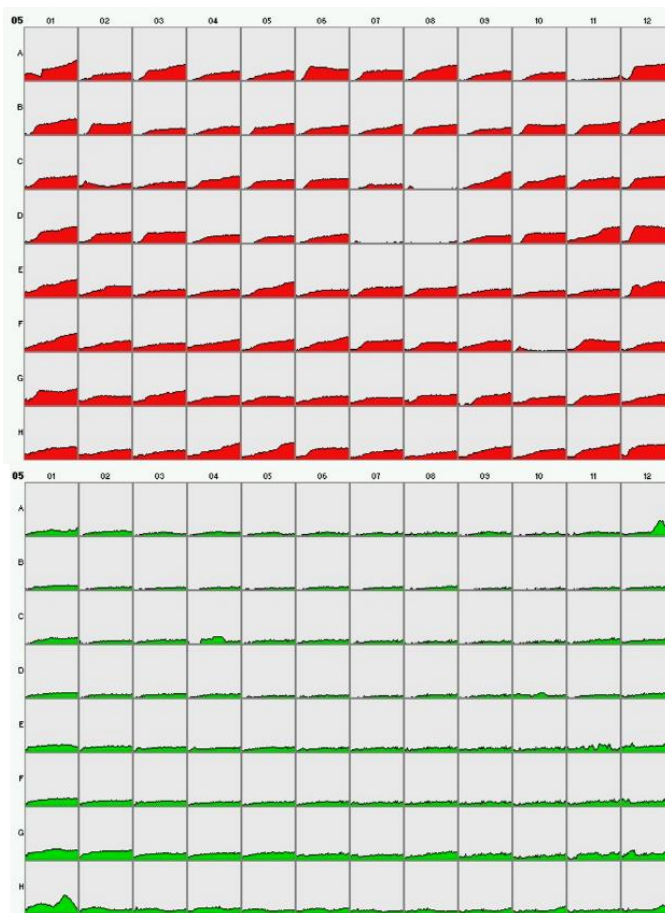


Figure 4.23: Data for biolog phenotype microarray PM5. Activity of biosynthetic pathways exhibited by the isolates was indicated by red (BLSM5B) and green (DR56) areas in the growth curve for each substrate

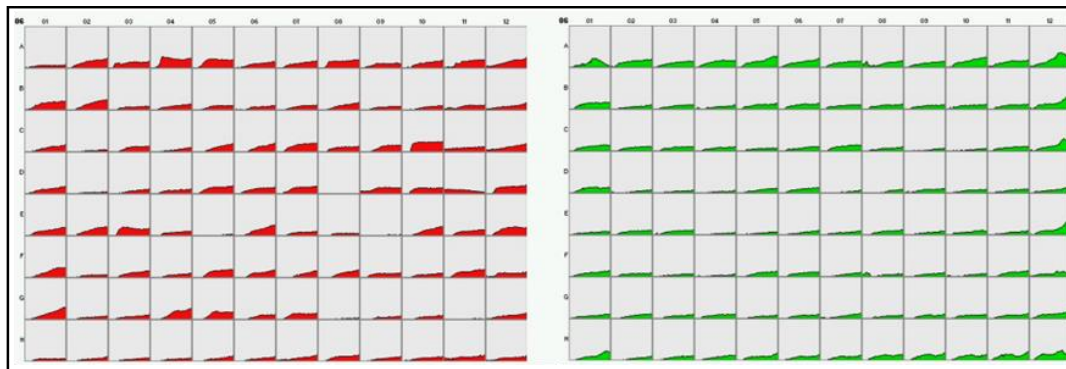
Table 4.6: Substrates in PM5 microplates that significantly supported the growth of isolate BLSM5B

Well	Substrate	Well	Substrate
A1	Negative Control	D12	2'-Deoxy Cytidine
A3	L-Alanine	E1	Putrescine
A8	L-Glutamic Acid	E5	Pyridoxal
A12	2'-Deoxy Adenosine	E12	2'-Deoxy Uridine
B1	L-Glutamine	F1	Quinolinic Acid
B2	Glycine	F6	Hematin
B11	Guanosine	G1	Oxaloacetic Acid
B12	2'-Deoxy Guanosine	G3	Cyano-Cobalamine
C1	L-Proline	G9	Riboflavin
C4	L-Tryptophan	G11	Menadione
C9	(5) 4-Amino Imidazole-4(5)- Carboxamide	H4	Caprylic Acid
C10	Hypoxanthine	H5	D,L- α -Lipoic Acid (oxidized form)
C12	2'-Deoxy Inosine	H9	Tween 20
D1	L-Ornithine	H11	Tween 60
D11	Cytidine	H12	Tween 80

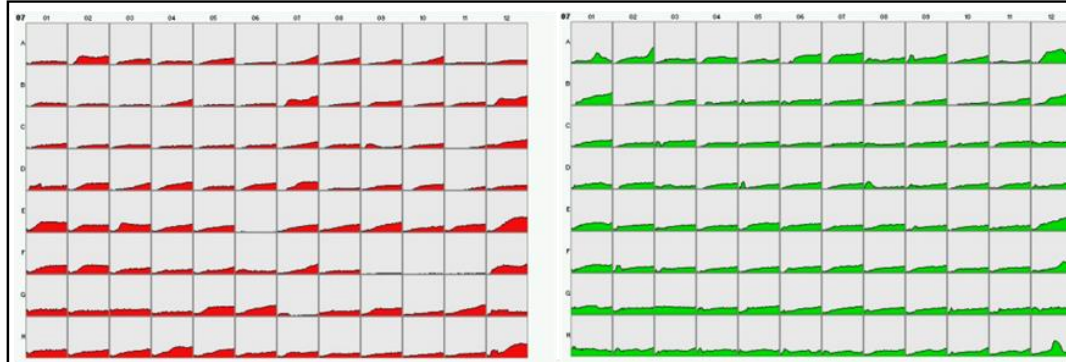
4.1.3.5 Peptide Nitrogen Sources

Using data from PM6, PM7, and PM8, the isolates BLSM5B and DR56 were able to use around 70.57% (72/94 in plate PM6, 65/94 in plate PM7, and 62/94 in plate PM8) and 72.34% (62/95 in plate PM6, 76/95 in plate PM7, and 66/95 in plate PM8) of tested peptide nitrogen sources, respectively (Figure 4.24). About 25 compounds significantly support the growth of isolate BLSM5B (Table 4.7). Whereas there were 16 compounds that significantly supported the growth of isolate DR56 (Table 4.7). Notably, Met-His, Thr-Arg, Gly-Asn, and Thr-Gln significantly supported the growth of both isolates BLSM5B and DR56 (Table 4.8 and Table 4.9). In comparison, the growth of isolates BLSM5B and DR56 was inhibited by 86 and 81 different compounds, respectively (Appendix 2). There was an apparent growth in the negative control without any peptide nitrogen source (Well A1) of PM6, PM7, and PM8 microplates inoculated with DR56 without any nitrogen source (Figure 4.24). Overall, using data from PM6 to PM8, isolates BLSM5B and DR56 presented 199 and 204 nitrogen pathways, respectively (Figure 4.24). Overall, isolate DR56 was more efficient using peptide nitrogen sources than isolate BLSM5B.

PM6



PM7



PM8

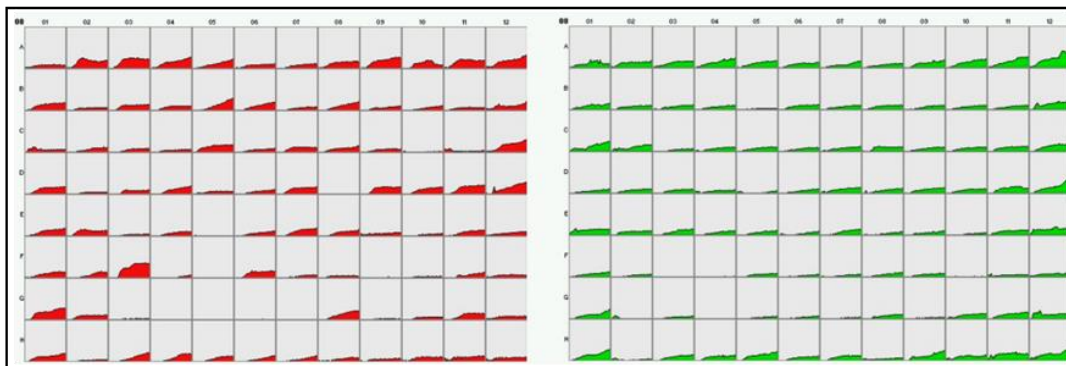


Figure 4.24: Data for biolog phenotype microarray PM6, PM7, and PM8. Utilisation of the peptide nitrogen sources by the isolates was indicated by red (BLSM5B) and green (DR56) areas in the growth curve for each substrate

Table 4.7: Substrates in PM6 microplates that significantly supported the growth of isolate BLSM5B and DR56

BLSM5B		DR56	
Well	Substrate	Well	Substrate
A4	Ala-Arg	A5	Ala-Asn
B2	Ala-Thr	A10	Ala-Lys
C10	Asp-Glu	B12	Arg-Lys
F1	Gly-Thr	C12	Asp-Lys
G1	His-Tyr	E12	Gly-Ser
G4	Ile-Arg		

Table 4.8: Substrates in PM7 microplates that significantly supported the growth of isolate BLSM5B and DR56

BLSM5B		DR56	
Well	Substrate	Well	Substrate
B12	Met-His	A2	L-Glutamine
E1	Ser-Ala	A6	Lys-Ala
E9	Ser-Tyr	A7	Lys-Arg
E12	Thr-Arg	A12	Lys-Phe
G5	Tyr-Ala	B1	Lys-Pro
G6	Tyr-Gln	B12	Met-His
G11	Tyr-Lys	E12	Thr-Arg
H4	Val-Asn		
H12	γ -Glu-Gly		

Note: The substrates that supported the growth of both isolates DR56 and BLSM5B are indicated in bold text

Table 4.9: Substrates in PM8 microplates that significantly supported the growth of isolate BLSM5B and DR56

BLSM5B		DR56	
Well	Substrate	Well	Substrate
A3	Ala-Asp	A11	Glu-Ala
A4	Ala-Gln	A12	Gly-Asn
A9	Asp-Gln	D12	Thr-Gln
A12	Gly-Asn	H1	Gly-Gly-Ala
B5	His-His		
C12	Pro-Asn		
D11	Thr-Asp		
D12	Thr-Gln		
F3	β -Ala-Gly		
G1	γ -Glu-Gly		

Note: The substrates that supported the growth of both isolates DR56 and BLSM5B are indicated in bold text

4.1.3.6 Osmolytes

In general, isolate BLSM5B demonstrated adaptability to 46.32% (44/95 in plate PM9) of the tested osmolyte conditions, while isolate DR56 exhibited adaptability to 60% (57/95 in plate PM9) (Figure 4.25). Using data from PM9, isolate BLSM5B could metabolize up to 4% NaCl (PM9, Well A1-A4) (Figure 4.25). Interestingly, although isolate BLSM5B could not metabolize

6% NaCl alone, it exhibited metabolic activity when 6% NaCl was combined with KCl (PM9, Well C1), L-proline (PM9, Well C2), and trigonelline (PM9, Well C12) (Figure 4.25). Additionally, isolate BLSM5B also could metabolize up to 6% potassium chloride (PM9, Well D1-D4), 5% sodium sulfate (PM9, Well D5-D8), 20% ethylene glycol (PM9, Well D9-D12), 2% sodium formate (PM9, Well E2-E1), 3% urea (PM9, Well E7-E8), 100 mM sodium phosphate pH 7 (PM9, Well G1-G3), 50 mM ammonium sulfate pH 8 (PM9, Well G9-G11), and 100 mM sodium nitrate (PM9, Well H1-H6) (Figure 4.25). Besides that, isolate BLSM5B also could metabolize different concentrations of sodium lactate except for 8%, 9%, 10%, and 11% sodium lactate (PM9, Well F8-F11) (Figure 4.25). As for sodium nitrite, isolate BLSM5B could only be able to metabolize at a concentration of 10 mM (PM9, Well H7) (Figure 4.25). Notably, isolate BLSM5B could not metabolize sodium benzoate pH 5.2, ranging from 20-200 mM (PM9, Well G5-G8) (Figure 4.25). Osmolyte conditions that significantly supported the growth of the isolates BLSM5B included 1% NaCl, 20% ethylene glycol, 1% sodium lactate, 2% sodium lactate, 10 mM ammonium sulfate pH 8, and 10 mM sodium nitrate (Table 4.10). Overall, there was 51 osmolyte conditions that inhibited the growth of isolate BLSM5B (Appendix 2).

Isolate DR56, on the other hand, could metabolize 1%, 2%, 3%, 5%, 5.5%, and 6% NaCl (PM9, Well A1-A3, and A5-A7) (Figure 4.25). Additionally, isolate DR56 exhibited metabolic activity in 6% NaCl in the presence of ectoine, choline, phosphorylcholine, L-carnitine, N-acetyl-L-glutamine, glutathione, glycerol, trehalose, trimethylamine, octopine, and trigonelline (PM9, Well B7-B9, B12, C3, C6-C8, and C10-C12) (Figure 4.25). Moreover, isolate DR56 could metabolize up to 6% potassium chloride (PM9, Well D1-D4), 3% urea (PM9, Well E7-E8), 200 mM sodium phosphate pH 7 (PM9, Well G1-G4), and 100 mM ammonium sulfate pH 8 (PM9, Well G9-G12) (Figure 4.25). Isolate DR56 was also able to metabolize 2%, 4%, and 5% sodium

sulfate (PM9, Well D5, D7, and D8), 10% and 20% ethylene glycol (PM9, Well D10 and D12), as well as 3%, 4%, and 5% sodium formate (Figure 4.25). Although isolate DR56 could metabolize different concentrations of sodium lactate and sodium nitrate; however, it was unable to metabolize 11% sodium lactate (PM9, Well F11) and 60 mM sodium nitrate (PM9, Well H4) (Figure 4.25). In terms of sodium nitrite, isolate DR56 could only metabolize it at concentrations of 10mM, 20mM, and 80mM (PM9, Well H7) (Figure 4.25). Similar to isolate BLSM5B, isolate DR56 was also unable to metabolize any concentration of sodium benzoate at pH 5.2 (PM9, Well G5-G8) (Figure 4.25). Only one osmolyte condition that significantly supported the growth of the isolate DR56. Overall, there was 38 osmolyte conditions that inhibited the growth of isolate DR56 (Appendix 2).

4.1.3.7 pH

Overall, isolate BLSM5B demonstrated adaptability to 81.91% (77/94 in plate PM10) of the tested pH conditions, while isolate DR56 exhibited adaptability to 64.89% (57/95 in plate PM9) (Figure 4.25). Isolate BLSM5B could grow in the pH range between 3.5 and 10 (PM10, Well A1-A12), with significant growth was observed between pH 3.5 and 5 (Figure 4.25 and Table 4.11). When combined with various amino acids at a pH of 4.5, isolate BLSM5B exhibited growth in all substrates except when combined with the amino acids L-homoarginine (PM10, Well C11), anthranilic acid (PM10, Well D1), and p-amino-benzoic acid (PM10, Well D5) (Figure 4.25). There were 20 amino acids that significantly support the growth of isolate BLSM5B at pH 4.5 (Table 4.11). Additionally, when combined with various amino acids at a pH of 9.5, isolate BLSM5B exhibited growth in all tests except for following amino acids: glycine (PM10, Well E8), L-histidine (PM10, Well E9), L-isoleucine (PM10, Well E10), L-serine (PM10, Well F4), L-threonine (PM10, Well F5), L-tryptophan (PM10, Well F6), L-tyrosine (PM10, Well F7), L-valine

(PM10, Well F8), anthranilic acid (PM10, Well G1), agmatine (PM10, Well G4), cadaverine (PM10, Well G5), and phenylethylamine (PM10, Well G8) (Figure 4.25). Among the tested substrates, only pH 9.5 combined with L-proline (PM10, Well F3) significantly supports the growth of isolate BLSM5B (Table 4.11). Besides that, X- β -D-glucoside, X- β -D-galactoside, and X- β -D-glucuronide significantly support the growth of isolate BLSM5B except for X- α -D-galactoside (PM10, Well H4) and X- β -D-glucosaminide (PM10, Well H8) (Figure 4.25 and Table 4.11). Overall, there was 17 pH conditions that inhibited the growth of isolate BLSM5B (Appendix 2).

As for isolate DR56, it could grow in the pH range between 4 and 10 (PM10, Well A2-A12), (Figure 4.25). At a pH of 4.5, isolate DR56 exhibited growth with various amino acids, except for anthranilic acid (PM10, Well D1) and L-norleucine (PM10, Well D2) (Figure 4.25). Only the presence of 5-hydroxy tryptophan (PM10, Well D9) at a pH of 4.5 significantly supports the growth of isolate DR56 (Figure 4.25 and Table 4.11). Isolate DR56 also exhibited growth in the presence of eight types of amino acids at pH 9.5, namely L-glutamic acid, glycine, L-histidine, L-leucine, L-lysine, anthranilic acid, creatine, and urea (PM10, Well E6, E8-E9, E11-E12, G1, G10, and G12) (Figure 4.25). Additionally, metabolic activity of isolate DR56 also was observed in the well containing X-caprylate, X- α -D-glucoside, X- β -D-glucoside, X- α -D-galactoside, X- β -D-galactoside, X- α -D-glucuronide, X- β -D-glucuronide, X- β -D-galactosaminide, X- α -D-mannoside, X-PO₄, X-SO₄ except for X- β -D-glucosaminide (PM10, Well H8) (Figure 4.25). The growth of both isolates BLSM5B and DR56 was significantly supported by 5-hydroxy tryptophan at pH 4.5 (Table 4.11). Overall, there was 32 pH conditions that inhibited the growth of isolate DR56 (Appendix 2).

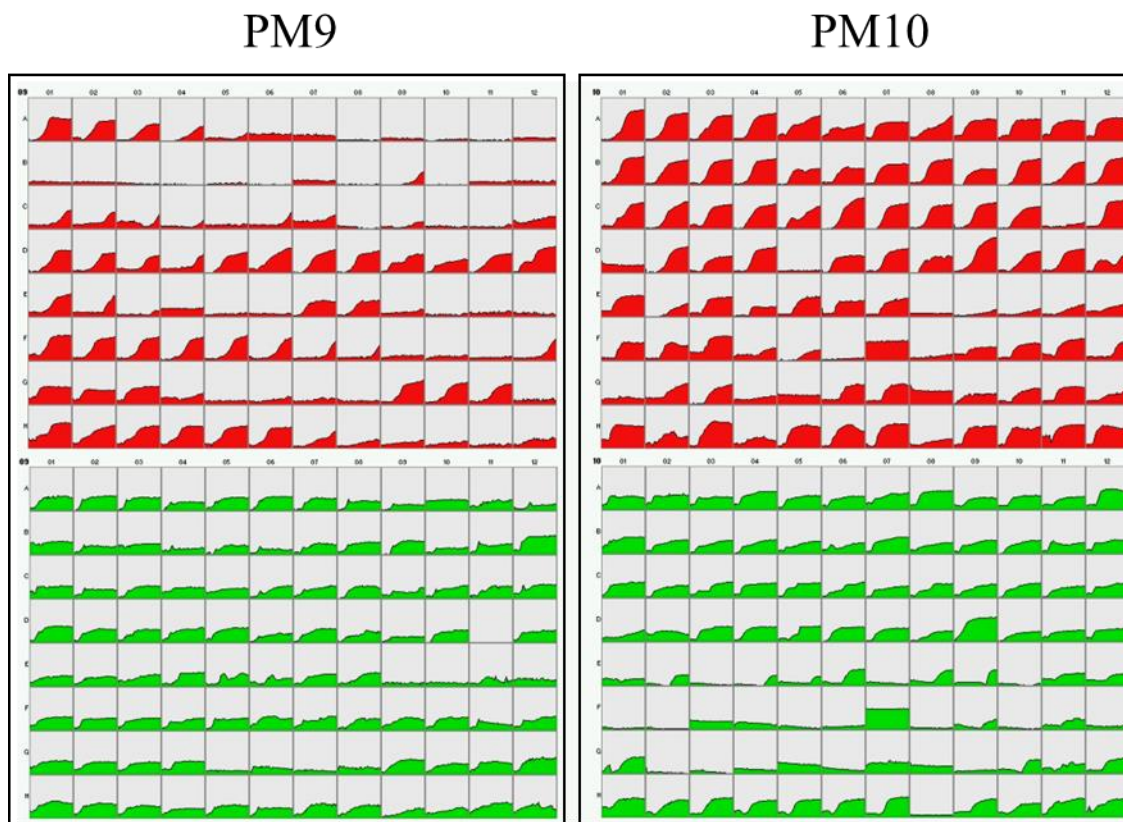


Figure 4.25: Data for biolog phenotype microarray PM9 (Osmolytes) and PM10 (pH). The metabolic activity was indicated by red (BLSM5B) and green (DR56) areas in the growth curve for each tested condition

Table 4.10: Osmolytes conditions in PM9 microplates that significantly supported the growth of isolate BLSM5B. There were no osmolytes conditions that significantly support the growth of isolate DR56

Well	Substrate	Well	Substrate
A1	1% NaCl	F2	2% Sodium Lactate
D12	20% Ethylene Glycol	G9	10 mM Ammonium Sulfate pH 8
F1	1% Sodium Lactate	H1	10 mM Sodium Nitrate

Table 4.11: pH conditions in PM10 microplates that significantly supported the growth of isolate BLSM5B and DR56

BLSM5B			
Well	Substrate	Well	Substrate
A1	pH 3.5	C6	pH 4.5 + L-Tryptophan
A2	pH 4	C7	pH 4.5 + L-Citrulline
A3	pH 4.5	C8	pH 4.5 + L-Valine
A4	pH 5	C9	pH 4.5 + Hydroxy-L-Proline
B1	pH 4.5	C12	pH 4.5 + L-Homoserine
B2	pH 4.5 + L-Alanine	D2	pH 4.5 + L-Norleucine
B3	pH 4.5 + L-Arginine	D4	pH 4.5 + α -Amino-N-Butyric Acid
B4	pH 4.5 + L-Asparagine	D7	pH 4.5 + D-Lysine
B8	pH 4.5 + Glycine	D9	pH 4.5 + 5-Hydroxy Tryptophan
B10	pH 4.5 + L-Isoleucine	D11	pH 4.5 + Trimethylamine-N-oxide
B12	pH 4.5 + L-Lysine	F3	pH 9.5 + L-Proline
C1	pH 4.5 + L-Methionine	H3	X- β -D-Glucoside
C2	pH 4.5 + L-Phenylalanine	H5	X- β -D-Galactoside
C3	pH 4.5 + L-Proline	H7	X- β -D-Glucuronide
C4	pH 4.5 + L-Serine		

Table 4.11 continued

DR56			
Well	Substrate	Well	Substrate
D9	pH 4.5 + 5-Hydroxy Tryptophan		

Note: The pH conditions that supported the growth of both isolates DR56 and BLSM5B are indicated in bold text

4.1.3.8 Summary of Substrates Utilisation by Isolates BLSM5B and DR56

In this study, there were variation observed in the metabolic capabilities and adaptability of the two isolates: BLSM5B and DR56. The most aggressive isolate in this study, BLSM5B, demonstrated a higher utilisation ratio in carbon (65.26%), nitrogen (72.63%), phosphorus (88.14%), and sulphur (74.29%) sources. Additionally, it displayed a diverse range of biosynthetic pathways (93.62%), and higher pH (81.91%) adaptability (Table 4.12). The less aggressive isolate, isolate DR56, on the other hand, displayed higher utilisation ratio in peptide nitrogen source (72.34%) and adaptability in varied osmolyte (60.00%) conditions (Table 4.12).

Table 4.12: Types of substrates and their utilisation ratio for isolates BLSM5B and DR56

Substrate	BLSM5B	DR56
Carbon sources	65.26%	4.73%
Nitrogen sources	72.63%	57.89%
Phosphorus sources	88.14%	81.36%
Sulphur sources	74.29%	62.86%

Table 4.12 continued

Biosynthetic pathways	93.62%	21.28%
Peptide nitrogen sources	70.57%	72.34%
Osmolytes	46.32%	60.00%
pH	81.91%	64.89%

Note: High utilization ratios (%) are indicated in bold

4.1.4 Substrate Utilisation Differences between Isolates BLSM5B and DR56

There was significant variation in the utilisation of various carbon sources (PM1 and PM2) when the two isolates, BLSM5B and DR56, were compared (Figure 4.26). The utilisation of N-acetyl-D-glucosamine (PM1, Well A3), dulcitol (PM1, Well A12), D-mannitol (PM1, Well B11), myo-inositol (PM1, Well F3), α -cyclodextrin (PM2, Well A3), γ -cyclodextrin (PM2, Well A5), amygdalin (PM2, Well B4), D-arabitol (PM2, Well B6), D-raffinose (PM2, Well D1), xylitol (PM2, Well D8), L-isoleucine (PM2, Well G9), L-lysine (PM2, Well G11), L-phenylalanine (PM2, Well H2), and D,L-carnitine (PM2, Well H5) by isolate BLSM5B was significantly higher than the isolate DR56 (Figure 4.26). As for nitrogen sources (PM3), isolate BLSM5B demonstrated a significantly higher utilisation of L-histidine (Well B3) and Ala-Asp (Well H1) compared to isolate DR56 (Figure 4.26). In terms of biosynthetic pathways/nutrient supplements (PM5), isolate BLSM5B exhibited a significant utilisation of L-alanine (Well A3), L-aspartic acid (Well A5), L-glutamic acid (Well A8), 2'-deoxy adenosine (Well A12), L-glutamine (Well B1), glycine (Well B2), 2'-deoxy guanosine (Well B12), cytidine (Well D11), 2'-deoxy cytidine (Well D12), and tween 80 (Well H12), as compared to isolate DR56 (Figure 4.26). Isolate BLSM5B also displayed

greater levels of utilisation of two peptide nitrogen sources (PM6 and PM8): Asp-Glu (PM6, Well C10) and β -Ala-Gly (PM8, Well F3), as compared to isolate DR56 (Figure 4.26).

As for the growth under various osmolytes (PM9), isolate DR56 exhibited a significant growth in 5%, 6.5%, 8%, and 9% NaCl (Wells A5, A8, A10, and A11, respectively) in comparison to isolate BLSM5B (Figure 4.26). Since the slopes for the growth in 6.5%, 8%, and 9% NaCl (Wells A8, A10, and A11, respectively) for both isolates (BLSM5B and DR56) did not meet the criteria established for this study, the differences were not taken into account. Similarly, the growth of isolates BLSM5B and DR56 in 6% NaCl (Well A7) and 6% NaCl incorporated with N-N dimethyl glycine (Well A3), or β -glutamic acid (Well C4) were also not taken into account for the same reason. On the other hand, isolate DR56 presented a significant growth in 6% NaCl incorporated with choline (Well B8), phosphorylcholine (Well B9), L-carnitine (Well B12), trehalose (Well C8), trimethylamine (Well C10), and octopine (Well C11) as compared to isolate BLSM5B (Figure 4.26). Comparing isolates BLSM5B and DR56, the former showed significantly greater growth at 3% sodium sulfate (Well D6) and ethylene glycol (5% and 15%, Well D9 and D11, respectively) (Figure 4.26). Whereas, as compared to isolate BLSM5B, isolate DR56 showed significant growth in the presence of 80 mM sodium nitrite (Well H11) (Figure 4.26).

In terms of the growth under various pH conditions (PM10), isolate BLSM5B showed significant growth at pH 8.5 (Well A9) as compared to isolate DR56 (Figure 4.26). When combined with glycine (amino acid) at a pH of 4.5 (Well B8), isolate BLSM5B showed significant growth compared to isolate DR56 (Figure 4.26). On the other hand, isolate DR56 displayed significant growth at pH 4.5 when combined with p-aminobenzoic Acid (Well D5) in comparison to isolate BLSM5B (Figure 4.26). When combined with L-arginine (Well E3), L-aspartic acid

(Well E5), L-glutamine (Well E7), L-methionine (Well F1), L-phenylalanine (Well F2), L-proline (Well F3), L-ornithine (Well F10), L-homoarginine (Well F11), L-norleucine (Well G2), L-norvaline (Well G3), and putrescine (Well G6) at a pH of 9.5, isolate BLSM5B presented significant growth compared to isolate DR56 (Figure 4.26). Notably, isolate BLSM5B also displayed significant growth when compared to isolate DR56 at pH 9.5 (Well E1) (Figure 4.26); however, at the same pH (Well A11), there was no significant difference between the two isolates.

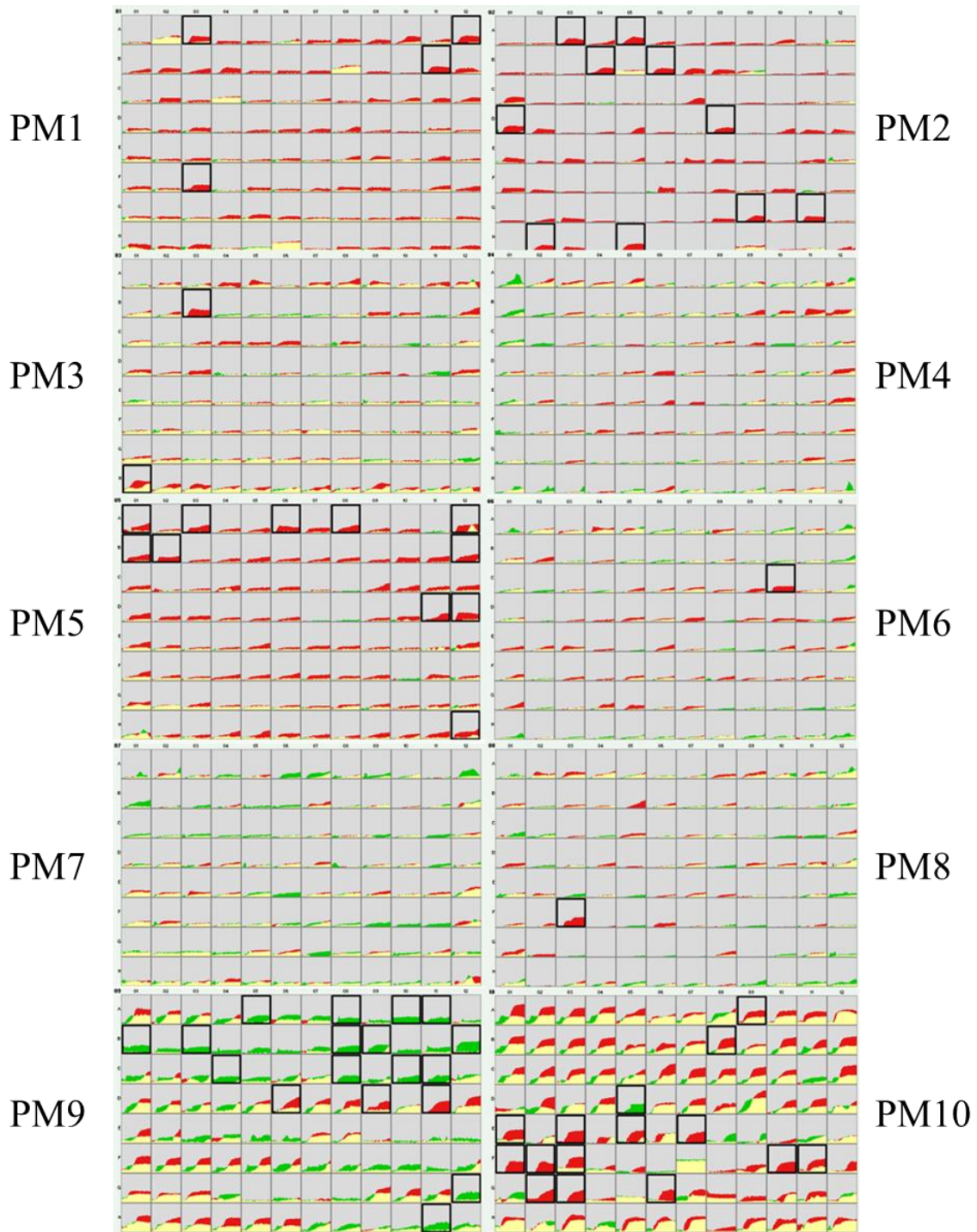


Figure 4.26: Data for biolog phenotype microarray PM 1-10 plates comparing isolate BLSM5B (most aggressive) and isolate DR56 (least aggressive). Red presented the metabolic fingerprint of isolate BLSM5B; green presented the metabolic fingerprint of isolate DR56; and yellow presented the common fingerprints of both isolates. The boxed well indicates a significant difference in substrate utilisation

4.2 Disease Confirmation Methods

4.2.1 Re-isolation from Infected Tissue

The bole and the root tissues of uninoculated seedlings did not produce brown pigmentation when plated on *Ganoderma* selective medium (GSM) (Figure 4.27A). However, tissues of all the infected seedlings (bole and root tissues), developed brown pigments identical to those produced by *G. boninense* when plated on the GSM (Figure 4.27B). *Ganoderma boninense* took around seven to 14 days to grow full plate on GSM. When the white mycelium grew on the infected tissue was inoculated on malt extract agar (MEA), it displayed a similar morphology to the original *G. boninense* isolates. Out of 240 inoculated seedlings, a total of 60 (25%) *G. boninense* pure cultures were successfully obtained from the infected tissue on GSM. During the incubation period, a majority of the infected tissue plated on GSM showed contamination by other fungi (Figure 4.28), thus making it impossible to isolate pure cultures of *G. boninense* from those plates. Additionally, some of the infected tissue plated on GSM did not produce fungal mycelia, despite showing brown pigmentation. Aside from that, the most commonly isolated fungi on contaminated GSM were identified, namely *Duportella trigonosperma*, *Curvularia aeria*, *Peniophora malaiensis*, *Curvularia eragrostidis*, and *Marasmius palmivorus* (Appendix 3).

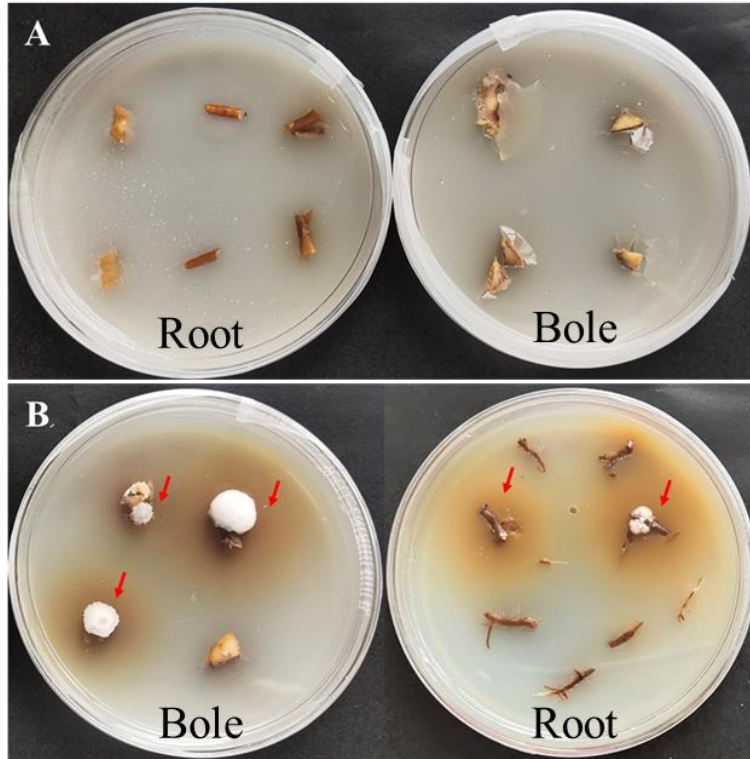


Figure 4.27: Re-isolation on *Ganoderma* selective medium. (A) The bole and the roots of uninoculated seedlings. (B) The bole and the roots of inoculated seedlings. Brown pigmentation forms around the infected tissue (red arrow)



Figure 4.28: Contaminated *Ganoderma* selective medium

4.2.2 Re-isolation from Fruiting Body

The fruiting body harvested from infected seedlings also exhibited brown pigmentation similar to the infected tissue when inoculated on GSM (Figure 4.29). When the white mycelium grew on the fruiting body was inoculated on MEA, it displayed morphology consistent with the original *G. boninense* isolates. From a total of 240 inoculated seedlings, 167 (69.58%) produces fruiting bodies. However, only 36.67% (88/167) *G. boninense* pure culture were successfully re-isolated from the fruiting body on GSM. Similarly, throughout the incubation period, most of the fruiting bodies plated on GSM were contaminated by other fungi (Figure 4.28 and Appendix 3), making it difficult to isolate pure cultures of *G. boninense* from those plates. In addition, in the present study, not all of the inoculated seedlings produced fruiting bodies.



Figure 4.29: Fruiting body inoculated on *Ganoderma* selective medium exhibited brown pigmentation (red arrow)

4.2.3 Molecular Identification

4.2.3.1 Identification of Fungi Isolated from Bole and Root Tissue on GSM

All the identity of fungi isolated from the bole and root tissue plated on GSM was verified as *G. boninense* based on the DNA sequence amplified with ITS1/ITS4 primer pair (650 bp DNA fragment) (Appendix 4).

4.2.3.2 Identification of Fungi Isolated from Fruiting Body on GSM

The identity of the fungi isolated from the fruiting bodies plated on GSM was confirmed as *G. boninense* via the sequence of DNA amplified using ITS1/ITS4 primer pair (650 bp DNA fragment) (Appendix 5).

4.2.3.3 Identification of Fungi Based on Genomic DNA of inoculated Bole and Root Tissues

The amplification of the genomic DNA extracted from the bole and root tissue of inoculated seedlings using the GanET/ITS3 primer pair produced a 320 bp DNA fragment identical to the amplicon of DNA from *G. boninense* pure culture. DNA bands were absent in lane 1 and 2 for the bole and the root tissue of uninoculated seedlings (Figure 4.30). Further validation by sequencing of the ITS1/ITS4 primer pair amplified PCR products of the DNA extracted from the infected bole and the root tissue confirmed the presence of *G. boninense* in the infected seedling (Appendix 6). A total of 110 (45.83%) *G. boninense* DNA were successfully recovered from 240 inoculated seedlings (Appendix 6). The rest of the genomic DNA samples (130) did not have amplification even though the inoculated seedlings showed some lesions on the infected tissues.

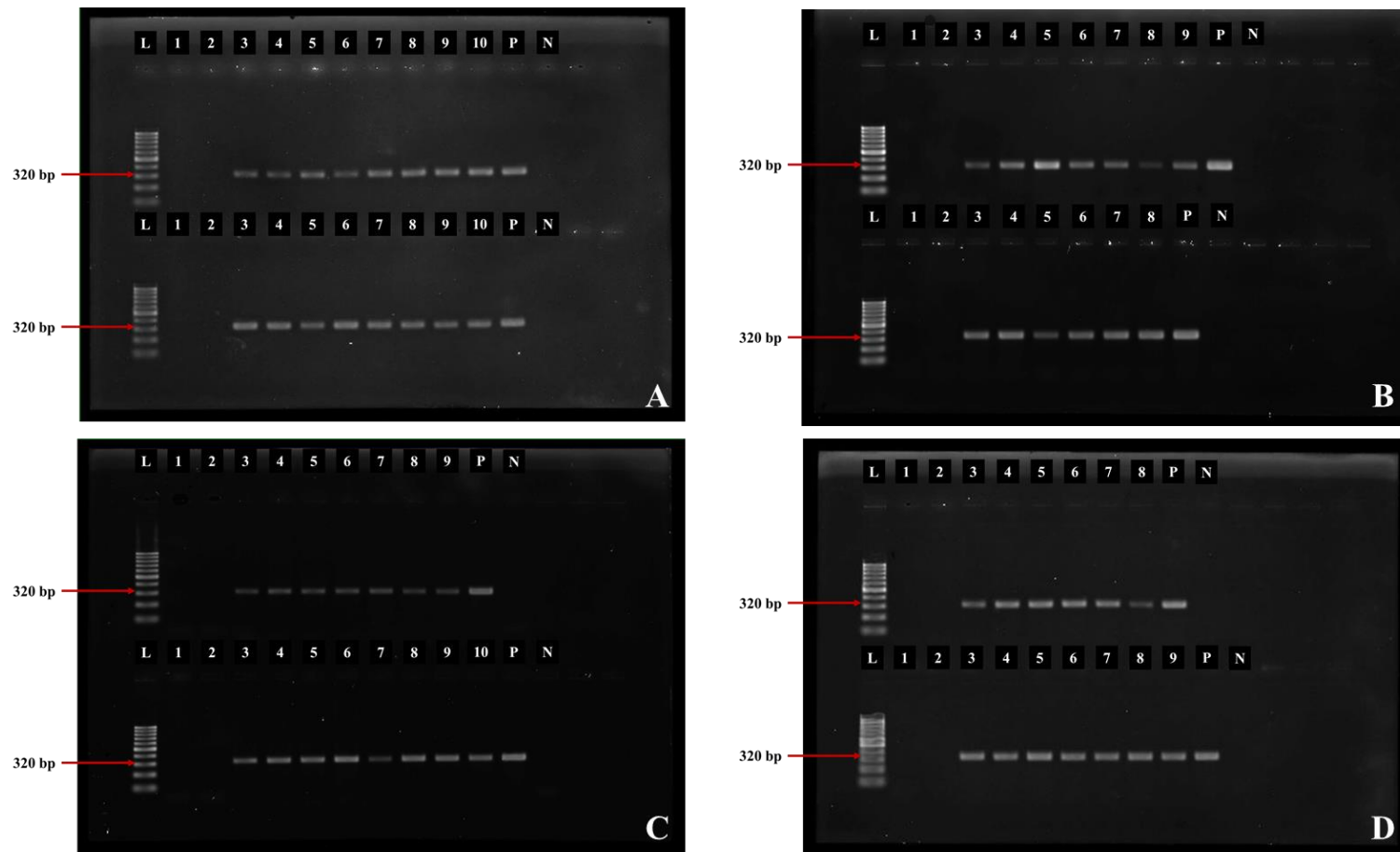


Figure 4.30: The amplification of fungal DNA recovered from the bole (top lane) and the root (bottom lane) tissue using the GanET/ITS3 primer pair after (A) three, (B) four, (C) five, and (D) six months after inoculation. “L”, “P”, and “N” indicate 100bp DNA ladder, positive control, and negative control, respectively. Lane 1 and 2 (A to D) is the DNA recovered from uninoculated oil palm seedlings. The remainder is the DNA recovered from oil palm seedlings inoculated with isolate BLSM5B, DR56, DR51B, IGKI3, BLSM4A, and BLSM5A

4.2.3.4 Comparison of Disease Confirmation Methods

Among the disease confirmation methods evaluated in this study, fungal DNA detection from infected tissues has the highest success rate (45.83%) in confirming the presence of *G. boninense* compared to fungal culture established from re-isolation from infected tissue (25%) and fruiting body (36.67%) of *G. boninense* (Figure 4.31).

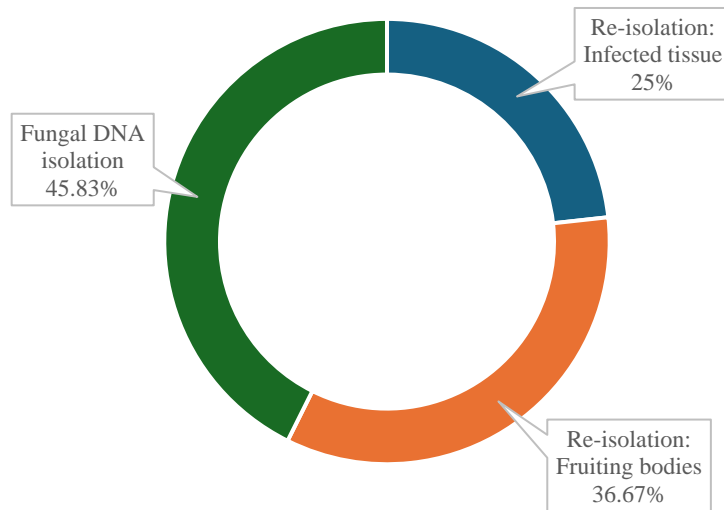


Figure 4.31: Success rate of confirming the presence of *Ganoderma boninense* based on PCR amplification using genomic DNA of infected tissue and fungal culture established from re-isolation from infected tissue and fruiting body of *Ganoderma boninense*

CHAPTER 5

DISCUSSION

5.1 *Ganoderma boninense* Isolates Aggressiveness

Ganoderma boninense is a main culprit of basal stem rot (BSR) that threatened the sustainability of oil palm industry. This disease causes yield decline and palm death several years after observation of initial disease symptoms (Kamu, 2018). However, there is limited information on the aggressiveness of *G. boninense* isolates reported in Sarawak in a wider geographical context, despite the serious effects of *Ganoderma* infection on the oil palm industry.

In the present study, it was observed that seedlings inoculated with the *G. boninense* isolates exhibited signs and symptoms such as necrosis or chlorosis leaves and the appearance of the fruiting body as early as two months after inoculation (MAI), which is similar to studies done by Kok et al. (2013) and Lo et al. (2023). Despite having necrotic leaves, some of the inoculated seedlings did not produce fruiting bodies. The necrotic leaves could be attributed to the impact of bole rotting, which disrupts the vascular systems of the infected seedlings, prevents water and nutrient uptake, and leads to leaf necrosis or wilting (Khoo and Chong, 2023).

Most of the inoculated seedlings displayed external symptoms by the end of three months post-inoculation. At 4 MAI, most inoculated seedlings produced disease incidence of more than 50%, indicating the rapid progression of the disease. Each isolate used in this study demonstrated different levels of disease severity index (DSI). This suggests that the level of disease severity depends on the aggressiveness of the isolates, as stated by Pariaud et al. (2009), aggressive pathogens will inflict more damage to plant hosts.

A significant effect of *G. boninense* inoculation on seedling growth was observed in the period between 3 MAI for height and 4 MAI for number of leaves, leaf area, and fresh root mass. Other studies reported the effect was evident as early as 2 MAI (Goh et al., 2014), while others observed an effect at 6 MAI (Lo et al., 2023). These variations may be attributed to the isolates aggressiveness as well as environmental conditions under which the seedlings were grown. Disease kinetics were generally progressed more rapidly with highly aggressive isolate (Breton et al., 2006) and in environments with shaded conditions with optimal temperatures and higher humidity (Rees et al., 2007).

Out of the five vegetative growth parameters measured, only the bole size remained unaffected throughout the course of this study. This finding aligns with the research conducted by Faizah et al. (2022) and Lo et al. (2023), who reported that the aerial parts of the inoculated seedlings were generally unaffected by the *G. boninense* infection in the early stage. Most of the chlorophyll content and the photosynthesis rate of the inoculated seedlings was significantly impacted at 5 MAI. This is because the disease is progressing to an advanced stage, affecting the seedlings vascular system. Since nitrogen and magnesium play essential roles in chlorophyll biosynthesis (Rissler et al., 2002), the inability of seedlings to absorb these nutrients results in a reduction in chlorophyll content (Rakib et al., 2019).

All seedlings in this study showed increasing fresh root mass throughout the study, including those inoculated with the most aggressive isolate, BLSM5B. This could be due to the localised initial point of contact, as the surface area of the rubberwood block (RWB) in contact with the seedlings' roots is 36 cm² (6 cm × 6cm). Therefore, only the roots close to the RWB will be penetrated or enveloped by the fungus, which then progresses upwards to the seedling bole.

Roots located further from the inoculum might not be affected by the infection and continue growing. This was evident in the findings of Rees et al. (2009), who described the initial stage of *Ganoderma* infection, where the fungal hyphae penetrate the outer layers of the root and spread longitudinally to the lower part of the stem. Additionally, the attachment of hyphae to the root surface was either localized to the initial point of contact or, in some cases, the fungus completely enveloped the root.

In terms of the relationship between disease severity index (DSI) and aggressiveness parameters, only the chlorophyll content and photosynthetic rate of infected seedlings showed a significant negative correlation with the DSI. This indicates that as the disease severity increases, the chlorophyll content and photosynthetic rate of infected seedlings decrease. Similarly, Rakib et al. (2019) and Goh et al. (2016) also reported a decrease in chlorophyll content as a disease advances. The reduction in chlorophyll content could be attributed to chloroplast damage resulting from pathogen infections in plants. When chloroplasts are damaged, chlorophyllase, an enzyme that degrades chlorophyll—interacts with chlorophyll, leading to chlorophyll degradation (Hao et al., 2009; Sun et al., 2017). Since photosynthesis takes place in the chloroplasts, the damages caused by pathogen infection also reduced the efficiency of photosynthesis. Conversely, there was no correlation between DSI and vegetative growth of infected seedlings, indicating that the vegetative growth measurement did not reflect the disease development in this study. This could be due to the localized nature of infection, as the inoculation was performed on the roots of the oil palm seedlings. Consequently, infected seedlings might exhibit symptoms such as lesions in the roots and bole without immediately impacting the above-ground vegetative growth. Oil palm infections by *G. boninense* are often asymptomatic in the early stages and become noticeable only when the disease has progressed significantly. (60-70%) (Chong et al., 2017). Therefore, assessing

the chlorophyll content and photosynthetic rate of infected seedlings could be a more reliable indicator of the disease progress than vegetative growth measurements.

In addition, there were a significant positive relationship between DSI and the *in vitro* growth rate of *G. boninense* on MEA. This suggests that when a pathogen grows faster, it tends to induce more severe disease. This agreed with earlier reports by Kok et al. (2013), who also found a low linear correlation between the mycelia growth rate of *G. boninense* on MEA and DSI. Even though the relationships between aggressiveness and growth rates is weak, it should not be overlooked since the isolates tested in this study capable to produced high DSI values. Further research involving a broader range of isolates to validate these observations may be needed. This is because pathogens that grow rapidly have the capacity to disseminate more rapidly and exert a greater impact on the development of epidemics by infecting host plants more effectively (Thrall et al., 2005). Both faster growth and high levels of pathogenicity are crucial traits for a pathogen since they give a competitive advantage that facilitates host colonisation (Meyer et al., 2010).

Data from this study indicate that the *in vitro* growth rate and physical characteristics (pigments) of *G. boninense* are greatly influenced both by the genotype of isolates and the different compositions of solid media used. This finding aligns with PatilArti and PatilKalpana (2016), who observed that fungi isolated from different infected plants exhibited varying growth rates and colony characteristics when exposed to different types of media. Additionally, it is worth noting that among the culture media assessed in this study, malt extract agar (MEA) stood out as the medium where the majority of *G. boninense* isolates exhibited uniform growth coverage compared to other medium. This result was tallied with Alizadeh et al. (2011), who also discovered variations in the growth of distinct *G. boninense* isolates when cultured on different media, owing to

disparities in nutrient composition. Consequently, if the research objective prioritizes the uniform growth of *G. boninense*, culturing on MEA is recommended, but this choice should be contingent on the specific goals of the research.

Malt extract agar allowed all *G. boninense* isolates in this study to grow uniformly; hence, it was employed to compare the *in vitro* growth rates of *G. boninense* isolates revived from original culture stock and those that were reisolated from the fruiting bodies collected from infected seedlings (in the current study). According to Butt et al. (2006), phenotypic changes associated with culture degeneration typically include changes in colour, growth rate, shape, production of spores, and a decline in yield production. Most of the *G. boninense* isolates reisolated in this study grew faster than those from the original culture stock. The slow *in vitro* growth rates of the original culture stock may indicate that the *G. boninense* isolates are undergoing degeneration. This was similar to the findings of a study on *Volvariella volvacea*, a basidiomycete, which displayed symptoms of degeneration after successive subculturing: slow mycelial growth rates (Chen et al., 2019). Additionally, degeneration of cultural stability on artificial growth media is a common feature of filamentous fungi (Li et al., 2014; Song et al., 2022).

Nevertheless, the original *G. boninense* culture stock used to prepare *Ganoderma* inoculum for artificial inoculation in this study was capable of inducing BSR in the seedlings. This suggests that the original *G. boninense* isolates do not lose their virulence despite degeneration (slow *in vitro* growth rates). According to Butt et al. (2006), stable strains conserve virulence for several generations, whereas unstable strains usually become attenuated after a few subcultures. As a result, an adequate culture preservation strategy is important for guaranteeing the viability and genetic stability of *G. boninense* for future research.

Interestingly, the original culture stock for isolate BLSM5B grew faster than those reisolated from the fruiting body on MEA. This observation suggests that the reisolated BLSMSB may have adapted to the specific conditions or nutrient availability of the fruiting body environment, which differ from the stock culture conditions. The composition of the MEA used in this study includes maltose, dextrin, glycerol, peptone and agar (Zimbro et al., 2009), whereas oil palm seedlings contain very high starch content (Rees et al., 2009). Starch, a major polysaccharide was utilised as a significant carbon source during BSR, as confirmed by transmission electron microscopy of bole tissues (Rees et al., 2009; Cooper et al., 2011). These environmental and nutritional differences could have influenced its growth rate, resulting in slower growth after reisolation due to sensitivity to changes in these factors. Further research is needed to confirm this hypothesis.

5.2 *Ganoderma boninense* Substrates Utilisation

Ganoderma boninense, a soil-borne fungus, has been regarded as a serious threat to the oil palm industry in many countries. It inflicts an annual economic loss of approximately USD 500 million in Malaysia (Kamu et al., 2021). As stated by Ries et al. (2018), nutrient acquisition and subsequent metabolic processes are vital for promoting fungal fitness, survival, and virulence within the host. However, the metabolic phenotype of this pathogen is still poorly understood. In this study, the most aggressive (BLSM5B) and least aggressive (DR56) *G. boninense* isolates were selected for a comprehensive study of their metabolic capabilities utilising the phenotype microarrays system (PMs).

Data obtained from PMs demonstrated that the most aggressive isolate, BLSM5B, outperforms the less aggressive isolate, DR56, in terms of carbon, nitrogen, phosphorus, and

sulphur sources utilisation. These data imply that isolate BLSM5B has a broader metabolic profile and greater adaptability for survival in its natural environment. The ability to use a diverse range of nutrients is fundamental for most organisms. This includes the capacity to rapidly adapt to fluctuating nutrient availability through regulating nutrient uptake and metabolic pathways (Ramachandra et al., 2014). This adaptability is critical because, without the capability to efficiently utilize the nutrients available at the host site, a fungus cannot succeed as a pathogen (Brock, 2009). Thus, rapid adaptation to changing microenvironments is vital for a successful infection.

Carbon sources are vital nutrients for most microorganisms (Wang et al., 2015) and are ubiquitous in the environment. However, isolate DR56 displays a narrow range of carbon utilisation (4.73%), which may suggest lower fitness compared to isolate BLSM5B. Fungi's ability to utilize a diverse array of carbon sources is crucial for their colonization and overall fitness, especially in environments where glucose is limited but other carbon sources are abundant, which enhances their pathogenicity by facilitating effective proliferation and adaptation to different environments (Lok et al., 2021). This adaptability is essential for pathogens to colonize and thrive in a diverse environment, thereby enhancing their pathogenic potential.

Many microorganisms exhibit a preference for carbon and nitrogen sources that could be metabolized rapidly, thus providing instant energy for growth and colonisation within specific niches (Ruijter and Visser, 1997; Schure et al., 2000). Interestingly, the utilisation rate of carbon sources was lower than that of nitrogen sources for both isolates (BLSM5B and DR56), suggesting that *G. boninense* may rely more on nitrogen-based metabolism. Similarly, the same observation was made in *Epicoccum latusicollum*, the causal agent of tobacco leaf spot (Li et al., 2023).

In terms of utilisation of peptide nitrogen sources, both isolates BLSM5B and DR56 exhibited efficient metabolism, with more than 70% utilisation. This indicates that both isolates can break down peptides and use the resulting amino acids for their growth and metabolic needs. This advantageous trait may be attributed to the ability to produce a diverse array of peptidase enzymes that can cleave the peptide bonds in peptides, breaking them down into individual amino acids or shorter peptides that can be readily assimilated for various cellular processes. Peptidases are a large family of hydrolases found in all living things that accelerate several biological processes by breaking down peptide bonds (Kos, 2023). Consequently, this gives advantage for survival of *G. boninense* isolates in environment where peptides are more available than free amino acids.

Both isolates, BLSM5B and DR56, demonstrated remarkable utilisation of phosphorus (P) sources exceeding 80%. This strongly suggests that phosphorus is indeed an essential nutrient for the growth of *G. boninense*. Ayundra et al. (2022) observed higher content of available P and total P in the soil of diseased plants compared to healthy ones, indicating that the abundant availability of P nutrients may favour *G. boninense* infection in oil palm plantations. Consequently, the regulation of phosphorus nutrients could hold the potential to suppress or mitigate *Ganoderma* infection in the field. However, it's worth noting that P is a macronutrient required in relatively large amounts to support plant growth, yield, and disease resistance. Plant metabolism is frequently hampered by nutritional deficiencies, resulting in a weakened plant with lower disease resistance (Wahid et al., 2004). As a result, the ideal disease management strategy should effectively control the disease while simultaneously maintaining the health of the plant.

In this study, both isolates, BLSM5B and DR56, also exhibited a moderately high utilisation of sulphur (S) sources (>60%). Govender et al. (2020) found high content of lignin and

S along with other elemental nutrients (iron, silicon, titanium, and copper) in the root of susceptible oil palm genotype. Collectively, these elemental nutrients could have contributed to the heightened lignin content in the root tissues (Govender et al., 2020). Additionally, plants with high lignin content may have a weaker ability to accumulate lignin during defence response compared to a plant with constitutively lower lignin content (Govender et al., 2020). Since lignin serves as the initial line of defence against pathogen attack, this suggests that S may be related to a plant's defence response to pathogens.

Isolate BLSM5B in this study displays a diversity of biosynthetic pathway (93.62%) in comparison to isolate DR56 (21.28%). Biosynthetic pathways involve chemical reaction that produce specific molecule by converting simple chemical building block substrates into more complex product (Berg et al., 2002). This suggests that isolate BLSM5B possesses the ability to produce a wide range of secondary metabolites for its survival. For instance, *Aspergillus fumigatus* produces various secondary metabolites, such as fumitremorgins, fumagillins, pseurotins, fumigaclavines, gliotoxins, and helvolic acid derivatives, owing to its exceptional adaptability to different environmental conditions (Zhang et al., 2022). This adaptability may provide a competitive advantage in resource-scarce or challenging environments by enabling the production of vital molecules even when substrates are limited.

Isolate DR56 also had a wide range of adaptabilities in osmolyte conditions, as opposed to isolate BLSM5B. The strong metabolic abilities of isolate DR56 in various osmotic conditions revealed the fungal adaptation to variation osmolytes in their niche, either in soil due to transition between dry and wet seasons or in host due to abiotic stress. Isolate BLSM5B and DR56 both demonstrated the ability to metabolize sodium chloride (NaCl) up to 4% (≈ 0.07 M) and 6% (≈ 0.1

M) sodium chloride (NaCl), respectively. This tallied with previous study conducted by Lim et al. (2018), which reported that *G. boninense* growth was slower on media containing 0.4 M and could not survive when exposed to media with 1 M NaCl. These results collectively suggest that *G. boninense* are sensitive to high NaCl concentrations, which could have implications for their ability to survive in saline environments. Additionally, both isolates BLSM5B and DR56 demonstrated the ability to metabolized up to 6% potassium chloride (PM9, well D1-D4), indicating that potassium (K) is another crucial nutrient that greatly promotes the growth of *G. boninense*. Periasamy et al. (2023) found that K has the most significant effect on the growth of *G. boninense* mycelia, with mycelia growth being restricted when K was removed from the solid media in which it was grown. Potassium is among the 16 mineral nutrients that support plant growth, yield, and disease resistance (Soumare et al., 2023). Notably, it has been identified as the most prevalent nutrient element in oil palm root tissue (Govender et al., 2020). Moreover, Govender et al. (2020) discovered that the highest K content was found in BSR-intermediate tolerant genotypes and commercial crosses with the highest yield, implying that K may have been used by the plant for the synthesis of cellulose, protein, and starch - components of yield. The susceptibility of oil palm could be related to abundance of K in root tissue, which is useful for the metabolism of *G. boninense* during infection.

Overall, isolate BLSM5B displays a wide range of adaptability in various pH conditions compared to isolate DR56. This adaptability is particularly evident when examining its growth on the PM10 microplate, where isolate BLSM5B exhibited growth across a pH range of 3 to 10. Based on the PMs data, the optimum pH for isolate BLSM5B falls within the range of 3.5 to 5, indicating a preference for acidic conditions. This observation is in line with the findings of Peng et al. (2019), who discovered that pH regimes 4 to 5 were optimal for *G. boninense* mycelial growth. Similarly,

Nawawi and Ho (1990) found that the ideal pH for *G. boninense* mycelial growth *in vitro* was 3.7 to 5.0. Furthermore, isolate BLSM5B demonstrated both decarboxylase and deaminase activity in this study, suggesting its ability to counteract conditions of both high and low pH in the presence of amino acids. However, it's important to note that no activities were observed at pH 4.5 and pH 9.5 in the presence of certain amino acids. These findings provide significant information for the development of basal stem rot control methods, as they highlight how pH conditions and the type of amino acids affect the growth and physiological activity of the pathogen.

Besides the variation in the range of substrate utilisation of isolates BLSM5B and DR56, the comparisons of substrates utilisation between isolates also showed a significant difference in their utilisation in certain substrates. Since all microorganisms require nutrients and minerals for growth, enhancing the amount of substrates that cannot be used by *G. boninense* or decreasing the amount of sources that can be utilized might be able to suppress *G. boninense* growth in their niche, or affect the infection caused by this pathogen and subsequently depress the disease losses. However, this hypothesis requires further studies due to complex nature of microbial metabolism. Furthermore, pathogen can adapt to changing condition over time. Nevertheless, phenotypic characterizations of *G. boninense* increased understanding on the survivability of the fungal in the environment which it is likely to thrive in food vehicles and infected hosts, as well as aid in disease intervention design development. In addition, the metabolic profile obtained from this study might provide a basis for developing improved media for *G. boninense* isolation and detection.

5.3 *Ganoderma* Disease Confirmation Methods

In the past, numerous methods have been employed to confirm the presence of *G. boninense* in infected seedlings. However, each of these approaches has its own advantages and

disadvantages. This investigation assessed the accuracy and reliability of techniques employed in *Ganoderma* infection studies to confirm the presence of *G. boninense* in infected seedlings, including re-isolation on *Ganoderma* selective medium (GSM) from infected tissue and fruiting bodies, as well as direct detection from infected tissue.

Among the techniques employed in this study, the molecular detection of fungal DNA isolated from infected tissue demonstrated the highest recovery percentage. This indicates the efficacy of PCR coupled with DNA sequencing in disease diagnosis. Comparatively to traditional culture-based techniques, which is time-consuming, low detection rates, and less accuracy (identification relying primarily on morphological traits), molecular detection generally has higher sensitivity and specificity, as well as rapid disease detection (Liu et al., 2023). Furthermore, the amplification of fungal DNA extracted from the infected tissue using the ITS3/GanET primers without subsequent sequencing demonstrated its reliability in detecting the presence of the pathogen. All the amplified DNA, with a 320 bp DNA fragment identical to the amplicon of DNA from *G. boninense* pure culture, were later confirmed as *G. boninense* via sequencing with the ITS1/ITS4 primer pair. Based on this study, it can be concluded that molecular detection methods could potentially replace the use of GSM for detecting the presence of *G. boninense* in infected tissue. However, in this study the use of was necessary in order to compare different techniques for reisolating *G. boninense*. Therefore, it is important to seek alternative ingredients that are safe and readily available to replace pentachloronitrobenzene and Ridomil, as GSM currently has no equivalent substitutes.

However, the major drawback of traditional PCR techniques is their inability to detect a low amount of DNA, which could lead to false-negative results in PCR (Yang and Rothman, 2004).

Advances in PCR technology have led to the development of molecular detection technologies such as quantitative PCR (qPCR), digital PCR (dPCR), next-generation sequencing, among others, which offer increased automation, detection rates, and specificity (Liu et al., 2023). Nonetheless, these technologies often necessitate relatively complex and costly instrumentation.

In this study, some of the infected tissue plated on GSM exhibited brown pigmentation but did not produce fungal mycelia. This brown pigmentation was indicative of laccase production, an enzyme characteristic of basidiomycete (Uber et al., 2023).). This suggests that the seedling tissue might be contaminated with other basidiomycetes capable of producing ligninolytic enzymes, which cause the brown pigmentation on GSM due to the presence of tannic acid—a component of GSM used to indicate laccase production (Ariffin and Idris, 1992; Uber et al., 2023). Nonetheless, as GSM was specifically formulated for the reisolation of *G. boninense*, it did not promote the growth of fungal mycelia, but still produce the pigmentation.

Since GSM alone as a tool for *Ganoderma* detection in infected seedlings has limitations, coupling it with molecular identification is advisable for precise and reliable detection. Disease confirmation via identification of fruiting bodies formed around the seedlings also could be considered as reliable method after molecular detection of fungal DNA isolated from infected tissue. However, it should be noted that not all infected seedlings will produce fruiting bodies. This is because the production of the fruiting body only occurs when the *G. boninense* dikaryotic mycelia under the ideal environmental conditions (Jazuli et al., 2022).

CHAPTER 6

CONCLUSION AND RECOMMENDATIONS

6.1 Conclusions

In this study, all six *G. boninense* isolates assessed were confirmed to be pathogenic to oil palm seedlings, resulting in varying levels of disease severity index. Among these isolates, BLSM5B could be the most aggressive isolate, with DSI value of 98.67% and the fastest in vitro growth rate of 0.47 cm day⁻¹, whereas isolate DR56, with the lowest DSI value of 43.99%, was the least aggressive and had the least impact on the physiological parameters of the infected seedlings. These isolate stands out as a promising candidate for future research on disease management and control strategies. The observed signs and symptoms, such as formation of fruiting bodies, lesions, and necrosis or necrotic leaves in infected oil palm seedlings, further confirm the pathogenicity of the *G. boninense* isolates used in this study.

Both chlorophyll content and photosynthesis rate measurement negatively correlated with the disease severity index, revealed that both parameters are sensitive to *G. boninense* infection. In contrast, there was no correlation between seedlings vegetative growth measurements and the disease severity index. Nevertheless, it remains essential to evaluate vegetative growth for disease scoring for disease severity and disease incidence calculation purpose.

Substrate utilisation profile of the most aggressive (BLSM5B) and least aggressive (DR56B) isolates revealed variation in their metabolic capabilities. Notably, isolate BLSM5B displayed a higher degree of metabolic versatility across multiple categories including carbon, nitrogen, phosphorus, and sulphur sources, biosynthetic pathways, and various pH conditions,

compared to the least aggressive isolate, DR56. In contrast, isolate DR56 exhibited a specific strength in the utilisation of peptide nitrogen sources and demonstrated adaptability to various osmolyte conditions. This information provides valuable insights into the nutrient preferences of *G. boninense* isolates with varying degrees of aggressiveness and their overall metabolic profiles, shedding light on their survival strategies in both environmental and host contexts. These findings suggest that adjusting external factors such as the nutrient levels, the type of osmolytes present in the soil, and soil pH may offer promising approaches for developing basal stem rot disease management strategies; however, these adjustments must be made carefully to avoid compromising the health of the oil palm.

Among the disease confirmation methods evaluated in this study, direct detection from plant tissues is the most recommended approach due to its reliability, precision, and speed compared to culture-based methods. In the case where re-isolation becomes necessary, the integration of molecular identification enhances the reliability and precision of the disease confirmation. These findings provide valuable guidance for researchers, allowing them to choose methods that align best with their research objectives.

6.2 Recommendations

This study utilized rubberwood blocks as a source of inoculum, which effectively induced *G. boninense* infection. However, the availability of rubberwood blocks is limited particularly in Sarawak and can be tedious to prepare. Therefore, immersing oil palm seedling roots in *G. boninense* mycelial suspension could be a more practical alternative for future research but it requires further optimization and validation to ensure its effectiveness.

Research on the manipulation of macronutrient and micronutrient for oil palm seedling in relation to *Ganoderma* infection could be highly valuable. This information will not only contribute to a deeper understanding of the nutrient dynamics involved in disease development but also provide insights into the development of targeted nutrient management strategies. By optimising nutrient availability for oil palm seedlings, we may enhance their resistance to *Ganoderma* infection and promote their overall health and productivity.

REFERENCES

- Abdul Hamid, Z. A. (2016). *Accumulation of carbohydrate reserve and its composition in oil palm trunk* [Doctoral dissertation, Universiti Sains Malaysia].
- Abdullah, R. (2011). World palm oil supply, demand, price and prospects: Focus on Malaysian and Indonesian palm oil industries. *Oil Palm Industry Economic Journal*, 11, 13–25.
- Abubakar, A., Ishak, M. Y., & Makmom, A. A. (2021). Impacts of and adaptation to climate change on the oil palm in Malaysia: A systematic review. *Environmental Science and Pollution Research*, 28, 54339–54361. <https://doi.org/10.1007/s11356-021-15890-3>
- Agrios, G. N. (2005). *Plant Pathology* (5th ed.). Elsevier Academic Press. <https://doi.org/10.1016/C2009-0-02037-6>
- Akoglu, H. (2018). User's guide to correlation coefficients. *Turkish Journal of Emergency Medicine*, 18(3), 91–93. <https://doi.org/10.1016/j.tjem.2018.08.001>
- Akond, M. A., Jahan, M. N., Sultana, N., Rahman, F., & Immunology. (2016). Effect of temperature, pH and NaCl on the isolates of Actinomycetes from straw and compost samples from Savar, Dhaka, Bangladesh. *American Journal of Microbiology*, 1(2), 10–15.
- Alexander, A., Abdullah, S., Dayou, J., & Chong, K. P. (2022). Cell wall-glycolipids profiling of oil palm roots during *Ganoderma boninense* infection using gas chromatography-mass spectrometry. *Journal of Oil Palm Research*, 34(4), 1–14. <https://doi.org/10.21894/jopr.2022.0013>

- Alexander, A., Sipaut, C. S., Dayou, J., & Chong, K. P. (2017). Oil palm roots colonisation by *Ganoderma boninense*: an insight study using scanning electron microscopy. *Journal of Oil Palm Research*, 29(2), 262–266. <https://doi.org/10.21894/jopr.2017.2902.10>
- Alizadeh, F., Abdullah, S. N. A., Khodavandi, A., Abdullah, F., Yusuf, U. K., & Chong, P. P. (2011). Differential expression of oil palm pathology genes during interactions with *Ganoderma boninense* and *Trichoderma harzianum*. *Journal of Plant Physiology*, 168(10), 1106–1113.
- Alizadeh, F., Abdullah, S. N. A., Khodavandi, A., & Chong, P. P. (2013). Improvement in *in vitro* growth rates of *Ganoderma* species with industrial wood waste supplements. *African Journal of Microbiology Research*, 7(29), 3772–3788. <https://doi.org/10.5897/AJMR12.2076>
- Amanda, W. I., & Prakoso, H. (2017, October 18–20). Modified *Ganoderma* selective medium to meet Indonesia's government regulation. *IOP Conference Series: Earth and Environmental Science* [Conference paper]. International Biotechnology Conference on Estate Crops 2017, Jakarta, Indonesia.
- Ariffin, D., Idris, A., & Singh, G. (2000). Status of *Ganoderma* in oil palm. In J. Flood, P. D. Bridge, & M. Holderness (Eds.), *Ganoderma Diseases of Perennial Crops* (pp. 49–68). CABI Publishing.
- Ariffin, D., & Idris, A. S. (1992). *The Ganoderma selective medium (GSM)*. Palm Oil Research Institute Malaysia,.

- As'wad, A. W. M., Sariah, M., Paterson, R. R. M., Abidin, M. A. Z., & Lima, N. (2011). Ergosterol analyses of oil palm seedlings and plants infected with *Ganoderma*. *Crop Protection*, *30*(11), 1438–1442.
- Avery, S. V., Singleton, I., Magan, N., & Goldman, G. H. (2019). The fungal threat to global food security. *Fungal Biology*, *123*(8), 555–557. <https://doi.org/10.1016/j.funbio.2019.03.006>
- Ayundra, S. D., Suwandi, S., Herlinda, S., Hamidson, H., Wandri, R., & Asmono, D. (2022). Soil physicochemical properties in respect to plant health in *Ganoderma*-infested oil palm plantation. *Journal of Scientific Agriculture*, *6*, 9–13. <https://doi.org/10.25081/jsa.2022.v6.7446>
- Aziz, M. H. A., Khairunniza-Bejo, S., Wayayok, A., Hashim, F., Kondo, N., & Azmi, A. N. N. (2021). Temporal changes analysis of soil properties associated with *Ganoderma boninense* Pat. infection in oil palm seedlings in a controlled environment. *Agronomy*, *11*(11), 2279. <https://doi.org/10.3390/agronomy11112279>
- Basiron, Y. (2007). Palm oil production through sustainable plantations. *European Journal of Lipid Science and Technology*, *109*(4), 289–295.
- Belisario, A., Scotton, M., Santori, A., & Onofri, S. (2008). Variability in the Italian population of *Gnomonia leptostyla*, homothallism and resistance of *Juglans* species to anthracnose. *Forest Pathology*, *38*(2), 129–145. <https://doi.org/10.1111/j.1439-0329.2007.00540.x>
- Berg, J. M., Tymoczko, J. L., & Stryer, L. (2002). *Biochemistry* (5th ed.). W.H. Freeman.

- Bharudin, I., Ab Wahab, A. F. F., Abd Samad, M. A., Xin Yie, N., Zairun, M. A., Abu Bakar, F. D., & Abdul Murad, A. M. (2022). Review update on the life cycle, plant–microbe interaction, genomics, detection and control strategies of the oil palm pathogen *Ganoderma boninense*. *Biology*, *11*(2), 251. <https://doi.org/10.3390/biology11020251>
- Biondi, E. G., Tatti, E., Comparini, D., Giuntini, E., Mocali, S., Giovannetti, L., Bazzicalupo, M., Mengoni, A., & Viti, C. (2009). Metabolic capacity of *Sinorhizobium (Ensifer) meliloti* strains as determined by phenotype microArray analysis. *Applied and Environmental Microbiology*, *75*(16), 5396–5404. <https://doi.org/10.1128/AEM.00196-09>
- Bivi, M. S. H. R., Paiko, A. S., Khairulmazmi, A., Akhtar, M. S., & Idris, A. S. (2016). Control of basal stem rot disease in oil palm by supplementation of calcium, copper, and salicylic acid. *The Plant Pathology Journal*, *32*(5), 396–406.
- Bochner, B. R., Gadzinski, P., & Panomitros, E. (2001). Phenotype microarrays for high-throughput phenotypic testing and assay of gene function. *Genome Research*, *11*(7), 1246–1255. <https://www.ncbi.nlm.nih.gov/pmc/articles/PMC311101/pdf/X18.pdf>
- Borglin, S., Joyner, D., DeAngelis, K. M., Khudyakov, J., D’haeseleer, P., PJoachimiak, M., & Hazen, T. (2012). Application of phenotypic microarrays to environmental microbiology. *Current Opinion in Biotechnology*, *23*(1), 41–48. <https://doi.org/10.1016/j.copbio.2011.12.006>
- Brasier, C. M., & Webber, J. F. (1987). Positive correlations between *in vitro* growth rate and pathogenesis in *Ophiostoma ulmi*. *Plant Pathology*, *36*(4), 462–466.

- Brennan, J. M., Fagan, B., Van Maanen, A., Cooke, B. M., & Doohan, F. M. (2003). Studies on *in vitro* growth and pathogenicity of European *Fusarium* fungi. *European Journal of Plant Pathology*, *109*(6), 577–587.
- Breton, F., Hasan, Y., Lubis, Z., & De Franqueville, H. (2006). Characterization of parameters for the development of an early screening test for basal stem rot tolerance in oil palm progenies. *Journal of Oil Palm Research, Special Issue*, 24–36.
- Bridge, P. D., O’Grady, E. B., Pilott, C. A., & Sanderson, F. R. (2000). Development of molecular diagnostics for the detection of *Ganoderma* isolates pathogenic to oil palm. In J. Flood, P. D. Bridge, & M. Holderness (Eds.), *Ganoderma Diseases of Perennial Crops* (pp. 23–45). CABI Publishing. <https://doi.org/10.1079/9780851993881.0225>
- Brock, M. (2009). Fungal metabolism in host niches. *Current Opinion in Biotechnology*, *12*(4), 371–376. <https://doi.org/10.1016/j.mib.2009.05.004>
- Burdon, J. J. (1987). *Diseases and plant population biology*. Cambridge University Press.
- Butt, T. M., Wang, C., Shah, F. A., & Hall, R. (2006). Degeneration of entomogenous fungi. In *An ecological and societal approach to biological control* (pp. 213–226). https://doi.org/10.1007/978-1-4020-4401-4_10
- Campbell, C. L., & Madden, L. V. (1990). *Introduction to Plant Disease Epidemiology*. John Wiley & Sons, Inc. <https://doi.org/10.1017/S0007485300051890>
- Castillo, S. Y., Rodríguez, M. C., González, L. F., Zúñiga, L. F., Mestizo, Y. A., Medina, H. C., Montoya, C., Morales, A., Romero, H. M., & Sarria, G. A. (2022). *Ganoderma zonatum* Is

- the causal agent of basal stem rot in oil palm in Colombia. *Journal of Fungi*, 8(3), 230.
<https://doi.org/10.3390/jof8030230>
- Chan, J. J., Latiffah, Z., Liew, K. W., & Idris, A. S. (2011). Pathogenicity of monokaryotic and dikaryotic mycelia of *Ganoderma boninense* on oil palm seedlings and germinated seeds in Malaysia. *Australasian Plant Pathology*, 40(3), 222–227.
<https://doi.org/10.1007/s13313-011-0031-4>
- Chan, Y. (2003). Biostatistics 104: Correlational analysis. *Singapore Medical Journal*, 44(12), 614–619.
- Chen, X., Li, L., Wang, H., Huang, Y., Wang, M., & Zhang, C. (2016). Phenotypic fingerprints of *Ralstonia solanacearum* under various osmolytes and pH environments. *Plant Pathology Journal*, 15(3), 102–107.
- Chen, X., Zhang, Z., Liu, X., Cui, B., Miao, W., Cheng, W., & Zhao, F. (2019). Characteristics analysis reveals the progress of *Volvariella volvacea* mycelium subculture degeneration. *Frontiers in Microbiology*, 10, 2045.
<https://doi.org/https://doi.org/10.3389/fmicb.2019.02045>
- Chong, K. P., Atong, M., & Rosall, S. (2012). The role of syringic acid in the interaction between oil palm and *Ganoderma boninense* the causal agent of basal. *Plant Pathology*, 61, 953–963. <https://doi.org/10.1111/j.1365-3059.2011.02577.x>
- Chong, K. P., Dayou, J., & Alexander, A. (2017). Pathogenic nature of *Ganoderma boninense* and basal stem rot disease. In *Detection and Control of Ganoderma boninense in Oil Palm Crop* (pp. 5–12). Springer.

- Chong, K. P., Lum, M. S., Foong, C. P., Wong, C. M. V. L., Atong, M., & Rossall, S. (2011). First identification of *Ganoderma boninense* isolated from Sabah based on PCR and sequence homology. *African Journal of Biotechnology*, *10*(66), 14718–14723. <https://doi.org/10.5897/AJB11.1096>
- Chotivanich, K., Udomsangpetch, R., Simpson, J. A., Newton, P., Pukrittayakamee, S., Looareesuwan, S., & White, N. J. (2000). Parasite multiplication potential and the severity of *Falciparum* malaria. *The Journal of Infectious Diseases*, *181*(3), 1206–1209. <https://doi.org/10.1086/315353>
- Cooper, R. M., Flood, J., & Rees, R. W. (2011). *Ganoderma boninense* in oil palm plantations: Current thinking on epidemiology, resistance and pathology. *Planter*, *87*(1024), 515–526.
- Corley, R. H. V., Hardon, J. J., & Tan, G. Y. (1971). Analysis of growth of the oil palm (*Elaeis guineensis* Jacq.) I. Estimation of growth parameters and application in breeding. *Euphytica*, *20*(2), 307–315. <https://doi.org/10.1007/BF00056093>
- Corley, R. H. V., & Tinker, P. B. (2016). The classification and morphology of the oil palm. In *World agriculture series: The oil palm* (5th ed., Vol. 10, pp. 30–51). Wiley Blackwell. <https://doi.org/10.1002/9781118953297.ch2>
- Dayarathne, M. C., Mridha, A. U., & Wang, Y. (2020). Diagnosis of fungal plant pathogens using conventional and molecular approaches. In D. Kourouski (Ed.), *Diagnostics of plant diseases*. IntechOpen. <https://doi.org/10.5772/intechopen.94980>
- Dayou, J., Alexander, A., Sipaut, C. S., Chong, K. P., & Lee, P. C. (2014). On the possibility of using FTIR for detection of *Ganoderma boninense* in infected oil palm tree. *International*

- Journal of Advances in Agricultural and Environmental Engineering*, 1(1), 161–163.
<https://doi.org/10.15242/IJAAEE.C514559>
- Deans, A.-M., Lyke, K. E., Thera, M. A., Plowe, C. V., Koné, A., Doumbo, O. K., Kai, O., Marsh, K., Mackinnon, M. J., Raza, A., & Rowe, J. A. (2006). Low multiplication rates of African *Plasmodium falciparum* isolates and lack of association of multiplication rate and red cell selectivity with malaria virulence. *The American Journal of Tropical Medicine and Hygiene*, 74(4), 554–563. <https://doi.org/10.4269/ajtmh.2006.74.554>
- Dislich, C., Keyel, A. C., Salecker, J., Kisel, Y., Meyer, K. M., Auliya, M., Barnes, A. D., Corre, M. D., DarrasKevin, Faust, H., Hess, B., Klasen, S., Knohl, A., Kreft, H., Meijide, A., Nurdiansyah, F., Otten, F., Pe'er, G., Steinebach, S., Tarigan, S., Tölle, M. H., Tschardtke, T., & Wiegand, K. (2017). A review of the ecosystem functions in oil palm plantations, using forests as a reference system. *Biological Reviews*, 92, 1539–1569. <https://doi.org/10.1111/brv.12295>
- Doehlemann, G., Ökmen, B., Zhu, W., & Sharon, A. (2017). Plant pathogenic fungi. *Microbiology Spectrum*, 5(1), 1–23. <https://doi.org/10.1128/microbiolspec.FUNK-0023-2016>.
- Fabien, F. T., Hanafi, M. M., Idris, A. S., Kadir, J., Jamaludin, N., Mohidin, H., & Syed, R. S. O. (2014). Effect of micronutrients-enriched fertilizers on basal stem rot disease incidence and severity on oil palm (*Elaeis guineensis* Jacq.) seedlings. *American Journal of Applied Sciences*, 11(10), 1841–1859.
- Faizah, R., Putrato, R. A., Raharti, V. R., Supena, N., Sukma, D., Budiani, A., Wening, S., & Sudarsono, S. (2022). Defense response changes in roots of oil palm (*Elaeis guineensis*

- Jacq.) seedlings after internal symptoms of *Ganoderma boninense* Pat. infection. *BMC Plant Biology*, 22(1), 1–23. <https://doi.org/10.1186/s12870.022.03493.0>
- Ferdous Alam, A. S. A., Er, A. C., & Begum, H. (2015). Malaysian oil palm industry: Prospect and problem. *Journal of Food Agriculture and Environment*, 13(2), 143–148.
- Fleck, C. B., Schöbel, F., & Brock, M. (2011). Nutrient acquisition by pathogenic fungi: Nutrient availability, pathway regulation, and differences in substrate utilization. *International Journal of Medical Microbiology*, 301(5), 400–407. <https://www.sciencedirect.com/science/article/abs/pii/S1438422111000245?via%3Dihub>
- Fleiss, S., Hill, J. K., McClean, C., & Lucey, J. M. (2017). *Potential impacts of climate change on oil palm cultivation. A science-for-policy paper by the SEnSOR programme.* <http://www.sensorproject.net/wp-content/uploads/2018/01/Climate-change-report-FINAL.pdf>
- Flood, J., Bridge, P. D., & Pilotti, C. A. (2022). Basal stem rot of oil palm revisited. *Annals of Applied Biology*, 181(2), 160–181. <https://doi.org/10.1111/aab.12772>
- Goh, K. J., Dickinson, M., Alderson, P., V, Y. L., & Supramaniam, C. V. (2016). Development of an *in planta* infection system for the early detection of *Ganoderma* spp. in oil palm. *Journal of Plant Pathology*, 98(2), 245–254.
- Goh, Y. K., Marzuki, N. F., Tung, H. J., Goh, Y. K., & Goh, K. J. (2013, November 22–23). Growth of different *Ganoderma* isolates on palm extract media and media with various sugar compound under in-vitro conditions. *Sustainable Management of Pests and*

- Ganoderma Disease in Oil Palm: The Way Forward* [Conference paper]. 5th MPOB-IOPRI International Seminar, Kuala Lumpur, Malaysia.
- Goh, Y. K., Ng, F. W., Kok, S. M., Goh, Y. K., & Goh, K. J. (2014). Aggressiveness of *Ganoderma boninense* isolates on the vegetative growth of oil palm (*Elaeis guineensis*) seedling at different age. *Malaysian Applied Biology*, 43(2), 9–16.
- Govender, N., Idris, A. S., & Wong, M.-Y. (2020). Root lignin composition and content in oil palm (*Elaeis guineensis* Jacq.) genotypes with different defense responses to *Ganoderma boninense*. *Agronomy*, 10, 1487. <https://doi.org/10.3390/agronomy10101487>
- Govender, N., & Wong, M.-Y. (2017). Detection of oil palm root penetration by agrobacterium-mediated transformed *Ganoderma boninense*, expressing green fluorescent protein. *Phytopathology*, 107(4), 483–490. <https://doi.org/10.1094/PHYTO-02-16-0062-R>
- Gurmit, S. (1990, September 11). *Ganoderma*-The scourge of oil palm in the coastal area. *Proceedings of Ganoderma Workshop*, Selangor, Malaysia.
- Gusarov, I., Shatalin, K., Starodubtseva, M., & Nudler, E. (2009). Endogenous nitric oxide protects bacteria against a wide spectrum of antibiotics. *Science*, 325(5946), 1380–1384. <https://www.ncbi.nlm.nih.gov/pmc/articles/PMC2929644/pdf/nihms228901.pdf>
- Hao, S., Liu, S., Zhang, Z., Gui, H., Duan, J., & Chen, Q. (2009). Characteristics of chlorophyll metabolism and chlorophyll fluorescence in the silvered leaf of summer squash. *Acta Horticulturae Sinica*, 6, 879–884.

- Hendricks, K. E., Christman, M. C., & Roberts, P. D. (2017). A statistical evaluation of methods of in-vitro growth assessment for *Phyllosticta citricarpa*: Average colony diameter vs. area. *PLoS One*, *12*(1). <https://doi.org/10.1371/journal.pone.0170755>
- Heriansyah, C., & Tan, C. (2005). Nursery practices for production of superior oil palm planting materials. *Planter*, *81*(948), 159–171.
- Hilmi, N. H. Z., Idris, A. S., Maizatul-suriza, M., Madihah, A. Z., & Nur-Rashyeda, R. (2022). Molecular PCR assays for detection of *Ganoderma* pathogenic to oil palm in Malaysia. *Malaysian Applied Biology*, *51*(1), 171–182. <https://doi.org/10.55230/mabjournal.v51i1.2157>
- Hirschmann, R. (2022). *Palm oil industry in Malaysia - Statistics & facts*. statista. Retrieved March 30, 2022 from https://www.statista.com/topics/5814/palm-oil-industry-in-malaysia/#topicHeader__wrapper
- Ho, Y. W., & Nawawi, A. (1985). *Ganoderma boninense* Pat. from basal stem rot of oil palm (*Elaeis guineensis*) in Peninsular malaysia. *Pertanika*, *8*(5), 425–428.
- Horsfall, J. G., & Cowling, E. B. (1978). Pathometry: The measurement of plant disease. In G. H. James & B. C. Ellis (Eds.), *Plant Disease: An Advanced Treatise: How Disease Develops in Populations* (Vol. 2, pp. 119–136). Academic Press. https://books.google.com.my/books?hl=en&lr=&id=umvlsq_8J6YC&oi=fnd&pg=PA119ots=WsSOzfbH8l&sig=ODVIE05Q898XtIUMIQbWXPbt14&redir_esc=y#v=onepage&q&f=false

- Husin, N. A., Khairunniza-Bejo, S., Abdullah, A. F., Kassim, M. S. M., Ahmad, D., & Aziz, M. H. A. (2020). Classification of basal stem rot disease in oil palm plantations using terrestrial laser scanning data and machine learning. *Agronomy*, *10*(11), 1624. <https://doi.org/10.3390/agronomy10111624>
- Idris, A., Ariffin, D., Watt, T., & Swinburne, T. (2001, August 20-22). Distribution of species of *Ganoderma* basal stem rot of oil palms in relation to the environmental conditions in Peninsular Malaysia. *Cutting-edge technologies for sustained competitiveness* [Conference session]. 2001 PIPOC International Palm Oil Congress, Agriculture Conference, Kuala Lumpur, Malaysia.
- Idris, A. S., Ariffin, D., Swinburne, T., & Watt, T. (2000a). The identity of *Ganoderma* species responsible for BSR disease of oil palm in Malaysia–Pathogenicity test. *MPOB Information Series*, *103*(77b), 1–4.
- Idris, A. S., Ariffin, D., Swinburne, T. R., & Watt, T. A. (2000b). The identity of *Ganoderma* species responsible for BSR disease of oil palm in Malaysia–Morphological characteristics. *MPOB Information Series*, *102*(77a), 102.
- Idris, A. S., Kushairi, A., Ismail, S., & Ariffin, D. (2004). Selection for partial resistance in oil palm progenies to *Ganoderma* basal stem rot. *Journal of Oil Palm Research*, *16*(2), 12–18.
- Idris, A. S., Yamaoka, M., Hayakawa, S., Basri, M. W., Noorhasimah, I., & Ariffin, D. (2003). PCR technique for detection of *Ganoderma*. *MPOB Information Series*, *202*(188), 1–3.

- Irzykowska, L., & Bocianowski, J. (2008). Genetic variation, pathogenicity and mycelial growth rate differentiation between *Gaeumannomyces graminis* var. tritici isolates derived from winter and spring wheat. *Annals of Applied Biology*, *152*(3), 369–375.
- Jazuli, N. A., Kamu, A., Chong, K. P., Gabda, D., Hassan, A., Idris, A. S., & Ho, C. M. (2022). A review of factors affecting *Ganoderma* basal stem rot. *Plants*, *11*, 2462. <https://doi.org/10.3390/plants11192462>
- Jin, J., Lee, M., Bai, B., Sun, Y., Qu, J., Alfiko, Y., Lim, C. H., Suwanto, A., Sugiharti, M., & Wong, L. (2016). Draft genome sequence of an elite Dura palm and whole-genome patterns of DNA variation in oil palm. *DNA Research*, *23*(6), 527–533. <https://www.ncbi.nlm.nih.gov/pmc/articles/PMC5144676/pdf/dsw036.pdf>
- Kamu, A. (2018). Identifying the early visible symptoms of the *Ganoderma*-infected oil palms: A case study on the infected palms which collapsed within twelve months after disease census. *ASM Science Journal*, *11*(Special), 156–163.
- Kamu, A., Chong, K. P., Idris, A. S., Darmesah, G., & Ho, C. M. (2021). Estimating the yield loss of oil palm due to *Ganoderma* basal stem rot disease by using Bayesian Model Averaging. *Journal of Oil Palm Research*, *33*(1), 46–55. <https://doi.org/10.21894/jopr.2020.0061>
- Khankahdan, H. H., Rastegar, S., Golein, B., Golmohammadi, M., & Jahromi, A. A. (2021). Relationship among vegetative growth and nutrient elements in the scion of different Persian lime accessions and its effect on WBDL phytoplasma. *Journal of Plant Diseases and Protection*, *129*, 145–154. <https://doi.org/10.1007/s41348-021-00527-x>

- Khoo, Y. W., & Chong, K. P. (2023). *Ganoderma boninense*: General characteristics of pathogenicity and methods of control. *Frontiers in Plant Science*, *14*, 1156869. <https://doi.org/10.3389/fpls.2023.1156869>
- Kinge, T. R., & Mih, A. M. (2011). *Ganoderma ryvardense* sp. nov. associated with basal stem rot (BSR) disease of oil palm in Cameroon. *Mycosphere*, *2*(2), 179-188.
- Knudsen, G. R., & Stack, J. P. (1991). Modeling growth and dispersal of fungi in natural environments. In D. K. Arora, B. Rai, K. G. Mukerji, & G. R. Knudsen (Eds.), *Handbook of Applied Mycology, Vol. I: Soil and Plants*. Marcel Dekker, Inc.
- Kok, S. M., Goh, Y. K., Tung, H. J., Goh, K. J., Wong, W. C., & Goh, Y. K. (2013). *In vitro* growth of *Ganoderma boninense* isolates on novel palm extract medium and virulence on oil palm (*Elaeis guineensis*) seedlings. *Malaysian Journal of Microbiology*, *9*(1), 33–42. <https://doi.org/10.21161/mjm.45212>
- Kos, J. (2023). Peptidases: Role and function in health and disease. *International Journal of Molecular Sciences*, *24*, 7823. <https://doi.org/10.3390/ijms24097823>
- Kranz, J. (1988). Measuring plant disease. In J. Kranz & J. Rotem (Eds.), *Experimental techniques in plant disease epidemiology* (pp. 35–50). Springer. https://doi.org/10.1007/978-3-642-95534-1_4
- Lee, D. H., Roux, J., Wingfield, B. D., & Wingfield, M. (2015). Variation in growth rates and aggressiveness of naturally occurring self-fertile and self-sterile isolates of the wilt pathogen *Ceratocystis albifundus*. *Plant Pathology*, *64*(5), 1103–1109. <https://doi.org/10.1111/ppa.12349>

- Li, L., Hu, X., Xia, Y., Xiao, G., Zheng, P., & Wang, C. (2014). Linkage of oxidative stress and mitochondrial dysfunctions to spontaneous culture degeneration in *Aspergillus nidulans*. *Molecular & Cellular Proteomics*, *13*, 449–461. <https://doi.org/10.1074/mcp.M113.028480>
- Li, Z., Hu, J.-R., Li, W.-H., Wang, H.-c., Guo, Z.-N., Cheng, X., Cai, L.-T., & Shi, C.-H. (2023). Characteristics of *Epicoccum latusicollum* as revealed by genomic and metabolic phenomic analysis, the causal agent of tobacco *Epicoccus* leaf spot. *Frontiers in Plant Science*, *14*, 1199956. <https://doi.org/10.3389/fpls.2023.1199956>
- Lim, F.-H., Rasid, A. O., Idris, A. S., & Parveez, G. K. A. (2018). Molecular cloning of *Ganoderma boninense* Hog1-type mitogen-activated protein kinase (MAPK) cDNA and transcriptional response to salinity stress. *Journal of Oil Palm Research*, *30*(3), 380–389. <https://doi.org/10.21894/jopr.2018.0032>
- Lim, T. K., Chiung, G. F., & Ko, W.-H. (1992). Basal stem rot of oil palm caused by *Ganoderma boninense*. *Plant Pathology Bulletin*, *1*, 147–152.
- Liu, L., Kloepper, J. W., & Tuzun, S. (1995). Induction of systemic resistance in cucumber against bacterial angular leaf spot by plant growth-promoting rhizobacteria. *Phytopathology*, *85*(8), 843–847.
- Liu, Q., Jin, X., Cheng, J., Xhou, H., Zhang, Y., & Dai, Y. (2023). Advances in the application of molecular diagnostic techniques for the detection of infectious disease pathogens (Review). *Molecular Medicine Reports*, *27*(5), 104. <https://doi.org/10.3892/mmr.2023.12991>

- Lo, M. L., Thanh, T. A. V., Midot, F., Lau, S. Y. L., Wong, W. C., Tung, H. J., Jee, M. S., Chin, M.-Y., & Melling, L. (2023). Comparison of *Ganoderma boninense* Isolate's Aggressiveness Using Infected Oil Palm Seedlings. *Journal of Microbiology*, *61*(4), 449–459. <https://doi.org/10.1007/s12275-023-00040-w>
- Lok, B., Adam, M. A. A., Kamal, L. Z. M., Chukwudi, N. A., Sandai, R., & Sandai, D. (2021). The assimilation of different carbon sources in *Candida albicans*: Fitness and pathogenicity. *Medical Mycology*, *59*(2), 115–125. <https://doi.org/10.1093/mmy/myaa080>
- Lu, Y., & Yao, J. (2018). Chloroplasts at the crossroad of photosynthesis, pathogen infection and plant defense. *International Journal of Molecular Sciences*, *19*(12), 1–37. <https://doi.org/10.3390/ijms19123900>
- Magan, N. (2001). Physiological approaches to improving the ecological fitness of fungal biocontrol agents. In T. M. Butt, C. W. Jackson, & N. Magan (Eds.), *Fungi as Biocontrol Agents: Progress, Problems and Potential*. CABI Publishing. <https://doi.org/10.1079/9780851993560.0239>
- Mahidin, M. U. (2021). *Selected Agricultural Indicators, Malaysia, 2021*. Ministry of Economy Department of Statistics Malaysia. Retrieved March 6, 2023 from <https://dev.dosm.gov.my/portal-main/release-content/selected-agricultural-indicators-malaysia-2021>
- Mandal, P. K., Kochu Babu, M., Jayanthi, M., & Satyavani, V. (2014). PCR based early detection of *Ganoderma* sp. causing basal stem rot of oil palm in India. *Journal of Plantation Crops*, *42*(3), 392–394.

- Mendiburu, F. D., & Yaseen, M. (2020). *agricolae: Statistical procedures for agricultural research*. In (Version R package 1.4.0) <https://cran.r-project.org/package=agricolae>
- Mercière, M., Boulord, R., Carasco-Lacombe, C., Klopp, C., Lee, Y.-P., Tan, J.-S., Syed Alwee, S. S. R., Zaremski, A., De Franqueville, H., Breton, F., & Camus-Kulandaivelu, L. (2017). About *Ganoderma boninense* in oil palm plantations of Sumatra and peninsular Malaysia: Ancient population expansion, extensive gene flow and large scale dispersion ability. *Fungal Biology*, *121*(6–7), 529–540. <https://doi.org/10.1016/j.funbio.2017.01.001>
- Meyer, S. E., Stewart, T., E., & Clement, S. (2010). The quick and the deadly: Growth vs virulence in a seed bank pathogen. *New Phytologist*, *187*, 209–216. <https://doi.org/10.1111/j.1469-8137.2010.03255.x>
- Michalska, A. M., Sobkowiak, S., Flis, B., & Zimnoch-Guzowski, E. (2016). Virulence and aggressiveness of *Phytophthora infestans* isolates collected in Poland from potato and tomato plants identified no strong specificity. *European Journal of Plant Pathology*, *144*(2), 325–336. <https://doi.org/10.1007/s10658-015-0769-6>
- Midot, F., Lau, S. Y. L., Wong, W. C., Tung, H. J., Yap, M. L., Lo, M. L., Jee, M. S., Dom, S. P., & Melling, L. (2019). Genetic diversity and demographic history of *Ganoderma boninense* in oil palm plantations of Sarawak, Malaysia inferred from ITS regions. *Microorganisms*, *7*(10), 1–17, Article 464. <https://doi.org/10.3390/microorganisms7100464>
- Miller, R. N. G., Holderness, M., & Bridge, P. D. (2000). Molecular and morphological characterisation of *Ganoderma* in oil-palm plantings. In J. Flood, P. D. Bridge, & M.

- Holderness (Eds.), *Ganoderma Diseases of Perennial Crops* (pp. 159–182). CABI Publishing.
- Miller, R. N. G., Holderness, M., Bridge, P. D., Chung, G., & Zakaria, M. H. (1999). Genetic diversity of *Ganoderma* in oil palm plantings. *Plant pathology*, 48(5), 595–603.
- Moncalvo, J. M. (2000). Systematics of *Ganoderma*. In J. Flood, P. D. Bridge, & M. Holderness (Eds.), *Ganoderma diseases of perennial crops*. CABI Publishing. <https://doi.org/10.1079/9780851993881.0225>
- MPOB. (2021). *Oil palm planted area 2021*. Retrieved March 10, 2022 from <https://bepi.mpob.gov.my/index.php/en/area/area-2021/oil-palm-planted-area-as-at-dec-2021>
- MPOC. (2020). *Malaysian palm oil industry*. Malaysian Palm Oil Council. Retrieved January 21, 2022 from <https://mpoc.org.my/malaysian-palm-oil-industry/>
- Muchaamba, F., Eshwar, A. K., Stevens, M., von Ah, U., & Tasara, T. (2019). Variable carbon source utilization, stress resistance and virulence profiles among *Listeria monocytogenes* strains responsible for listeriosis outbreaks in Switzerland. *Frontiers in Microbiology*, 10, 957. <https://www.ncbi.nlm.nih.gov/pmc/articles/PMC6510287/pdf/fmicb-10-00957.pdf>
- Murphy, D. (2014). The future of oil palm as a major global crop: Opportunities and challenges. *Journal of Oil Palm Research*, 26(1), 1–24.

- Naher, L., Yusuf, U. K., Siddiquee, S., Ferdous, J., & Rahman, M. A. (2012). Effect of media on growth and antagonistic activity of selected *Trichoderma* strains against *Ganoderma*. *African Journal of Microbiology Research*, 6(48), 7449–7453.
- Nawawi, A., & Ho, Y. W. (1990). Effect of temperature and pH on growth pattern of *Ganoderma boninense* from oil palm in Peninsular Malaysia. *Pertanika Journal of Tropical Agricultural Science*, 13(3), 303–307.
- Pariaud, B., Ravigné, V., Halkett, F., Goyeau, H., Carlier, J., & Lannou, C. (2009). Aggressiveness and its role in the adaptation of plant pathogens. *Plant Pathology*, 58(3), 409–424.
- Parkash, V., Sharma, D. B., Snider, J., Bag, S., Roberts, P., Tabassum, A., West, D., Khanal, S., Suassuna, N., & Chee, P. (2021). Effect of cotton leafroll dwarf virus on physiological processes and yield of individual cotton plants. *Frontiers in Plant Science*, 12, 1–16. <https://doi.org/10.3389/fpls.2021.734386>
- Paterson, R. R., Kumar, L., Taylor, S., & Lima, N. (2015). Future climate effects on suitability for growth of oil palms in Malaysia and Indonesia. *Scientific Reports*, 5(1), 1–11. <https://doi.org/10.1038/srep14457>
- Paterson, R. R. M. (2019). *Ganoderma boninense* disease deduced from simulation modelling with large data sets of future Malaysian oil palm climate. *Phytoparasitica*, 47, 255–262. <https://doi.org/10.1007/s12600-019-00723-4>
- Paterson, R. R. M. (2020). Oil palm survival under climate change in Malaysia with future basal stem rot assessments. *Forest Pathology*, 50(6), 1–8, Article e12641. <https://doi.org/10.1111/efp.12641>

- Paterson, R. R. M., Kumar, L., Shabani, F., & Lima, N. (2017). World climate suitability projections to 2050 and 2100 for growing oil palm. *The Journal of Agricultural Science*, *155*(5), 689–702. <https://doi.org/10.1017/S0021859616000605>
- PatilArti, & PatilKalpana. (2016). Impact of different culture media on the growth rate of fungi isolated from different infected plants. *International Journal of Recent Scientific Research*, *7*(6), 12080–12083.
- Peng, S. H. T., Yap, C. K., Ren, P. F., & Chai, E. W. (2019). Effects of environment and nutritional conditions on mycelial growth of *Ganoderma boninense*. *International Journal of Oil Palm*, *2*(3), 95–107.
- Periasamy, G., Yun, W. M., Vadamalai, G., Ho, C. L., Naidu, Y. R., & Sundram, S. (2023). Ligninolytic enzymes profiling in association with the aggressiveness of *Ganoderma boninense* isolates. *Malaysian Journal of Microbiology*, *19*(1), 11–21. <https://doi.org/10.21161/mjm.221549>
- Pilott, C. A., Gorea, E. A., & Bonneau, L. (2018). Basidiospores as sources of inoculum in the spread of *Ganoderma boninense* in oil palm plantations in Papua New Guinea. *Plant Pathology*, *67*(9), 1829–2028. <https://doi.org/10.1111/ppa.12915>
- Pilotti, C. A. (2005). Stem rots of oil palm caused by *Ganoderma boninense*: Pathogen biology and epidemiology. *Mycopathologia*, *159*(1), 129–137.
- Pilotti, C. A., Killah, G., Rama, D., Gorea, E. A., & Mudge, A. M. (2021). A preliminary study to identify and distinguish southern tropical populations of *Ganoderma boninense* from oil

- palm via mating assays, sequence data, and microsatellite markers. *Mycologia*, 113(3), 574–585. <https://doi.org/10.1080/00275514.2020.1858687>
- Pilotti, C. A., Sanderson, F. R., Aitken, E. A. B., & Armstrong, W. (2004). Morphological variation and host range of two *Ganoderma* species from Papua New Guinea. *Mycopathologia*, 158, 251–265.
- Pinzari, F., Ceci, A., Abu Samra, N., Canfora, L., Maggi, O., & Persiani, A. (2016). Phenotype MicroArray™ system in the study of fungal functional diversity and catabolic versatility. *Research in Microbiology*, 167(9–10), 710–722. <https://doi.org/10.1016/j.resmic.2016.05.008>
- Pornsuriya, C., Sunpapao, A., Srihanant, N., Worapattamasri, K., Kittimorakul, J., Phithakkit, S., & Petcharat, V. (2013). A survey of diseases and disorders in oil palms of Southern Thailand. *Plant Pathology Journal*, 12(4), 169–175.
- Purba, A., Basyuni, M., Putri, L. A. P., Chalil, D., Hayati, R., Arifiyanto, D., & Syahputra, I. (2019, October 24–25). *Sequence analysis of Ganoderma boninense isolates from oil palm* [Conference Paper]. International Conference on Agriculture, Environment, and Food Security Medan, Indonesia.
- Purnamasari, M. I., Agustina, D., Prihatna, C., & Suwanto, A. (2018). A rapid inoculation method for infection of *Ganoderma* in oil palm. *International Journal of Oil Palm*, 1(1), 1–9.
- R Core Team. (2021). *R: A language and environment for statistical computing*. In (Version 1.4.1106) R Foundation for Statistical Computing. <https://www.R-project.org/>

- Rakib, M., Borhan, A., & Jawahir, A. (2019). The relationship between SPAD chlorophyll and disease severity index in *Ganoderma*-infected oil palm seedlings. *Journal of the Bangladesh Agricultural University*, 17(3), 355–358.
- Rakib, M. R. M., Bong, C. F. J., Khairulmazmi, A., & Idris, A. S. (2014). Genetic and morphological diversity of *Ganoderma* species isolated from infected oil palms (*Elaeis guineensis*). *International Journal of Agriculture And Biology*, 16(4), 691–699.
- Rakib, M. R. M., Bong, C. F. J., Khairulmazmi, A., & Idris, A. S. (2015). Aggressiveness of *Ganoderma boninense* and *G. zonatum* isolated from upper-and basal stem rot of oil palm (*Elaeis guineensis*) in Malaysia. *Journal of Oil Palm Research*, 27(3), 229–240.
- Rakib, M. R. M., Clament, C. F. S., Dayang Syazanie, A. E., & Darwana, D. (2020). Investigation on *Ganoderma* infection in oil palm based on the cultural characteristics and somatic compatibility: A case study in Sandakan, Sabah. *ASM Science Journal*, 13(6), 23–29.
- Ramachandra, S., Linde, J., Brock, M., Guthke, R., Hube, B., & Brunke, S. (2014). Regulatory networks controlling nitrogen sensing and uptake in *Candida albicans*. *PLoS One*, 9(3), e92734. <https://doi.org/10.1371/journal.pone.0092734>
- Rebitanim, N. A., Hanafi, M. M., Idris, A. S., Abdullah, S. N. A., Mohidin, H., & Rebitanim, N. Z. (2020). GanoCare® improves oil palm growth and resistance against *Ganoderma* basal stem rot disease in nursery and field trials. *BioMed Research International*, 2020, 1–16. <https://doi.org/10.1155/2020/3063710>
- Rees, R. W., Flood, J., Hasan, Y., & Cooper, R. M. (2007). Effects of inoculum potential, shading and soil temperature on root infection of oil palm seedlings by the basal stem rot pathogen

- Ganoderma boninense*. *Plant Pathology*, 56(5), 862–870. <https://doi.org/10.1111/j.1365-3059.2007.01621.x>
- Rees, R. W., Flood, J., Hasan, Y., Potter, U., & Cooper, R. M. (2009). Basal stem rot of oil palm (*Elaeis guineensis*); Mode of root infection and lower stem invasion by *Ganoderma boninense*. *Plant Pathology*, 58(5), 982–989. <https://doi.org/10.1111/j.1365-3059.2009.02100.x>
- Ries, L. N. A., Beattie, S., Cramer, R. A., & Goldman, G. H. (2018). Overview of carbon and nitrogen catabolite metabolism in the virulence of human pathogenic fungi. *Molecular Microbiology*, 107(3), 277–297. <https://doi.org/10.1111/mmi.13887>
- Rissler, H. M., Collakova, E., DellaPenna, D., Whelan, J., & Pogson, B. J. (2002). Chlorophyll biosynthesis. Expression of a second *Chl I* gene of magnesium chelatase in arabidopsis supports only limited chlorophyll synthesis. *Plant Physiology*, 128, 770–779. <https://doi.org/10.1104/pp.010625>
- Ruijter, G. J. G., & Visser, J. (1997). Carbon repression in aspergilli. *FEMS Microbiology Letters*, 151(2), 103–114. <https://doi.org/10.1111/j.1574-6968.1997.tb12557.x>
- Rupaedah, B., Prasetyo, A. E., Hidayat, F., Asiani, N., Wahid, A., Nurlaila, & Lutfia, A. (2024). Evaluation of microbial biocontrol agents for *Ganoderma boninense* management in oil palm nurseries. *Journal of the Saudi Society of Agricultural Sciences*, 23(3), 236–244. <https://doi.org/10.1016/j.jssas.2023.12.001>

- Sapak, Z., Meon, S., & Ahmad, Z. A. M. (2008). Effect of endophytic bacteria on growth and suppression of *Ganoderma* infection in oil palm. *International Journal of Agriculture And Biology*, *10*, 127–132.
- Sariah, M., Hussin, M. Z., Miller, R. N. G., & Holderness, M. (1994). Pathogenicity of *Ganoderma boninense* tested by inoculation of oil palm seedlings. *Plant Pathology*, *43*(3), 507–510.
- Sarkar, M. S. K., Begum, R. A., & Pereira, J. J. (2020). Impacts of climate change on oil palm production in Malaysia. *Environmental Science and Pollution Research*, *27*(9), 9760–9770. <https://doi.org/10.1007/s11356-020-07601-1>
- Schure, E. G. t., Riel, N. A. W. v., & Verrips, C. T. (2000). The role of ammonia metabolism in nitrogen catabolite repression in *Saccharomyces cerevisiae*. *FEMS Microbiology Reviews*, *24*(1), 67–83. <https://doi.org/10.1111/j.1574-6976.2000.tb00533.x>
- Seem, R. C. (1984). Disease incidence and severity relationships. *Annual Review of Phytopathology*, *22*, 133–150. <https://doi.org/10.1146/annurev.py.22.090184.001025>
- Singh, M. P. (2009). Application of Biolog FF MicroPlate for substrate utilization and metabolite profiling of closely related fungi. *Journal of Microbiological Methods*, *77*(1), 102–108. <https://www.sciencedirect.com/science/article/pii/S0167701209000347?via%3Dihub>
- Singh, R., Ong-Abdullah, M., Low, E.-T. L., Abdul Manaf, M. A., Rosli, R., Nookiah, R., Ooi, L. C.-L., Ooi, S. E., Chan, K. L., Halim, M. A., Azizi, N., Nagappan, J., Bacher, B., Lakey, N., Smith, S. W., He, D., Hogan, M., Budiman, M. A., Lee, E. K., DeSalle, R., Kudrna, D., Goicoechea, J. L., Wing, R., Wilson, R. K., Fulton, R. S., Ordway, J. M., Martienssen, R. A., & Sambanthamurthi, R. (2013). Oil palm genome sequence reveals divergence of

- interfertile species in old and new worlds. *Nature*, 500(7462), 335–339.
<https://doi.org/10.1038/nature12309>
- Slowik, A. R., Hesketh, H., Sait, S. M., & de Fine Licht, H. H. (2023). A rapid method for measuring *in vitro* growth in Entomopathogenic fungi. *Insects*, 14(8), 703.
<https://doi.org/10.3390/insects14080703>
- Song, H., Bao, Y., Zhang, M., Liu, S., Yu, C., Dai, J., Wu, C., Tang, D., & Fang, W. (2022). An inactivating mutation in the vacuolar arginine exporter gene *Vae* results in culture degeneration in the fungus *Metarhizium robertsii*. *Environmental Microbiology*, 24, 2924–2937. <https://doi.org/10.1111/1462-2920.15982>
- Soumare, A., Sarr, D., & Diédhiou, A. G. (2023). Potassium sources, microorganisms and plant nutrition: Challenges and future research directions. *Pedosphere*, 33(1), 105–115.
<https://doi.org/10.1016/j.pedsph.2022.06.025>
- Strange, R. N., & Scott, P. R. (2005). Plant disease: A threat to global food security. *Annual Review of Phytopathology*, 43, 83–116. <https://doi.org/10.1146/annurev.phyto.43.113004.133839>
- Sun, Y., Wang, Y., Xiao, H., Gu, X., Pan, L., & Tu, K. (2017). Hyperspectral imaging detection of decayed honey peaches based on their chlorophyll content. *Food Chemistry*, 235, 194–202.
- Supramani, S., Rejab, N. A., Ilham, Z., Wan-Mohtar, W. A. A. Q. I., & Ghosh, S. (2021). Basal stem rot of oil palm incited by *Ganoderma* species: A review. *European Journal of Plant Pathology*, 164, 1–20. <https://doi.org/10.1007/s10658-022-02546-2>

- Tee, S.-S., Tan, Y.-C., Abdullah, F., Ong-Abdullah, M., & Ho, C.-L. (2013). Transcriptome of oil palm (*Elaeis guineensis* Jacq.) roots treated with *Ganoderma boninense*. *Tree Genetics and Genomes*, 9(2), 377–386.
- Teoh, C. H. (2002). *The palm oil industry in Malaysia* (From seed to frying pan, Issue).
- Thompson, A. (1931). *Stem-rot of the oil palm in Malaya* (Vol. 6). Straits Settlements and F.M.S., Science Series.
- Thrall, P., Barrett, L., Burdon, J., & Alexander, H. (2005). Variation in pathogen aggressiveness within a metapopulation of the *Cakile maritima*—*Alternaria brassicicola* host-pathogen association. *Plant Pathology*, 54(3), 265–274.
- Thynne, E., McDonald, M. C., & Solomon, P. S. (2015). Phytopathogen emergence in the genomics era. *Trends in Plant Science*, 20(4), 246–255.
<https://doi.org/10.1016/j.tplants.2015.01.009>
- Turner, P. D. (1981). *Oil palm diseases and disorders*. Oxford University Press.
- Uber, T. M., Backes, E., Saute, V. M. S., da Silva, B. P., Corrêa, R. C. G., Kato, C. G., Seixas, F. A. V., Bracht, A., & Peralta, R. M. (2023). Enzymes from basidiomycetes—Peculiar and efficient tools for biotechnology. In G. Brahmachari (Ed.), *Biotechnology of Microbial Enzymes* (2nd ed., pp. 129–164). Academic Press. <https://doi.org/10.1016/B978-0-443-19059-9.00023-2>

- Utomo, C., & Niepold, F. (2000). Development of diagnostic methods for detecting *Ganoderma*-infected oil palms. *Journal of Phytopathology*, 148(9–10), 507–514. <https://doi.org/10.1046/j.1439-0434.2000.00478.x>
- van Dijk, L. J. A., Ehrlén, J., & Tack, A. J. M. (2021). Direct and insect-mediated effects of pathogens on plant growth and fitness. *Journal of Ecology*, 109, 2769–2779. <https://doi.org/1111/1365-2745.13689>
- Voigt, K., Cigelnik, E., & O'donnell, K. (1999). Phylogeny and PCR identification of clinically important Zygomycetes based on nuclear ribosomal-DNA sequence data. *Journal of Clinical Microbiology*, 37(12), 3957–3964. <https://doi.org/10.1128/jcm.37.12.3957-3964.1999>
- Wahid, M. B., Abdullah, S. N. A., & Henson, I. E. (2004). Oil palm-achievements and potential. *Plant Production Science*, 8, 288–297. <https://doi.org/10.1626/pps.8.288>
- Wang, H.-C., Li, L.-C., Cai, B., Cai, L.-T., Chen, X.-J., Yu, Z.-H., & Zhang, C.-Q. (2018). Metabolic phenotype characterization of *Botrytis cinerea*, the causal agent of gray mold. *Frontiers in Microbiology*, 9, 470. <https://www.ncbi.nlm.nih.gov/pmc/articles/PMC5859374/pdf/fmicb-09-00470.pdf>
- Wang, H., Huang, Y., Xia, H., Wang, J., Wang, M., Zhang, C., & Lu, H. (2015). Phenotypic analysis of *Alternaria alternata*, the causal agent of tobacco brown spot. *Plant Pathology Journal*, 14(2), 79.
- White, T. J., Bruns, T., Lee, S., & Taylor, J. (1990). Amplification and direct sequencing of fungal ribosomal RNA genes for phylogenetics. In M. A. Innis, D. H. Gelfand, J. J. Sninsky, & T.

- J. White (Eds.), *PCR Protocols: A guide to Methods and Applications* (Vol. 18, pp. 315–322). Academic Press.
- Wong, L. C., Bong, C.-F. J., & Idris, A. S. (2012). *Ganoderma* species associated with basal stem rot disease of oil palm. *American Journal of Applied Sciences*, 9(6), 879–885.
- Wong, W. C., Tung, H. J., Nurul Fadhilah, M., Midot, F., Lau, S. Y. L., Melling, L., Astari, S., Hadziabdic, D., Trigiano, R. N., Goh, K. J., & Goh, Y. K. (2021). Genetic diversity and gene flow amongst admixed populations of *Ganoderma boninense*, causal agent of basal stem rot in African oil palm (*Elaeis guineensis* Jacq.) in Sarawak (Malaysia), Peninsular Malaysia, and Sumatra (Indonesia). *Mycologia*, 113(5), 902–917. <https://doi.org/10.1080/00275514.2021.1884815>
- Yang, H., & Luo, P. (2021). Changes in photosynthesis could provide important insight into the interaction between wheat and fungal pathogens. *International Journal of Molecular Sciences*, 22(8865), 1–15. <https://doi.org/10.3390/ijms22168865>
- Yang, S., & Rothman, R. E. (2004). PCR-based diagnostics for infectious diseases: Uses, limitations, and future applications in acute-care settings. *The Lancet Infectious Diseases*, 4(6), 337–348. [https://doi.org/10.1016/S1473-3099\(04\)01044-8](https://doi.org/10.1016/S1473-3099(04)01044-8)
- Zakaria, L. (2023). Basal stem rot of oil palm-The pathogen, disease incidence, and control methods. *Plant Disease*, 107(3), 603–615. <https://doi.org/10.1094/PDIS-02-22-0358-FE>
- Zakaria, L., Kulaveraasingham, H., Tan, S. G., Adbdullah, F., & Ho Yin, W. (2005). Random amplified polymorphic DNA (RAPD) and random amplified microsatellite (RAMS) of

Ganoderma from infected oil palm and coconut stumps in Malaysia. *Asia-Pacific Journal of Molecular Biology and Biotechnology*, 13(1), 23–34.

Zhan, F., Xie, Y., Zhu, W., Sun, D., McDonald, B. A., & Zhan, J. (2016). Linear correlation analysis of *Zymoseptoria tritici* aggressiveness with *in vitro* growth rate. *Phytopathology*, 106(11), 1255–1261. <https://doi.org/10.1094/PHYTO-12-15-0338-R>

Zhang, R., Wang, H., Chen, B., Dai, H., Sun, J., Han, J., & Liu, H. (2022). Discovery of anti-MRSA secondary metabolites from a marine-derived fungus *Aspergillus fumigatus*. *Marine Drugs*, 20(5), 302. <https://doi.org/10.3390/md20050302>

Zhou, L.-W., Cao, Y., Wu, S.-H., Vlasák, J., Li, D.-W., Li, M.-J., & Dai, Y.-C. (2015). Global diversity of the *Ganoderma lucidum* complex (Ganodermataceae, Polyporales) inferred from morphology and multilocus phylogeny. *Phytochemistry*, 114, 7–15. <https://doi.org/10.1016/j.phytochem.2014.09.023>

Zimbro, M. J., Power, D. A., Miller, S. M., Wilson, G. E., & Johnson, J. A. (Eds.). (2009). *Difco™ & BBL™ Manual: Manual of Microbiological Culture Media* (2nd ed.). BD Diagnostics – Diagnostic Systems. <https://www.bd.com/resource.aspx?IDX=9572>.

APPENDICES

Appendix 1: 10× Phosphate buffered saline (PBS) recipe

Composition	Amount
Sodium Chloride, NaCl (Fisher, Leicestershire, UK)	80 g
Potassium Chloride, KCl (Merck, Darmstadt, Germany)	2 g
Disodium Hydrogen Phosphate, Na ₂ HPO ₄ (Merck, Darmstadt, Germany)	14.4 g
Potassium Dihydrogen Phosphate, KH ₂ PO ₄ (Merck, Darmstadt, Germany)	2.4 g
Ultra-Pure Water, UPW	Top up to 1000 mL

To prepare 10× PBS, all the reagent salts were dissolved in 900 mL of UPW, and the pH was adjusted to 7.4 with hydrochloric acid (HCl) (Fisher, Scientific, Selangor, Malaysia) or sodium hydroxide (NaOH) (System®, Selangor, Malaysia) before adding UPW to achieve the final volume (1000 mL). Finally, the PBS solution was autoclaved at 121 °C for 15 minutes and kept at 4 °C until used

Appendix 2: Substrates (PM1-PM8), osmolytes (PM9), and pH (PM10) conditions that inhibited the growth of isolates BLSM5B and DR56

Microplate	Substrates	
	BLSM5B	DR56
PM1	L-Arabinose, D-Xylose, L-Lactic Acid, Formic Acid, D-Ribose, Acetic Acid, 1,2-Propanediol, Lactulose, D-Threonine, Glyoxylic Acid, D-Malic Acid, Tyramine, D-Psicose, L-Lyxose, and Glucuronamide.	L-Arabinose, D-Saccharic Acid, Succinic Acid, L-Aspartic Acid, L-Proline, D-Alanine, D-Mannose, Dulcitol, D-Serine, D-Sorbitol, Glycerol, L-Fucose, D-Glucuronic Acid, D-Gluconic Acid, D,L- α -Glycerol-Phosphate, D-Xylose, L-Lactic Acid, Formic Acid, D-Mannitol, L-Glutamic Acid, D-Glucose-6-Phosphate, D-Galactonic Acid- γ -Lactone, D,L-Malic Acid, D-Ribose, Tween 20, L-Rhamnose, D-Fructose, Acetic Acid, α -D-Glucose, Maltose, D-Melibiose, Thymidine, D-Aspartic Acid, D-Glucosaminic Acid, 1,2-Propanediol, Tween 40, α -Keto-Glutaric Acid, α -Keto-Butyric Acid, α -Methyl-D-Galacto, α -D-Lactose, Lactulose, Sucrose, Uridine, L-Glutamine, m-Tartaric Acid, D-Glucose-1-Phosphate, D-Fructose-6-Phosphate, Tween 80, α -Hydroxy Glutaric Acid- γ -Lactone, α -Hydroxy Butyric Acid, β -Methyl-D-Glucoside, Maltotriose, 2-Deoxy Adenosine, Adenosine, Glycyl-L-Aspartic Acid, Citric Acid, myo-Inositol, D-Threonine, Fumaric Acid, Bromo Succinic Acid, Propionic Acid, Mucic Acid, Glycolic Acid, Glyoxylic Acid, D-Cellobiose, Inosine, Glycyl-LGlutamic Acid, Tricarballic Acid, L-Serine, L-Threonine, L-Alanine, L-Alanyl-Glycine, Acetoacetic Acid, N-Acetyl- β -D-Mannosamine, Mono Methyl Succinate, Methyl Pyruvate, D-Malic Acid, L-Malic Acid, Glycyl-L-Proline, p-Hydroxy Phenyl Acetic Acid, m-Hydroxy Phenyl Acetic Acid, Tyramine, D-Psicose, L-Lyxose, Glucuronamide, Pyruvic Acid, L-Galactonic Acid- γ -Lactone, D-Galacturonic Acid, Phenylethyl-amine, and 2-Aminoethanol

Appendix 2 continued

<p>PM2</p>	<p>Chondroitin Sulfate C, Inulin, Mannan, N-Acetyl-D-Galactosamine, N-Acetyl-Neuraminic Acid, β-D-Allose, D-Arabinose, 2-Deoxy-D-Ribose, I-Erythritol, D-Fucose, 3-0-β-D-Galacto-pyranosyl-D-Arabinose, L-Glucose, Lactitol, D-Melezitose, Maltitol, α-Methyl-D-Glucoside, 3-Methyl-Glucose, β-Methyl-D-Glucuronic Acid, α-Methyl-D-Mannoside, β-Methyl-D-Xyloside, Sedoheptulosa, L-Sorbose, D-Tagatose, Turanose, N-Acetyl-D-Glucosaminitol, Citramalic Acid, 2-Hydroxy Benzoic Acid, γ-Hydroxy Butyric Acid, α-KetoValeric Acid, Malonic Acid, Melibionc Acid, Oxalic Acid, Oxalomalic Acid, D-Ribono-1,4-Lactone, Sorbic Acid, D-Tartaric Acid, L-Tartaric Acid, Acetamide, L-Arginine, Glycine, L-Histidine, L-Homoserine, L-Leucine, L-Methionine, L-Ornithine, L-Valine, Sec-Butylamine, D,L-Octopamine, Putrescine, Dihydroxy Acetone, and 2,3-Butanone.</p>	<p>Chondroitin Sulfate C, α-Cyclodextrin, β-Cyclodextrin, γ-Cyclodextrin, Dextrin, Gelatin, Glycogen, Inulin, Mannan, Pectin, N-Acetyl-D-Galactosamine, N-Acetyl-Neuraminic Acid, β-D-Allose, Amygdalin, D-Arabinose, D-Arabitol, L-Arabitol, Arbutin, I-Erythritol, D-Fucose, 3-0-β-D-Galacto-pyranosyl-D-Arabinose, Gentiobiose, L-Glucose, Lactitol, D-Melezitose, Maltitol, α-Methyl-D-Glucoside, β-Methyl-D-Galactoside, 3-Methyl-Glucose, β-Methyl-D-Glucuronic Acid, α-Methyl-D-Mannoside, β-Methyl-D-Xyloside, D-Raffinose, Salicin, Sedoheptulosa, L-Sorbose, Stachyose, D-Tagatose, Turanose, Xylitol, N-Acetyl-D-Glucosaminitol, γ-Amino Butyric Acid, δ-AminoValeric Acid, Butyric Acid, Capric Acid, Caproic Acid, Citraconic Acid, Citramalic Acid, D-Glucosamine, 2-Hydroxy Benzoic Acid, 4-Hydroxy Benzoic Acid, β-Hydroxy Butyric Acid, γ-Hydroxy Butyric Acid, α-KetoValeric Acid, Itaconic Acid, 5-Keto-D-Gluconic Acid, D-Lactic Acid MethylEster, Malonic Acid, Melibionc Acid, Oxalic Acid, Oxalomalic Acid, Quinic Acid, D-Ribono-1,4-Lactone, Sebacic Acid, Sorbic Acid, Succinamic Acid, D-Tartaric Acid, L-Tartaric Acid, Acetamide, L-Alaninamide, N-Acetyl-L-Glutamic Acid, L-Arginine, Glycine, L-Histidine, L-Homoserine, Hydroxy-L-Proline, L-Isoleucine, L-Leucine, L-Lysine, L-Methionine, L-Ornithine, L-Phenylalanine, L-Pyroglutamic Acid, L-Valine, D,L-Carnitine, Sec-Butylamine, D,L-Octopamine, Putrescine, Dihydroxy Acetone, and 2,3-Butanediol, 3-Hydroxy2-Butanone.</p>
<p>PM3</p>	<p>Bluret, L-isoleucine, L-lysine, L-methionine, L-threonine, D-lysine, D-valine, L-citrulline, Hydroxylamine, Methylamine, N-butylamine, Ethylamine, Ethylenediamine, Putrescine, β-phenylethyl-amine, Glucuronamide, D-glucosamine, N-acetyl-D-galactosamine, N-acetyl-D-mannosamine, Guanosine, Thymine, Thymidine, Uracil, Uridine, D,L-α-amino-caprylic acid, and α-amino-N-valeric acid.</p>	<p>Bluret, L-cysteine, L-histidine, L-proline, L-serine, L-threonine, D-alanine, D-asparagine, D-aspartic acid, D-glutamic acid, D-lysine, D-serine, D-valine, N-acetyl-D,L-glutamic acid, L-pyroglutamic acid, Hydroxylamine, Methylamine, N-amylamine, N-butylamine, Ethanolamine, Ethylenediamine, β-phenylethyl-amine, Tyramine, Formamide, D-glucosamine, D-galactosamine, D-mannosamine, Adenine, Cytidine, Thymine, Thymidine, Uracil, Uridine, Xanthosine, Uric acid, Alloxan, D,L-α-amino-caprylic acid, Ala-his, and Met-ala.</p>

Appendix 2 continued.

PM4	<p>Hypophosphite, Dithiophosphate, Phospho-glycolic acid, 2-deoxy-D-glucose 6-phosphate, Cytidine-5'-monophosphate, Uridine-2'-monophosphate, Methylene diphosphonic acid, S-methyl-L-cysteine, Lanthionine, Glutathione, D,L-ethionine, Thiourea, 1-thio-β-D-glucose, D,L-lipoamide, p-amino benzene sulfonic acid, and Tetramethylene sulfone.</p>	<p>Hypophosphite, Guanosine-3'-monophosphate, 2-deoxy-D-glucose 6-phosphate, Cytidine-3'-monophosphate, O-phospho-L-serine, Uridine-2'-monophosphate, Phosphoryl choline, O-phosphoryl-ethanolamine, Phosphono acetic acid, 2-aminoethyl phosphonic acid, Methylene diphosphonic acid, Tetrathionate, Thiophosphate, Dithiophosphate, D-cysteine, L-cysteic acid, Cysteamine, Cystathionine, Lanthionine, Glutathione, D,L-ethionine, D-Methionine, D,L-lipoamide, and p-amino benzene sulfonic acid.</p>
PM5	<p>Adenosine, L-Serine, trans-4-Hydroxy L-Proline, D-Aspartic Acid, D-Glutamic Acid, and Thymine.</p>	<p>L-Alanine, L-Arginine, L-Asparagine, L-Aspartic Acid, L-Cysteine, L-Glutamic Acid, Adenosine-3',5'-cyclic monophosphate, Adenine, Adenosine, L-Glutamine, Glycine, L-Histidine, L-Isoleucine, L-Leucine, L-Lysine, L-Methionine, L-Phenylalanine, Guanosine-3',5'-cyclic monophosphate, Guanine, Guanosine, 2'-Deoxy Guanosine, L-Serine, L-Threonine, L-Tryptophan, L-Tyrosine, L-Valine, L-Isoleucine + L-Valine, trans-4-Hydroxy L-Proline, (5) 4-Amino Imidazole-4(5)- Carboxamide, Hypoxanthine, 2'-Deoxy Inosine, L-Citrulline, Chorismic Acid, (-)Shikimic Acid, L-Homoserine Lactone, D-Alanine, D-Aspartic Acid, D-Glutamic Acid, D,L-α,ε-Diaminopimelic Acid, Cytosine, Cytidine, Putrescine, Spermidine, Spermine, Pyridoxine, Pyridoxal, Pyridoxamine, β-Alanine, D-Pantothenic Acid, Orotic Acid, Uracil, Uridine, 2'-Deoxy Uridine, Nicotinamide, β-Nicotinamide Adenine Dinucleotide, δ-Amino-Levulinic Acid, Hematin, Deferoxamine Mesylate, D-(+)-Glucose, N-Acetyl D-Glucosamine, Thymine, Thymidine, nosine + Thiamine, Thiamine, myo-Inositol, D,L-α-Hydroxy-Butyric Acid, α-Keto- Butyric Acid, Caprylic Acid, D,L-α-Lipoic Acid (oxidized form), D,L-Mevalonic Acid, D,L-Carnitine, Choline, Tween 20, and Tween 60.</p>
PM6	<p>Ala-Trp, Arg-Glu, Arg-Phe, Arg-Trp, Asp-Leu, Asp-Trp, Glu-Glu, Glu-Trp, Gly-Gly, Gly-Lys, Gly-Met, Gly-Trp, Gly-Val, His-Val, Ile-Ile, Ile-Met, Ile-Phe, Ile-Pro, Ile-Trp, Ile-Tyr, Ile-Val, Leu-Ala, and Leu-Asp.</p>	<p>Ala-Thr, Ala-Tyr, Arg-Tyr, Asn-Val, Asp-Asp, Asp-Glu, Asp-Trp, Asp-Val, Cys-Gly, Glu-Asp, Glu-Glu, Glu-Ser, Glu-Trp, Glu-Val, Gly-Cys, Gly-Gly, Gly-His, Gly-Leu, Gly-Met, Gly-Pro, Gly-Trp, Gly-Tyr, Gly-Val, His-Leu, His-Lys, His-Met, His-Pro, Ile-Ala, Ile-Gln, Ile-Gly, Ile-Ile, Ile-Met, and Ile-Tyr.</p>

Appendix 2 continued.

PM7	Leu-Trp, Lys-Ala, Lys-Lys , Lys-Pro, Lys-Ser , Lys-Thr, Lys-Tyr , Lys-Val, Met-Asp, Met-Glu , Met-Lys, Met-Met, Met-Phe, Phe-Ala, Phe-Ile, Phe-Pro, Pro-Hyp , Pro-Pro, Ser-Phe, Trp-Ala, Trp-Asp, Trp-Glu, Trp-Gly, Trp-Leu, Trp-Phe , Trp-Ser, Trp-Trp , Trp-Tyr, Tyr-Glu, and Tyr-Phe ..	Leu-Val, Lys-Glu, Lys-Lys , Lys-Ser , Lys-Trp, Lys-Tyr , Met-Glu , Met-Val, Phe-Trp, Pro-Asp, Pro-Hyp , Trp-Phe , Trp-Trp , Tyr-Phe , Tyr-Trp, Val-Asn, Val-Asp, Val-Gly, and Val-His.
PM8	Gly-Ile, Ile-Leu, Leu-Tyr, Lys-Gly, Met-Tyr , Phe-Glu, Phe-Tyr, Phe-Val, Pro-Arg, Pro-Ile, Pro-Trp , Ser-Asp, Trp-Val, Tyr-Val, Val-Lys , Val-Met , β-Ala-His , Met-β-Ala , D-Ala-D-Ala , D-Ala-Gly, D-Ala-Leu , D-Leu-D-Leu , D-Leu-Tyr , Gly-D-Ala , Gly-D-Asp , Gly-D-Ser , Gly-D-Thr , Gly-D-Val , Leu-D-Leu , Phe- β -Ala, D-Ala-Gly-Gly , γ-D-Glu-Gly , and Leu-Gly-Gly.	His-His, Met-Thr, Pro-Glu, Pro-Ser, Pro-Trp , Val-Ala, Val-Glu, Val-Lys , Val-Met , β -Ala-Ala, β -Ala-Gly, β-Ala-His , Met-β-Ala , β -Ala-Phe, D-Ala-D-Ala , D-Ala-Leu , D-Leu-D-Leu , D-Leu-Gly, D-Leu-Tyr , γ -D-Glu-Gly, Gly-D-Ala , Gly-D-Asp , Gly-D-Ser , Gly-D-Thr , Gly-D-Val , Leu-D-Leu , D-Ala-Gly-Gly , γ-D-Glu-Gly , and Gly-Phe-Phe.
PM9	5% NaCl, 5.5% NaCl, 6% NaCl, 6.5% NaCl , 7% NaCl , 8% NaCl , 9% NaCl , 10% NaCl , 6% NaCl, 6% NaCl + Betaine, 6% NaCl + N-N Dimethyl glycine , 6% NaCl + Sarcosine, 6% NaCl + Dimethyl sulphonyl propionate , 6% NaCl + MOPS , 6% NaCl + Ectoine, 6% NaCl + Choline, 6% NaCl + Phosphorylcholine, 6% NaCl + Creatine , 6% NaCl + Creatinine , 6% NaCl + L-Carnitine, 6% NaCl + N-Acetyl-L-glutamine, 6% NaCl + β-Glutamic acid , 6% NaCl + γ-Amino-N-butyric acid , 6% NaCl + Glutathione, 6% NaCl + Glycerol, 6% NaCl + Trehalose, 6% NaCl + Trimethylamine-N-oxide , 6% NaCl + Trimethylamine, 6% NaCl + Octopine, 3% Sodium Formate, 4% Sodium Formate, 5% Sodium Formate, 6% Sodium Formate , 4% Urea , 5% Urea , 6% Urea , 7% Urea , 8% Sodium Lactate, 9% Sodium Lactate, 10% Sodium Lactate, 11% Sodium Lactate , 200 mM Sodium Phosphate pH 7, 20 mM Sodium Benzoate pH 5.2 , 50 mM Sodium Benzoate pH 5.2 , 100 mM Sodium Benzoate pH 5.2 , 200 mM Sodium Benzoate pH 5.2 , 100 mM Ammonium Sulfate pH 8, 20mM Sodium Nitrite, 40mM Sodium Nitrite , 60mM Sodium Nitrite , 80mM Sodium Nitrite, and 100mM Sodium Nitrite .	4% NaCl, 6.5% NaCl , 7% NaCl , 8% NaCl , 9% NaCl , 10% NaCl , 6% NaCl, 6% NaCl + Betaine, 6% NaCl + N-N Dimethyl glycine, 6% NaCl + Sarcosine, 6% NaCl + Dimethyl sulphonyl propionate, 6% NaCl + MOPS , 6% NaCl + Creatine , 6% NaCl + Creatinine , 6% NaCl + KCl, 6% NaCl + L-Proline, 6% NaCl + β-Glutamic acid , 6% NaCl + γ-Amino-N-butyric acid , 6% NaCl + Trimethylamine-N-oxide , 3% Sodium Sulfate, 5% Ethylene Glycol, 15% Ethylene Glycol, 1% Sodium Formate, 2% Sodium Formate, 6% Sodium Formate , 4% Urea , 5% Urea , 6% Urea , 7% Urea , 11% Sodium Lactate , 20 mM Sodium Benzoate pH 5.2 , 50 mM Sodium Benzoate pH 5.2 , 100 mM Sodium Benzoate pH 5.2 , 200 mM Sodium Benzoate pH 5.2 , 60 mM Sodium Nitrate, 100 mM Sodium Nitrate, 40mM Sodium Nitrite , 60mM Sodium Nitrite , and 100mM Sodium Nitrite .

Appendix 2 continued.

PM10	<p>pH 4.5 + L-Homoarginine, pH 4.5 + Anthranilic Acid, pH 4.5 + p-AminoBenzoic Acid, pH 9.5 + Glycine, pH 9.5 + L-Histidine, pH 9.5 + L-Isoleucine, pH 9.5 + L-Serine, pH 9.5 + L-Threonine, pH 9.5 + L-Tryptophan, pH 9.5 + L-Tyrosine, pH 9.5 + L-Valine, pH 9.5 + Anthranilic Acid, pH 9.5 + Agmatine, pH 9.5 + Cadaverine, pH 9.5 + Phenylethylamine, X-α-D-Galactoside, and X-β-D-Glucosaminide,</p>	<p>pH 4.5 + L-Glutamic Acid, pH 4.5 + L-Leucine, pH 4.5 + Anthranilic Acid, pH 4.5 + L-Norleucine, pH 9.5, pH 9.5 + L-Alanine, pH 9.5 + L-Arginine, pH 9.5 + L-Asparagine, pH 9.5 + L-Aspartic Acid, pH 9.5 + L-Glutamine, pH 9.5 + L-Isoleucine, pH 9.5 + L-Methionine, pH 9.5 + L-Phenylalanine, pH 9.5 + L-Proline, pH 9.5 + L-Serine, pH 9.5 + L-Threonine, pH 9.5 + L-Tryptophan, pH 9.5 + L-Tyrosine, pH 9.5 + L-Valine, pH 9.5 + Hydroxy-L-Proline, pH 9.5 + L-Ornithine, pH 9.5 + L-Homoarginine, pH 9.5 + L-Homoserine, pH 9.5 + L-Norleucine, pH 9.5 + L-Norvaline, pH 9.5 + Agmatine, pH 9.5 + Cadaverine, pH 9.5 + Putrescine, pH 9.5 + Histamine, pH 9.5 + Phenylethylamine, pH 9.5 + Tyramine, pH 9.5 + TrimethylamineN-oxide, and X-β-D-Glucosaminide,</p>
------	---	---

Note: The substrates, osmolytes, and pH conditions that inhibited the growth of both isolates DR56 and BLSM5B are indicated in bold text

Appendix 3: Sequencing results of ITS1/ITS4 amplified PCR products of DNA extracted from fungi isolated from contaminated *Ganoderma* selective medium. Identification was based on BLAST searches of ITS sequences against those of deposited ITS sequences in GenBank (NCBI)

No.	Sample ID*	Scientific Name	Max Score	Total Score	Query Coverage	E Value	Percent Identity	Accession Length	Accession
1	NG.A9	<i>Duportella trigonosperma</i>	771	771	100%	0.0	99.76%	636 bp	MK588762.1
2	NG.A32	<i>Curvularia aerea</i>	887	887	100%	0.0	100%	549 bp	MF101868.1
3	NG.B6	<i>Peniophora malaiensis</i>	1033	1033	100%	0.0	99.82%	613 bp	MK588775.1
4	NG.B28	<i>Peniophora malaiensis</i>	891	891	100%	0.0	99.59%	636 bp	MH862297.1
5	NG B41	<i>Curvularia eragrostidis</i>	929	929	100%	0.0	100%	586 bp	MF038158.1
6	NG.C2	<i>Curvularia eragrostidis</i>	929	929	100%	0.0	100%	589 bp	MK886805.1
7	NG.C31	<i>Curvularia eragrostidis</i>	929	929	100%	0.0	100%	589 bp	MK886805.1
8	NG.C37	<i>Curvularia eragrostidis</i>	950	950	100%	0.0	100%	589 bp	MK886805.1
9	NG.D11	<i>Marasmius palmivorus</i>	1122	1122	100%	0.0	99.84%	701 bp	MN871733.1

Note: NG is referred to non-*Ganoderma*

Appendix 4: Sequencing results of ITS1/ITS4 amplified PCR products of DNA extracted from the fungus re-isolated on *Ganoderma* selective medium with morphology identical to the original *Ganoderma boninense* isolates. The identification was based on BLAST searches of ITS sequences against those of deposited ITS sequences in GenBank (NCBI)

No.	Sample ID*	Scientific Name**	Max Score	Total Score	Query Coverage	E Value	Percent Identity	Accession Length	Accession
1	PCB.B4	<i>Ganoderma boninense</i>	1090	1090	100%	0.0	100%	601 bp	MK713555.1
2	PCB.B8	<i>Ganoderma boninense</i>	1090	1090	100%	0.0	100%	601 bp	MK713555.1
3	PCB.B14	<i>Ganoderma boninense</i>	1090	1090	100%	0.0	100%	601 bp	MK713555.1
4	PCB.B19	<i>Ganoderma boninense</i>	1090	1090	100%	0.0	100%	601 bp	MK713555.1
5	PCB.B21	<i>Ganoderma boninense</i>	1090	1090	100%	0.0	100%	601 bp	MK713555.1
6	PCB.B25	<i>Ganoderma boninense</i>	1090	1090	100%	0.0	100%	601 bp	MK713555.1
7	PCB.B29	<i>Ganoderma boninense</i>	1090	1090	100%	0.0	100%	601 bp	MK713555.1
8	PCB.B33	<i>Ganoderma boninense</i>	1090	1090	100%	0.0	100%	601 bp	MK713555.1
9	PCB.B35	<i>Ganoderma boninense</i>	1090	1090	100%	0.0	100%	601 bp	MK713555.1
10	PCB.B36	<i>Ganoderma boninense</i>	1090	1090	100%	0.0	100%	601 bp	MK713555.1
11	PCB.B40	<i>Ganoderma boninense</i>	1051	1051	100%	0.0	100%	601 bp	MK713555.1
12	PCB.C5	<i>Ganoderma boninense</i>	1072	1072	100%	0.0	100%	601 bp	MK713555.1
13	PCB.C16	<i>Ganoderma boninense</i>	1072	1072	100%	0.0	100%	601 bp	MK713555.1
14	PCB.C26	<i>Ganoderma boninense</i>	1072	1072	100%	0.0	100%	601 bp	MK713555.1
15	PCB.D3	<i>Ganoderma boninense</i>	1077	1077	100%	0.0	100%	601 bp	MK713555.1
16	PCB.D6	<i>Ganoderma boninense</i>	1070	1070	100%	0.0	100%	601 bp	MK713555.1
17	PCB.D26	<i>Ganoderma boninense</i>	1070	1070	100%	0.0	100%	601 bp	MK713555.1
18	PCB.D33	<i>Ganoderma boninense</i>	1070	1070	100%	0.0	100%	601 bp	MK713555.1
19	PCB.D38	<i>Ganoderma boninense</i>	1070	1070	100%	0.0	100%	601 bp	MK713555.1
20	PCB.D39	<i>Ganoderma boninense</i>	1070	1070	100%	0.0	100%	601 bp	MK713555.1
21	PCB.E4	<i>Ganoderma boninense</i>	1072	1072	100%	0.0	100%	601 bp	MK713555.1
22	PCB.E6	<i>Ganoderma boninense</i>	1072	1072	100%	0.0	100%	601 bp	MK713555.1
23	PCB.E7	<i>Ganoderma boninense</i>	1072	1072	100%	0.0	100%	601 bp	MK713555.1
24	PCB.E13	<i>Ganoderma boninense</i>	1072	1072	100%	0.0	100%	601 bp	MK713555.1

Appendix 4 continued

25	PCB.E17	<i>Ganoderma boninense</i>	1072	1072	100%	0.0	100%	601 bp	MK713555.1
26	PCB.E20	<i>Ganoderma boninense</i>	1072	1072	100%	0.0	100%	601 bp	MK713555.1
27	PCB.E21	<i>Ganoderma boninense</i>	1072	1072	100%	0.0	100%	601 bp	MK713555.1
28	PCB.E23	<i>Ganoderma boninense</i>	1072	1072	100%	0.0	100%	601 bp	MK713555.1
29	PCB.E27	<i>Ganoderma boninense</i>	1072	1072	100%	0.0	100%	601 bp	MK713555.1
30	PCB.E36	<i>Ganoderma boninense</i>	1072	1072	100%	0.0	100%	601 bp	MK713555.1
31	PCB.F7	<i>Ganoderma boninense</i>	773	773	100%	0.0	100%	601 bp	MK713555.1
32	PCB.F9	<i>Ganoderma boninense</i>	773	773	100%	0.0	100%	601 bp	MK713555.1
33	PCB.F12	<i>Ganoderma boninense</i>	773	773	100%	0.0	100%	601 bp	MK713555.1
34	PCB.F15	<i>Ganoderma boninense</i>	773	773	100%	0.0	100%	601 bp	MK713555.1
35	PCB.F28	<i>Ganoderma boninense</i>	773	773	100%	0.0	100%	601 bp	MK713555.1
36	PCB.F32	<i>Ganoderma boninense</i>	773	773	100%	0.0	100%	601 bp	MK713555.1
37	PCB.G4	<i>Ganoderma boninense</i>	1000	1000	100%	0.0	100%	601 bp	MK713555.1
38	PCB.G10	<i>Ganoderma boninense</i>	1000	1000	100%	0.0	100%	601 bp	MK713555.1
39	PCB.G11	<i>Ganoderma boninense</i>	1000	1000	100%	0.0	100%	601 bp	MK713555.1
40	PCB.G16	<i>Ganoderma boninense</i>	1000	1000	100%	0.0	100%	601 bp	MK713555.1
41	PCB.G20	<i>Ganoderma boninense</i>	1000	1000	100%	0.0	100%	601 bp	MK713555.1
42	PCB.G21	<i>Ganoderma boninense</i>	1000	1000	100%	0.0	100%	601 bp	MK713555.1
43	PCB.G23	<i>Ganoderma boninense</i>	1000	1000	100%	0.0	100%	601 bp	MK713555.1
44	PCB.G31	<i>Ganoderma boninense</i>	1000	1000	100%	0.0	100%	601 bp	MK713555.1
45	PCB.G33	<i>Ganoderma boninense</i>	1000	1000	100%	0.0	100%	601 bp	MK713555.1
46	PCB.G35	<i>Ganoderma boninense</i>	1000	1000	100%	0.0	100%	601 bp	MK713555.1
47	PCB.G38	<i>Ganoderma boninense</i>	1000	1000	100%	0.0	100%	601 bp	MK713555.1
48	PCB.G41	<i>Ganoderma boninense</i>	1000	1000	100%	0.0	100%	601 bp	MK713555.1
49	PCR.B14	<i>Ganoderma boninense</i>	1090	1090	100%	0.0	100%	601 bp	MK713555.1
50	PCR.B40	<i>Ganoderma boninense</i>	1090	1090	100%	0.0	100%	601 bp	MK713555.1
51	PCR.C5	<i>Ganoderma boninense</i>	1072	1072	100%	0.0	100%	601 bp	MK713555.1
52	PCR.D33	<i>Ganoderma boninense</i>	1070	1070	100%	0.0	100%	601 bp	MK713555.1
53	PCR.E2	<i>Ganoderma boninense</i>	1072	1072	100%	0.0	100%	601 bp	MK713555.1
54	PCR.E4	<i>Ganoderma boninense</i>	1072	1072	100%	0.0	100%	601 bp	MK713555.1

Appendix 4 continued

55	PCR.E6	<i>Ganoderma boninense</i>	1072	1072	100%	0.0	100%	601 bp	MK713555.1
56	PCR.F28	<i>Ganoderma boninense</i>	773	773	100%	0.0	100%	601 bp	MK713555.1
57	PCR.F32	<i>Ganoderma boninense</i>	773	773	100%	0.0	100%	601 bp	MK713555.1
58	PCR.G10	<i>Ganoderma boninense</i>	994	994	100%	0.0	99.82%	601 bp	MK713555.1
59	PCR.G20	<i>Ganoderma boninense</i>	1000	1000	100%	0.0	100%	601 bp	MK713555.1
60	PCR.G35	<i>Ganoderma boninense</i>	1000	1000	100%	0.0	100%	601 bp	MK713555.1

Note: PCB is referred to pure cultures isolated from the bole and PCR is referred to pure cultures isolated from the root

Appendix 5: Sequencing results of ITS1/ITS4 amplified PCR products of pure cultures obtained from the fruiting body inoculated on *Ganoderma* selective medium. Identification was based on BLAST searches of ITS sequences against those of deposited ITS sequences in GenBank (NCBI)

No.	Sample ID*	Scientific Name	Max Score	Total Score	Query Coverage	E Value	Percent Identity	Accession Length	Accession
1	FB.B3	<i>Ganoderma boninense</i>	1077	1077	100%	0.0	100%	601 bp	MK713555.1
2	FB.B4	<i>Ganoderma boninense</i>	1077	1077	100%	0.0	100%	601 bp	MK713555.1
3	FB.B5	<i>Ganoderma boninense</i>	1077	1077	100%	0.0	100%	601 bp	MK713555.1
4	FB.B6	<i>Ganoderma boninense</i>	1077	1077	100%	0.0	100%	601 bp	MK713555.1
5	FB.B9	<i>Ganoderma boninense</i>	1077	1077	100%	0.0	100%	601 bp	MK713555.1
6	FB.B13	<i>Ganoderma boninense</i>	1077	1077	100%	0.0	100%	601 bp	MK713555.1
7	FB.B14	<i>Ganoderma boninense</i>	1077	1077	100%	0.0	100%	601 bp	MK713555.1
8	FB.B21	<i>Ganoderma boninense</i>	1077	1077	100%	0.0	100%	601 bp	MK713555.1
9	FB.B26	<i>Ganoderma boninense</i>	1077	1077	100%	0.0	100%	601 bp	MK713555.1
10	FB.B29	<i>Ganoderma boninense</i>	1077	1077	100%	0.0	100%	601 bp	MK713555.1
11	FB.B35	<i>Ganoderma boninense</i>	1077	1077	100%	0.0	100%	601 bp	MK713555.1
12	FB.B37	<i>Ganoderma boninense</i>	1077	1077	100%	0.0	100%	601 bp	MK713555.1
13	FB.B38	<i>Ganoderma boninense</i>	401	401	99%	3e-107	80.63%	601 bp	MK713555.1
14	FB.B40	<i>Ganoderma boninense</i>	1066	1066	100%	0.0	99.66%	601 bp	MK713555.1
15	FB.B42	<i>Ganoderma boninense</i>	1077	1077	100%	0.0	100%	601 bp	MK713555.1
16	FB.C16	<i>Ganoderma boninense</i>	1072	1072	100%	0.0	100%	601 bp	MK713555.1
17	FB.C17	<i>Ganoderma boninense</i>	1072	1072	100%	0.0	100%	601 bp	MK713555.1
18	FB.C22	<i>Ganoderma boninense</i>	1072	1072	100%	0.0	100%	601 bp	MK713555.1
19	FB.C24	<i>Ganoderma boninense</i>	1072	1072	100%	0.0	100%	601 bp	MK713555.1
20	FB.C26	<i>Ganoderma boninense</i>	1072	1072	100%	0.0	100%	601 bp	MK713555.1
21	FB.C33	<i>Ganoderma boninense</i>	1072	1072	100%	0.0	100%	601 bp	MK713556.1

Appendix 5 continued

22	FB.D1	<i>Ganoderma boninense</i>	1075	1075	100%	0.0	100%	601 bp	MK713555.1
23	FB.D4	<i>Ganoderma boninense</i>	1070	1070	100%	0.0	100%	601 bp	MK713555.1
24	FB.D5	<i>Ganoderma boninense</i>	1070	1070	100%	0.0	100%	601 bp	MK713555.1
25	FB.D9	<i>Ganoderma boninense</i>	1070	1070	100%	0.0	100%	601 bp	MK713555.1
26	FB.D12	<i>Ganoderma boninense</i>	1075	1075	100%	0.0	100%	601 bp	MK713555.1
27	FB.D19	<i>Ganoderma boninense</i>	1075	1075	99%	0.0	100%	601 bp	MK713555.1
28	FB.D23	<i>Ganoderma boninense</i>	1075	1075	99%	0.0	100%	601 bp	MK713555.1
29	FB.D25	<i>Ganoderma boninense</i>	1075	1075	100%	0.0	100%	601 bp	MK713555.1
30	FB.D26	<i>Ganoderma boninense</i>	1075	1075	100%	0.0	100%	601 bp	MK713555.1
31	FB.D28	<i>Ganoderma boninense</i>	1075	1075	100%	0.0	100%	601 bp	MK713555.1
32	FB.D32	<i>Ganoderma boninense</i>	1075	1075	100%	0.0	100%	601 bp	MK713555.1
33	FB.D33	<i>Ganoderma boninense</i>	1075	1075	100%	0.0	100%	601 bp	MK713555.1
34	FB.D38	<i>Ganoderma boninense</i>	1075	1075	100%	0.0	100%	601 bp	MK713555.1
35	FB.D39	<i>Ganoderma boninense</i>	1075	1075	100%	0.0	100%	601 bp	MK713555.1
36	FB.D42	<i>Ganoderma boninense</i>	1075	1075	100%	0.0	100%	601 bp	MK713555.1
37	FB.E2	<i>Ganoderma boninense</i>	1072	1072	100%	0.0	100%	601 bp	MK713555.1
38	FB.E4	<i>Ganoderma boninense</i>	1072	1072	100%	0.0	100%	601 bp	MK713555.1
39	FB.E7	<i>Ganoderma boninense</i>	1072	1072	100%	0.0	100%	601 bp	MK713555.1
40	FB.E11	<i>Ganoderma boninense</i>	1072	1072	100%	0.0	100%	601 bp	MK713555.1
41	FB.E12	<i>Ganoderma boninense</i>	1072	1072	100%	0.0	100%	601 bp	MK713555.1
42	FB.E13	<i>Ganoderma boninense</i>	1072	1072	100%	0.0	100%	601 bp	MK713555.1
43	FB.E16	<i>Ganoderma boninense</i>	1072	1072	100%	0.0	100%	601 bp	MK713555.1
44	FB.E17	<i>Ganoderma boninense</i>	1072	1072	100%	0.0	100%	601 bp	MK713555.1
45	FB.E19	<i>Ganoderma boninense</i>	1072	1072	100%	0.0	100%	601 bp	MK713555.1

Appendix 5 continued

46	FB.E20	<i>Ganoderma boninense</i>	1072	1072	100%	0.0	100%	601 bp	MK713555.1
47	FB.E21	<i>Ganoderma boninense</i>	1072	1072	100%	0.0	100%	601 bp	MK713555.1
48	FB.E22	<i>Ganoderma boninense</i>	1072	1072	100%	0.0	100%	601 bp	MK713555.1
49	FB.E27	<i>Ganoderma boninense</i>	1072	1072	100%	0.0	100%	601 bp	MK713555.1
50	FB.E28	<i>Ganoderma boninense</i>	1033	1033	100%	0.0	98.80%	601 bp	MK713555.1
51	FB.E29	<i>Ganoderma boninense</i>	1072	1072	100%	0.0	100%	601 bp	MK713555.1
52	FB.E33	<i>Ganoderma boninense</i>	1072	1072	100%	0.0	100%	601 bp	MK713555.1
53	FB.E36	<i>Ganoderma boninense</i>	1072	1072	100%	0.0	100%	601 bp	MK713555.1
54	FB.E37	<i>Ganoderma boninense</i>	1072	1072	100%	0.0	100%	601 bp	MK713555.1
55	FB.E38	<i>Ganoderma boninense</i>	1072	1072	100%	0.0	100%	601 bp	MK713555.1
56	FB.E40	<i>Ganoderma boninense</i>	1072	1072	100%	0.0	100%	601 bp	MK713555.1
57	FB.F9	<i>Ganoderma boninense</i>	773	773	100%	0.0	100%	601 bp	MK713555.1
58	FB.F10	<i>Ganoderma boninense</i>	773	773	100%	0.0	100%	601 bp	MK713555.1
59	FB.F12	<i>Ganoderma boninense</i>	773	773	100%	0.0	100%	601 bp	MK713555.1
60	FB.F15	<i>Ganoderma boninense</i>	773	773	100%	0.0	100%	601 bp	MK713555.1
61	FB.F18	<i>Ganoderma boninense</i>	863	863	100%	0.0	100%	601 bp	MK713555.1
62	FB.F19	<i>Ganoderma boninense</i>	763	763	100%	0.0	99.52%	601 bp	MK713555.1
63	FB.F20	<i>Ganoderma boninense</i>	773	773	100%	0.0	100%	601 bp	MK713555.1
64	FB.F21	<i>Ganoderma boninense</i>	773	773	100%	0.0	100%	601 bp	MK713555.1
65	FB.F23	<i>Ganoderma boninense</i>	773	773	100%	0.0	100%	601 bp	MK713555.1
66	FB.F24	<i>Ganoderma boninense</i>	773	773	100%	0.0	100%	601 bp	MK713555.1
67	FB.F27	<i>Ganoderma boninense</i>	773	773	100%	0.0	100%	601 bp	MK713555.1
68	FB.F29	<i>Ganoderma boninense</i>	773	773	100%	0.0	100%	601 bp	MK713555.1
69	FB.F30	<i>Ganoderma boninense</i>	773	773	100%	0.0	100%	601 bp	MK713555.1

Appendix 5 continued

70	FB.F31	<i>Ganoderma boninense</i>	773	773	100%	0.0	100%	601 bp	MK713555.1
71	FB.F32	<i>Ganoderma boninense</i>	773	773	100%	0.0	100%	601 bp	MK713555.1
72	FB.F36	<i>Ganoderma boninense</i>	773	773	100%	0.0	100%	601 bp	MK713555.1
73	FB.G1	<i>Ganoderma boninense</i>	1000	1000	100%	0.0	100%	601 bp	MK713555.1
74	FB.G8	<i>Ganoderma boninense</i>	1000	1000	100%	0.0	100%	601 bp	MK713555.1
75	FB.G10	<i>Ganoderma boninense</i>	1000	1000	100%	0.0	100%	601 bp	MK713555.1
76	FB.G12	<i>Ganoderma boninense</i>	1000	1000	100%	0.0	100%	601 bp	MK713555.1
77	FB.G13	<i>Ganoderma boninense</i>	1000	1000	100%	0.0	100%	601 bp	MK713555.1
78	FB.G14	<i>Ganoderma boninense</i>	1000	1000	100%	0.0	100%	601 bp	MK713555.1
79	FB.G17	<i>Ganoderma boninense</i>	1000	1000	100%	0.0	100%	601 bp	MK713555.1
80	FB.G20	<i>Ganoderma boninense</i>	1000	1000	100%	0.0	100%	601 bp	MK713555.1
81	FB.G21	<i>Ganoderma boninense</i>	1000	1000	100%	0.0	100%	601 bp	MK713555.1
82	FB.G22	<i>Ganoderma boninense</i>	1000	1000	100%	0.0	100%	601 bp	MK713555.1
83	FB.G23	<i>Ganoderma boninense</i>	1000	1000	100%	0.0	100%	601 bp	MK713555.1
84	FB.G29	<i>Ganoderma boninense</i>	1000	1000	100%	0.0	100%	601 bp	MK713555.1
85	FB.G32	<i>Ganoderma boninense</i>	1000	1000	100%	0.0	100%	601 bp	MK713555.1
86	FB.G33	<i>Ganoderma boninense</i>	1000	1000	100%	0.0	100%	601 bp	MK713555.1
87	FB.G35	<i>Ganoderma boninense</i>	1000	1000	100%	0.0	100%	601 bp	MK713555.1
88	FB.G37	<i>Ganoderma boninense</i>	1000	1000	100%	0.0	100%	601 bp	MK713555.1

Note: FB is referred to fruiting body

Appendix 6: Sequencing results of ITS1/ITS4 amplified PCR products of DNA extracted from the bole and the root tissue of infected seedlings. Identification was based on BLAST searches of ITS sequences against those of deposited ITS sequences in GenBank (NCBI)

No.	Sample ID	Scientific Name	Max Score	Total Score	Query Coverage	E Value	Percent Identity	Accession Length	Accession
1	B.B2	<i>Ganoderma boninense</i>	1075	1075	100%	0.0	100%	601 bp	MK713555.1
2	B.B4	<i>Ganoderma boninense</i>	1075	1075	100%	0.0	100%	601 bp	MK713555.1
3	B.B5	<i>Ganoderma boninense</i>	1075	1075	100%	0.0	100%	601 bp	MK713555.1
4	B.B14	<i>Ganoderma boninense</i>	1075	1075	100%	0.0	100%	601 bp	MK713555.1
5	B.B18	<i>Ganoderma boninense</i>	1075	1075	100%	0.0	100%	601 bp	MK713555.1
6	B.B19	<i>Ganoderma boninense</i>	1075	1075	100%	0.0	100%	601 bp	MK713555.1
7	B.B20	<i>Ganoderma boninense</i>	1075	1075	100%	0.0	100%	601 bp	MK713555.1
8	B.B21	<i>Ganoderma boninense</i>	1075	1075	100%	0.0	100%	601 bp	MK713555.1
9	B.B23	<i>Ganoderma boninense</i>	1075	1075	100%	0.0	100%	601 bp	MK713555.1
10	B.B25	<i>Ganoderma boninense</i>	1075	1075	100%	0.0	100%	601 bp	MK713555.1
11	B.B36	<i>Ganoderma boninense</i>	1075	1075	100%	0.0	100%	601 bp	MK713555.1
12	B.B37	<i>Ganoderma boninense</i>	1075	1075	100%	0.0	100%	601 bp	MK713555.1
13	B.B38	<i>Ganoderma boninense</i>	1075	1075	100%	0.0	100%	601 bp	MK713555.1
14	B.C16	<i>Ganoderma boninense</i>	1042	1042	100%	0.0	100%	601 bp	MK713555.1
15	B.C26	<i>Ganoderma boninense</i>	1042	1042	100%	0.0	100%	601 bp	MK713555.1
16	B.D3	<i>Ganoderma boninense</i>	1072	1072	100%	0.0	100%	601 bp	MK713555.1
17	B.D4	<i>Ganoderma boninense</i>	1072	1072	100%	0.0	100%	601 bp	MK713555.1
18	B.D6	<i>Ganoderma boninense</i>	1072	1072	100%	0.0	100%	601 bp	MK713555.1
19	B.D9	<i>Ganoderma boninense</i>	1072	1072	100%	0.0	100%	601 bp	MK713555.1
20	B.D20	<i>Ganoderma boninense</i>	1072	1072	100%	0.0	100%	601 bp	MK713555.1
21	B.D26	<i>Ganoderma boninense</i>	1072	1072	100%	0.0	100%	601 bp	MK713555.1

Appendix 6 continued

22	B.D31	<i>Ganoderma boninense</i>	1072	1072	100%	0.0	100%	601 bp	MK713555.1
23	B.D33	<i>Ganoderma boninense</i>	1072	1072	100%	0.0	100%	601 bp	MK713555.1
24	B.D35	<i>Ganoderma boninense</i>	1072	1072	100%	0.0	100%	601 bp	MK713555.1
25	B.D38	<i>Ganoderma boninense</i>	992	992	100%	0.0	99.81%	601 bp	MK713555.1
26	B.D39	<i>Ganoderma boninense</i>	1072	1072	100%	0.0	100%	601 bp	MK713555.1
27	B.D42	<i>Ganoderma boninense</i>	1072	1072	100%	0.0	100%	601 bp	MK713555.1
28	B.E2	<i>Ganoderma boninense</i>	1072	1072	100%	0.0	100%	601 bp	MK713555.1
29	B.E6	<i>Ganoderma boninense</i>	1072	1072	100%	0.0	100%	601 bp	MK713555.1
30	B.E7	<i>Ganoderma boninense</i>	1072	1072	100%	0.0	100%	601 bp	MK713555.1
31	B.E12	<i>Ganoderma boninense</i>	1072	1072	100%	0.0	100%	601 bp	MK713555.1
32	B.E13	<i>Ganoderma boninense</i>	1072	1072	100%	0.0	100%	601 bp	MK713555.1
33	B.E16	<i>Ganoderma boninense</i>	1072	1072	100%	0.0	100%	601 bp	MK713555.1
34	B.E17	<i>Ganoderma boninense</i>	1072	1072	100%	0.0	100%	601 bp	MK713555.1
35	B.E18	<i>Ganoderma boninense</i>	1072	1072	100%	0.0	100%	601 bp	MK713555.1
36	B.E20	<i>Ganoderma boninense</i>	1072	1072	100%	0.0	100%	601 bp	MK713555.1
37	B.E21	<i>Ganoderma boninense</i>	1072	1072	100%	0.0	100%	601 bp	MK713555.1
38	B.E23	<i>Ganoderma boninense</i>	1072	1072	100%	0.0	100%	601 bp	MK713555.1
39	B.E27	<i>Ganoderma boninense</i>	1072	1072	100%	0.0	100%	601 bp	MK713555.1
40	B.E28	<i>Ganoderma boninense</i>	1072	1072	100%	0.0	100%	601 bp	MK713555.1
41	B.E36	<i>Ganoderma boninense</i>	1072	1072	100%	0.0	100%	601 bp	MK713555.1
42	B.E38	<i>Ganoderma boninense</i>	1072	1072	100%	0.0	100%	601 bp	MK713555.1
43	B.F7	<i>Ganoderma boninense</i>	773	773	100%	0.0	100%	601 bp	MK713555.1
44	B.F12	<i>Ganoderma boninense</i>	773	773	100%	0.0	100%	601 bp	MK713555.1
45	B.F14	<i>Ganoderma boninense</i>	773	773	100%	0.0	100%	601 bp	MK713555.1

Appendix 6 continued

46	B.F23	<i>Ganoderma boninense</i>	773	773	100%	0.0	100%	601 bp	MK713555.1
47	B.F24	<i>Ganoderma boninense</i>	885	885	100%	0.0	99.41%	601 bp	MK713555.1
48	B.F25	<i>Ganoderma boninense</i>	773	773	100%	0.0	100%	601 bp	MK713555.1
49	B.F28	<i>Ganoderma boninense</i>	773	773	100%	0.0	100%	601 bp	MK713555.1
50	B.F29	<i>Ganoderma boninense</i>	773	773	100%	0.0	100%	601 bp	MK713555.1
51	B.F31	<i>Ganoderma boninense</i>	773	773	100%	0.0	100%	601 bp	MK713555.1
52	B.F32	<i>Ganoderma boninense</i>	773	773	100%	0.0	100%	601 bp	MK713555.1
53	B.G6	<i>Ganoderma boninense</i>	1000	1000	100%	0.0	100%	601 bp	MK713555.1
54	B.G9	<i>Ganoderma boninense</i>	1000	1000	100%	0.0	100%	601 bp	MK713555.1
55	B.G11	<i>Ganoderma boninense</i>	1000	1000	100%	0.0	100%	601 bp	MK713555.1
56	B.G12	<i>Ganoderma boninense</i>	1000	1000	100%	0.0	100%	601 bp	MK713555.1
57	B.G16	<i>Ganoderma boninense</i>	1000	1000	100%	0.0	100%	601 bp	MK713555.1
58	B.G18	<i>Ganoderma boninense</i>	1000	1000	100%	0.0	100%	601 bp	MK713555.1
59	B.G21	<i>Ganoderma boninense</i>	1000	1000	100%	0.0	100%	601 bp	MK713555.1
60	R.B2	<i>Ganoderma boninense</i>	1072	1072	100%	0.0	100%	601 bp	MK713555.1
61	R.B18	<i>Ganoderma boninense</i>	1072	1072	100%	0.0	100%	601 bp	MK713555.1
62	R.B20	<i>Ganoderma boninense</i>	1072	1072	100%	0.0	100%	601 bp	MK713555.1
63	R.B21	<i>Ganoderma boninense</i>	1072	1072	100%	0.0	100%	601 bp	MK713555.1
64	R.B23	<i>Ganoderma boninense</i>	1072	1072	100%	0.0	100%	601 bp	MK713555.1
65	R.B25	<i>Ganoderma boninense</i>	1072	1072	100%	0.0	100%	601 bp	MK713555.1
66	R.B28	<i>Ganoderma boninense</i>	1072	1072	100%	0.0	100%	601 bp	MK713555.1
67	R.B36	<i>Ganoderma boninense</i>	1072	1072	100%	0.0	100%	601 bp	MK713555.1
68	R.B37	<i>Ganoderma boninense</i>	1072	1072	100%	0.0	100%	601 bp	MK713555.1
69	R.B38	<i>Ganoderma boninense</i>	1072	1072	100%	0.0	100%	601 bp	MK713555.1

Appendix 6 continued

70	R.C16	<i>Ganoderma boninense</i>	1042	1042	100%	0.0	100%	601 bp	MK713555.1
71	R.C26	<i>Ganoderma boninense</i>	1042	1042	100%	0.0	100%	601 bp	MK713555.1
72	R.D4	<i>Ganoderma boninense</i>	1072	1072	100%	0.0	100%	601 bp	MK713555.1
73	R.D20	<i>Ganoderma boninense</i>	1072	1072	100%	0.0	100%	601 bp	MK713555.1
74	R.D31	<i>Ganoderma boninense</i>	1072	1072	100%	0.0	100%	601 bp	MK713555.1
75	R.D33	<i>Ganoderma boninense</i>	1072	1072	100%	0.0	100%	601 bp	MK713555.1
76	R.D39	<i>Ganoderma boninense</i>	1072	1072	100%	0.0	100%	601 bp	MK713555.1
77	R.D42	<i>Ganoderma boninense</i>	1062	1062	100%	0.0	99.66%	601 bp	MK713555.1
78	R.E1	<i>Ganoderma boninense</i>	1072	1072	100%	0.0	100%	601 bp	MK713555.1
79	R.E2	<i>Ganoderma boninense</i>	1072	1072	100%	0.0	100%	601 bp	MK713555.1
80	R.E6	<i>Ganoderma boninense</i>	1007	1007	100%	0.0	97.94%	601 bp	MK713555.1
81	R.E12	<i>Ganoderma boninense</i>	1072	1072	100%	0.0	100%	601 bp	MK713555.1
82	R.E16	<i>Ganoderma boninense</i>	1072	1072	100%	0.0	100%	601 bp	MK713555.1
83	R.E20	<i>Ganoderma boninense</i>	1072	1072	100%	0.0	100%	601 bp	MK713555.1
84	R.E21	<i>Ganoderma boninense</i>	1072	1072	100%	0.0	100%	601 bp	MK713555.1
85	R.E28	<i>Ganoderma boninense</i>	1072	1072	100%	0.0	100%	601 bp	MK713555.1
86	R.E36	<i>Ganoderma boninense</i>	1072	1072	100%	0.0	100%	601 bp	MK713555.1
87	R.E38	<i>Ganoderma boninense</i>	1072	1072	100%	0.0	100%	601 bp	MK713555.1
88	R.F2	<i>Ganoderma boninense</i>	773	773	100%	0.0	100%	601 bp	MK713555.1
89	R.F7	<i>Ganoderma boninense</i>	773	773	100%	0.0	100%	601 bp	MK713555.1
90	R.F12	<i>Ganoderma boninense</i>	773	773	100%	0.0	100%	601 bp	MK713555.1
91	R.F14	<i>Ganoderma boninense</i>	773	773	100%	0.0	100%	601 bp	MK713555.1
92	R.F21	<i>Ganoderma boninense</i>	773	773	100%	0.0	100%	601 bp	MK713555.1
93	R.F25	<i>Ganoderma boninense</i>	773	773	100%	0.0	100%	601 bp	MK713555.1

Appendix 6 continued

94	R.F28	<i>Ganoderma boninense</i>	773	773	100%	0.0	100%	601 bp	MK713555.1
95	R.F29	<i>Ganoderma boninense</i>	773	773	100%	0.0	100%	601 bp	MK713555.1
96	R.F31	<i>Ganoderma boninense</i>	773	773	100%	0.0	100%	601 bp	MK713555.1
97	R.F32	<i>Ganoderma boninense</i>	773	773	100%	0.0	100%	601 bp	MK713555.1
98	R.G6	<i>Ganoderma boninense</i>	1000	1000	100%	0.0	100%	601 bp	MK713555.1
99	R.G9	<i>Ganoderma boninense</i>	994	994	100%	0.0	99.82%	601 bp	MK713555.1
100	R.G10	<i>Ganoderma boninense</i>	1000	1000	100%	0.0	100%	601 bp	MK713555.1
101	R.G12	<i>Ganoderma boninense</i>	1000	1000	100%	0.0	100%	601 bp	MK713555.1
102	R.G16	<i>Ganoderma boninense</i>	1000	1000	100%	0.0	100%	601 bp	MK713555.1
103	R.G20	<i>Ganoderma boninense</i>	1000	1000	100%	0.0	97.94%	601 bp	MK713555.1
104	R.G21	<i>Ganoderma boninense</i>	1000	1000	100%	0.0	100%	601 bp	MK713555.1
105	R.G23	<i>Ganoderma boninense</i>	994	994	100%	0.0	99.82%	601 bp	MK713555.1
106	R.G24	<i>Ganoderma boninense</i>	1000	1000	100%	0.0	100%	601 bp	MK713555.1
107	R.G33	<i>Ganoderma boninense</i>	1000	1000	100%	0.0	100%	601 bp	MK713555.1
108	R.G35	<i>Ganoderma boninense</i>	1000	1000	100%	0.0	100%	601 bp	MK713555.1
109	R.G39	<i>Ganoderma boninense</i>	1000	1000	100%	0.0	100%	601 bp	MK713555.1
110	R.G41	<i>Ganoderma boninense</i>	1000	1000	100%	0.0	100%	601 bp	MK713555.1

Note: B is referred to bole tissue and R is referred to root tissue